Biogeosciences, 23, 1–63, 2026
https://doi.org/10.5194/bg-23-1-2026

Biogeosciences Open Access EGU

Research article

Plant belowground traits indicate increased plant-mediated methane transport along a peatland permafrost thaw gradient

Tiia M. Määttä[1], Samantha H. Bosman[2], Jeffrey P. Chanton[3], Patrick Crill[4], Suzanne B. Hodgkins[5], Jalisha Theanutti Kallingal[6], Rachel M. Wilson[3], Ruth Varner[4,7], and Avni Malhotra[1,8]

[1]Department of Geography, Faculty of Science, University of Zürich, Winterthurerstrasse 190, 8057 Zürich, Switzerland
[2]Department of Oceanography, Dalhousie University, Halifax, NS, Canada
[3]Department of Earth Ocean and Atmospheric Sciences, Florida State University, Tallahassee, Fl 32306, USA
[4]Department of Geological Sciences and Bolin Centre for Climate Research, Stockholm University, 106 91 Stockholm, Sweden
[5]Department of Microbiology, The Ohio State University, Columbus, OH, USA
[6]Department of Physical Geography and Ecosystem Science, Lund University, 223 62 Lund, Sweden
[7]Department of Earth Sciences and Institute for the Study of Earth, Oceans and Space, University of New Hampshire, Durham, NH, USA
[8]Biological Sciences Division, Pacific Northwest National Laboratory, 902 Battelle Boulevard, Richland, WA, USA

Correspondence: Tiia M. Määttä (tiia.maatta@geo.uzh.ch)

Received: 27 January 2026 – Discussion started: 29 January 2026
Revised: 17 June 2026 – Accepted: 30 June 2026 – Published:

Abstract. Permafrost thaw alters methane (CH_4) fluxes from subarctic peatland ecosystems. Collapsing permafrost palsas change hydrology, interstitial oxygen availability, and vegetation composition, and each of these factors contribute to net CH_4 flux by influencing CH_4 production, consumption and transport. Changes in plant-mediated CH_4 fluxes have mostly been estimated using aboveground characteristics, such as biomass and leaf area, leaving belowground parts (roots and rhizomes) understudied despite their direct contact to depth-dependent CH_4 flux processes. Here, we explored the potential of using root and rhizome traits as proxies for plant-mediated CH_4 cycling along a peatland permafrost thaw gradient in subarctic Sweden. We investigated changes in root and rhizome biomass, surface area (SA), diameter, tissue density (TD), and specific root length (SRL) along the permafrost thaw gradient, and how these traits relate to early-, middle-, peak- and season median CH_4 fluxes. We utilized chamber CH_4 flux and pore water CH_4 concentration and isotopic measurements during the productive season. Shrub SRL, diameter and isotopic data suggested increased plant-mediated carbon substrates available for acetoclastic methanogenesis across the thaw gradient. Root TD, proxy for root porosity, decreased with thaw and had negative correlations with CH_4 fluxes throughout the season. Simultaneously, herbaceous rhizome SA-CH_4 flux correlations were positive and pore water CH_4 concentrations were lowest in the fully thawed stage. These results indicated increasing herbaceous plant-mediated transport of acetoclastically-produced CH_4 with thaw. Our study demonstrates that integrating plant belowground traits with environmental and biogeochemical data can help improve CH_4 flux predictions in thawing landscapes and revealed key mechanistic insights regarding the interplay between substrate availability for methanogenesis and gas transport.

1 Introduction

Northern peatlands are significant net methane (CH_4) emitters primarily due to the predominance of anoxia throughout the peat depth profile (Gorham, 1991; McGuire et al., 2009; Zhuang et al., 2004). Owing to high organic carbon accumulation, high-latitude peatlands store approximately a third of the global carbon stock (Gorham, 1991), with a substantial fraction preserved in and beneath permafrost (Schuur et al., 2008). In the high latitudes, increasing air temperatures drive permafrost thaw, which can expose the previously frozen organic matter to soil decomposers, including methanogens. Together with altered hydrological and thermal conditions, these processes may increase CH_4 emissions and lead to positive climate feedback (Olefeldt et al., 2013; Schuur et al., 2008). Palsa mires with permafrost plateaus (palsas) are especially vulnerable to increasing temperatures and changes in precipitation (Luoto et al., 2004). Palsas are approximately 0.5–10 m high peat hummocks with a frozen core of peat and mineral soil. They form as a result of water-saturated peat freezing in winter and the dry surface peat protecting the frozen peat in summer, raising the peat above the surrounding mire (Luoto et al., 2004). In northern Fennoscandia, permafrost thaw has formed transitional gradients from frozen palsas and peat plateau to permafrost-free bogs and fens (Luoto et al., 2004; Olvmo et al., 2020). Following palsa collapse, soil moisture increases, shifting the system from an ombrotrophic bog-like system to a minerotrophic fen. Vegetation composition shifts from shrub-dominated on palsas to graminoid-dominated in fens, and soil redox and pH change, influencing methanogenic CH_4 production, methanotrophic CH_4 consumption, and CH_4 transport from the soil to the atmosphere, and net CH_4 fluxes (Perryman et al., 2020; Turetsky et al., 2014; Varner et al., 2022). Almost all arctic permafrost has been estimated to degrade and result in 120 ± 85 Gt of carbon emissions by 2100 (Lawrence et al., 2008; Schaefer et al., 2014). Together with the inevitable disappearance of palsa mires (Luoto et al., 2004; Olvmo et al., 2020), this highlights the urgent need to investigate the network of CH_4 flux controls in thawing palsa mires.

One of the key biotic CH_4 flux drivers in permafrost peatlands are wetland plants and the traits reflecting their adaptive and resource acquisition strategies. In general, plants contribute to CH_4 fluxes by mediating gas transport, providing carbon substrates for methanogens, and modifying the physicochemical properties of the rhizosphere (Chanton and Dacey, 1991; Laanbroek, 2010; Määttä and Malhotra, 2024; Noyce et al., 2014). As an adaptive strategy to anoxia, many wetland plant species develop aerenchyma which are air spaces within the plant stem, roots and rhizomes that transport oxygen (O_2) from the atmosphere to the roots and the surrounding soil (Armstrong et al., 1991; Končalová, 1990; Vroom et al., 2022). This plant-mediated gas transport mechanism enhances rhizosphere oxygenation and CH_4 consumption, but also simultaneously increases CH_4 transport from anoxic peat to the atmosphere (Laanbroek, 2010; Noyce et al., 2014; Ström et al., 2005). While peatlands store vast quantities of carbon, much of it is too recalcitrant to be directly utilized by methanogens particularly in deep peat (Hogg, 1993; Ström et al., 2005). The release of labile carbon substrates such as acetate and other organic acids by plant roots stimulates CH_4 production and emission (Joabsson and Christensen, 2001; Ström et al., 2003).

Studies using plant functional traits to predict CH_4 fluxes have primarily focused on aboveground features, such as plant green area, even though plant belowground biomass can exceed that aboveground especially in (sub)arctic ecosystems (Iversen et al., 2015; Malhotra and Roulet, 2015). Often, the aboveground traits have been used to estimate belowground characteristics, such as root porosity, based on the plant species or functional type (PFT) (e.g., Bouchard et al., 2007; Greenup et al., 2000; Iversen et al., 2015). However, above- and belowground plant traits and the functional connections between them have not been adequately studied in relation to carbon cycling and the use of aboveground traits as proxies for plant-mediated belowground carbon functioning remains unresolved (Iversen et al., 2015; Määttä and Malhotra, 2024).

Many studies have used above- and/or belowground biomass as CH_4 flux predictors but the direction of the relationship varies strongly between studies, species, and PFTs (e.g., Greenup et al., 2000; Joabsson and Christensen, 2001; Koelbener et al., 2010). While above and belowground biomass may reflect plant productivity, quantification of plant-mediated CH_4 fluxes may be better served by a knowledge of belowground traits more directly related to CH_4 production, consumption and transport. For example, root exudation in some instances can explain CH_4 flux variation better than biomass (Ström et al., 2005; Waldo et al., 2019). Because belowground traits, such as rooting depth, change with a deepening active layer (Blume-Werry et al., 2016; Iversen et al., 2015), assessing these trait variations and their effects on CH_4 fluxes along permafrost thaw gradients is essential.

Wetland CH_4 fluxes can be driven by plant-mediated carbon release and CH_4 and O_2 transport (Knox et al., 2021), which can be reflected in root and rhizome traits. Increases in root and rhizome tissue porosity (i.e., lower tissue density and larger diameter; Freschet et al., 2021a; Visser et al., 2000) can enhance plant-mediated gas transport and, depending on species and environmental conditions (e.g., water table level), can lead to increased CH_4 transport and net flux (Bhullar et al., 2013; Henneberg et al., 2016; van den Berg et al., 2020) or rhizospheric CH_4 oxidation and decreased net CH_4 flux (e.g., Fritz et al., 2011; Noyce et al., 2023). CH_4 production can be stimulated by increased labile carbon provision particularly from root exudation (Ström et al., 2003, 2012; Waldo et al., 2019) but also from rhizome and root decomposition (Hackney and De La Cruz, 1980; Scheffer and Aerts, 2000). Specific root length (SRL), the relationship between root length and dry mass, could be a proxy for carbon substrate provision, as high SRL is associated with low tissue density, shorter lifespan, high turnover rates (Bergmann et al., 2020; Eissenstat et al., 2000), and root exudation (Wen et al., 2022). However, studies on the relationships between different root traits, especially SRL and tissue density, in wetlands are rare (Iversen et al., 2015; Pan et al., 2019).

Here, we investigated (1) how root (biomass, surface area, diameter, tissue density, and SRL) and rhizome (biomass, surface area, diameter, and tissue density) traits vary along a peatland permafrost thaw gradient, (2) the correlation of these belowground traits with CH_4 fluxes, and (3) whether root and rhizome traits are strong predictors of CH_4 flux during early, middle and peak CH_4 flux during the productive season. We expected that root biomass, surface area and SRL would be highest at the intact and partly thawed permafrost stages due to lower soil moisture and high species diversity (Hough et al., 2022; Iversen et al., 2015; Keuper et al., 2017). We hypothesized that shrub rhizomes would be most abundant in the intact permafrost stage, whereas most herbaceous rhizome biomass would be found in the more thawed permafrost stage (Hough et al., 2022). We hypothesized that root and rhizome tissue density would decrease from intact to fully thawed permafrost due to increased soil moisture. We also expected that SRL would increase CH_4 flux (Saarnio et al., 2004; Ström and Christensen, 2007; Wen et al., 2022), while tissue density would have negative relationships with CH_4 fluxes throughout the productive season. We expected the trait-CH_4 flux relationships to be stronger for herbaceous plants than for shrubs at the middle and peak CH_4 flux periods, because herbaceous plants increase root biomass throughout the growing season in the tundra (Billings et al., 1978; Kummerow and Russell, 1980; Wang et al., 2016) whereas shrub root biomass can remain relatively constant (Wang et al., 2016).

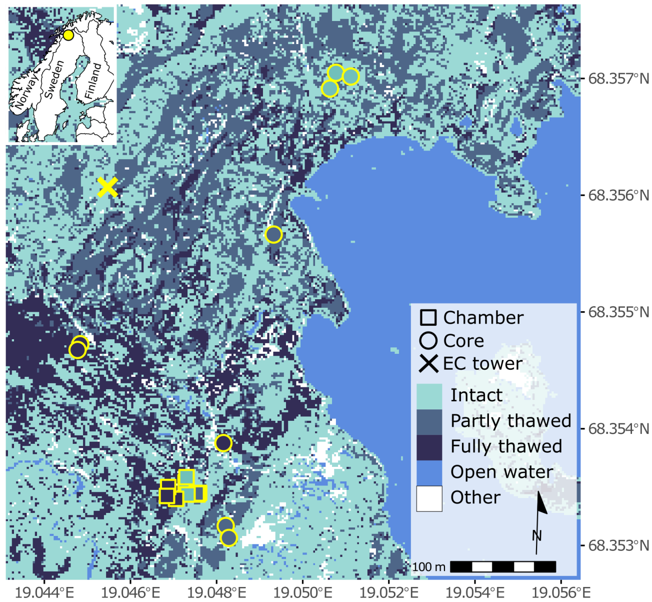

Figure 1. Location of the Stordalen mire and CH_4 flux and peat coring plots within the study area. Based on vegetation classification in 2014, the study area was classified into intact permafrost (tall shrub and hummock, in light blue), partly thawed permafrost (semi-wet and wet, in dark gray), fully thawed permafrost (tall graminoid, in dark blue), open water (bright blue) and other (rock and anthropogenic surfaces, in white) (Palace et al., 2018, 2022; Varner et al., 2022). Rectangles indicate automated chamber CH_4 flux measurement plots, circles indicate peat coring plots, and the cross represents the eddy covariance tower (ICOS: SE-Sto).

2 Materials and methods

2.1 Study area

The study area is the Stordalen mire in northern Sweden (68°22′ N 19°03′ E; Fig. 1). The mean annual temperature of the area was −0.5 °C and mean annual precipitation sum was 204 mm for period 1985–2023, based on measurements from a nearby meteorological station (Polarforskningssekretariatet and SMHI, 2025a, b). The area contains a permafrost thaw gradient ranging from palsa with intact permafrost to partly and fully thawed permafrost, each of which includes hydrological conditions and vegetation compositions typical for each thaw stage. The permafrost is largely intact in drained palsa with ericaceous shrubs (e.g., *Empetrum nigrum*, *Andromeda polifolia*, *Rubus chamaemorus*), hummock-forming *Eriophorum vaginatum*, mosses (e.g., *Dicranum* sp.) and lichens (Holmes et al., 2022; Hough et al., 2022; Malhotra and Roulet, 2015). In the partly thawed hydrologically perched stage, the vegetation is dominated by *Sphagnum* spp. and feather mosses as well as sedges, such as *Eriophorum vaginatum* and *Carex rotundata*, typical for ombrotrophic bogs (Holmes et al., 2022; Malhotra and Roulet, 2015). The fully thawed stage includes wet minerotrophic fens that have generally higher pH and their dominant vegetation includes *Eriophorum angustifolium*, *Equisetum fluviatile* and *Carex rostrata* (Holmes et al., 2022; Johansson et al., 2006; Malhotra and Roulet, 2015). In general, moisture increases from intact to fully thawed permafrost stages, due to improved connections to the ground water (2007–2017 mean annual water table level ± standard deviation at partly thawed stage: 9.1 ± 4.6 cm below peat surface, fully thawed stage: 2.1 ± 4.4 cm above peat surface) (Crill et al., 2023; Holmes et al., 2022; Malhotra and Roulet, 2015). The peat depth reaches down to 3 m and is underlain by silt (Johansson et al., 2006).

2.2 Peat cores

We took peat cores using a push corer ($d = 12$ cm, length = 45 cm) to obtain plant material for belowground trait measurements. Despite destructive sampling being restricted, we were able to obtain three cores per thaw stage ($n = 9$ cores in total). In addition, peat coring was not possible next to the CH_4 flux chambers and within the eddy covariance footprint, so we estimated the vegetation composition (vascular plant and moss species) in the chamber collars with vegetation surveys (point intercept method; Sect. A1, Table C1) and found representative vegetation patches for each chamber outside of the footprint. In the plot selection, emphasis was put on vascular plant species and secondarily on moss species cover. The peat cores were collected on the 21 July 2023. The tightly packed samples were put into a cooler with ice packs and stored frozen for four days. The samples were transported from Sweden to University of Zurich, Switzerland (11 h), and stored in a freezer in −20 °C until further processing.

2.3 Plant green area measurements

To compare the chamber and peat coring plots, and to provide a non-destructive aboveground plant trait comparison to the belowground traits, we estimated species-specific vascular plant green area (GA; Tables 1 and C2). We randomly assigned three (peat coring plots) to five (chamber plots) subquadrats (16.8 × 16.8 cm) of the vegetation survey grid (Sect. A1) for GA measurements using the function sample in R (R Core Team, 2025). We measured green leaf and stem dimensions (leaf width and length, stem length and diameter) per species within each subquadrat. We measured 10 leaves per species per subquadrat, with the exception of fully thawed stage chamber plots where we measured all leaves and stems. For *E. nigrum*, we estimated the total number of leaves by counting all the leaves of three stems roughly representing the majority of the stems within the subquadrat. We calculated species-specific leaf and stem area (m^2) based on geometric formulae, and GA was estimated based on the average number of green leaves and stems per m^2 multiplied by green leaf and stem area per m^2 (Wilson et al., 2007). Since the leaves of *Rubus chamaemorus* did not fit into a simple geometric formula, we estimated their green area using photos taken above the survey grid and ImageJ.JS v0.5.8 (Ouyang et al., 2019; Schneider et al., 2012) (see mean GA per species in Table C2).

2.4 Environmental variables

In order to compare the abiotic environmental characteristics of the peat coring plots with the chamber plots, we measured peat temperature (°C), pH, water table level (cm) and active layer depth (cm) at the individual plots (Table 2). Peat temperature was measured 2–3 times a day (08:00 a.m., 12:00 p.m., 05:00 p.m.) at 10 cm depth over a three-day period (23–25 July 2023) using a soil temperature probe (Testo 720, SN 03679207, Testo, Titisee-Neustadt, Germany). Active layer depth was measured with a metal rod.

We measured pH on 25 July 2023. For the intact and partly thawed plots, we took ca. 8.5 g of peat from 0.5 m distance from the chamber collar at ca. 5 cm depth (intact) or 7–10 cm depth (partly thawed). The pH was measured using a pH meter (826 pH mobile, SN 1826001012160, Metrohm, Herisau, Switzerland) and pH electrode (Polyplast, Ref 238380, SN13208, Hamilton, Reno, USA) by mixing the peat sample with $CaCl_2$ solution (10 mL 0.01 mol L^{-1} $CaCl_2$ per sample). At fully thawed plots, pH was measured directly from open water at ca. 5 cm depth. The electrode was always kept in liquid and when not in measurement solution, it was kept in a protective tube with KCl.

Half-hourly peat temperature data was measured with thermocouples installed at each chamber and acquired with CR10x data logger (Campbell Scientific Inc., UT, USA) (Bäckstrand et al., 2008; McCalley et al., 2014). As continuous soil moisture and water table level data were not available for the productive season in 2023, we used 10-year (2007-2017) water table depth (WTD) means and standard deviations per thaw stage from Crill et al., (2023) for a rough background estimate in soil moisture conditions. To estimate relationships between peat moisture and CH_4 fluxes, we also obtained soil moisture (volumetric water content, %VWC; Table C3) estimates for each chamber using soil moisture sensors (TMS-4 Standard, TOMST s.r.o., Prague, Czech Republic; Wild et al., 2019) at ca. 8 cm depth at ca. 1 m distance from the chambers. The soil moisture values were calibrated to peat using the myClim R package (Man et al., 2023; Wild et al., 2019). To obtain a representative estimate of the central tendency of the dominant peat moisture conditions at each chamber, we used overall chamber medians of daily-aggregated values (non-normal and distributions varied between chambers) from the May–August 2024 and 2025 periods.

2.5 Root and rhizome trait quantification

We cut the frozen peat cores horizontally into minimum 10 cm increments, and then further into four vertical parts (ca. 25 %) using a bandsaw. We randomly chose one of the quarters as a subsample for trait measurements. We thawed the subsamples in a refrigerator over 2–3 d and separated the aboveground vascular plants (see species-specific biomass in Table C4). We picked all living roots (light in color and elastic) and rhizomes (stiff, firm bark) from the subsample using tweezers and jeweler's glasses (2.5× magnification). Due to the very high amount of shrub roots, we took a further subsample (ca. 15 g fresh weight) from which we picked all shrub roots. We cleaned the roots and rhizomes with deionized water and grouped them into herbaceous and shrub PFTs based on a combination of branching patterns, color, and thickness (e.g., shrub roots were generally thinner and had higher branching density than herbaceous roots). The forb *Rubus chamaemorus* was grouped into shrub PFT (e.g., Blume-Werry et al., 2019), due to root identification challenges. We did not separate coarse and fine roots but instead focused on the average root system properties. The picked roots were stored in 70 % ethanol in a refrigerator (4 °C, max. 4 months).

We put the cleaned roots and rhizomes on a transparent tray filled with deionized water and scanned them with an Epson Perfection V700 Photo scanner (Epson, Japan), and analyzed them for root length, surface area and volume using WinRhizo Pro software (v. 2003b, Regent Instruments Inc., Québec, Canada). We used 1400 dpi for shrub roots with

Table 1. Vegetation characteristics at CH_4 flux chambers and corresponding peat coring plots at each permafrost thaw stage (intact, partly and fully thawed). "Core" refers to the plots where peat cores were taken for root and rhizome samples. "Species" includes the species encountered in the vegetation survey (Sect. A1), while vascular plant green area (GA) measurements also included species that were not included in the plant cover measurements. "Total" in GA is the mean vascular plant GA across plots per thaw stage. See vegetation coverage at the plot level in Table C1.

Thaw stage	Species	Mean plant cover (%)		Mean GA ($m^2\ m^{-2}$)	
		Chamber	Core	Chamber	Core
Intact	*Eriophorum vaginatum*	66	41		
	Andromeda polifolia	31	27		
	Vaccinium uliginosum	25	24		
	Empetrum nigrum	17	31		
	Rubus chamaemorus	10	15		
	Betula nana	8	20		
	Carex rotundata	4	0		
	Vaccinium vitis-idaea	0	4		
	Ptilidium ciliare	48	20		
	Sphagnum balticum	32	0		
	Dicranum sp.	8	27		
	Polytrichum sp.	0	20		
	Herbaceous	45	41	0.01	0.01
	Shrub	83	104	0.04	0.02
				Total: 1.98	Total: 3.61
Partly thawed	*C. rotundata*	48	48		
	E. vaginatum	0	42		
	V. oxycoccos	32	28		
	A. polifolia	28	24		
	E. angustifolium	0	16		
	Drosera rotundifolia	0	4		
	S. capillifolium	96	89		
	P. ciliare	0	16		
	Herbaceous	48	72	0.004	0.007
	Shrub	31	27	0.001	0.002
				Total: 0.05	Total: 0.09
Fully thawed	*E. angustifolium*	92	95		
	Equisetum fluviatile	32	44		
	Comarum palustre	4	12		
	S. riparium	26	96		
	Herbaceous	115	128	0.02	0.03
	Shrub	0	0	0.002	0
				Total: 0.32	Total: 0.8

Table 2. Peat characteristics at CH_4 flux chambers and peat coring plots per permafrost thaw stage (intact, partly and fully thawed). "Core" refers to the plots where peat cores were taken for root and rhizome samples. See peat characteristics at the plot level in Table C1. ± denotes one standard deviation of the mean. Peat temperature was measured at 10 cm depth. WTD = water table depth (cm from peat surface), VWC = volumetric water content. Note that WTD for chamber plots is the mean annual WTD across the 2007–2017 period per thaw stage (Crill et al., 2023), and that peat moisture was estimated as overall chamber medians of the 2024–2025 period (see Sect. 2.4).

Thaw stage	Mean peat temperature (°C)		Mean pH		WTD (cm)		Mean active layer depth (cm)		Peat moisture (VWC; %)	
	Chamber	Core	Chamber	Core	Chamber	Core	Chamber	Core	Chamber	Core
Intact	8.6 ± 1.1	8.4 ± 1.6	3.01	3.05	–	–	44.3	54	47.4 ± 11.2	–
Partly thawed	9.25 ± 0.6	9.6 ± 2.1	3.3	3.5	-9.1 ± 4.6	−20.9	>85	>85	76.9 ± 31.3	–
Fully thawed	9.05 ± 0.8	9.6 ± 2.1	4.9	5.5	2.1 ± 4.4	>0	>85	>85	100 ± 0	–

very fine roots (< 1 mm), 600 dpi for herbaceous roots, and 100–300 dpi for rhizomes. When rhizome length and diameter were not accurately calculated by WinRhizo, we measured them manually using ImageJ.JS. Then, all roots and herbaceous rhizomes were dried in 70 °C and woody shrub rhizomes in 102 °C for 4 d and weighed at 0.00001 g precision to obtain root and rhizome dry weight. To obtain a proxy of belowground gas transport potential (i.e., porosity), we calculated root and rhizome tissue density (TD, $g\,cm^{-3}$) by dividing their dry weight by fresh volume. For shrub rhizomes, the TD represents all the different rhizome tissues (e.g., bark, wood and pith). While this is not a direct measurement of the gas transport ability of a woody rhizome, low tissue density could indicate increased rhizome aeration (e.g., pith cavities) and possibly gas transport (Vroom et al., 2022). Specific root length (SRL, $m\,g^{-1}$) was calculated by dividing total root length by its dry weight.

Since peat core depths varied between plots, we standardized root total length ($m\,m^{-2}$), biomass ($g\,m^{-2}$) and surface area (SA, $m^2\,m^{-2}$) to 30 cm depth by taking into account core volume and peat bulk density. We also standardized the traits to 10 cm depth for depth-specific analyses. In addition, shrub root and rhizome biomass, length and SA were scaled from the sub-subsample to the increment level and to 30 cm standardized depth. We calculated root and rhizome volumes by summing diameter-class-specific volumes from WinRhizo (Rose, 2017). All traits were calculated per PFT but also summed (biomass, length, and SA) or biomass-weighted (TD, SRL, diameter) to get an across-PFTs trait estimate. We used the rest of the peat core sample (remaining ca. 75 %) to determine peat bulk density and gravimetric water content (GWC). We thawed the sample in a refrigerator over 2–3 d, removed the aboveground vascular plants, took a 5 ± 0.2 g subsample, and took its fresh and dry weight to obtain bulk density and GWC.

2.6 CH_4 flux measurements

CH_4 flux data were obtained from automated chambers (see data in Table C5). The details of the chamber measurement system in general are presented in Bäckstrand et al. (2008). In 2012, the chambers were replaced to similar design as in Bubier et al. (2003). In each thaw stage (intact, partly and fully thawed), three transparent automated gas flux chambers (basal area: 0.2 m^2, height: 15–75 cm) measured CH_4 and CO_2 every three hours with 5–8 min enclosure time and 5 min air flushing before and after closure (Bäckstrand et al. 2008; Holmes et al. 2022). The CH_4 concentrations were measured with a Los Gatos Research Fast Greenhouse Gas Analyzer (Los Gatos Research Inc, Los Gatos, CA, USA) and the timing control and data acquisition was done with Campbell CR10x data logger (Campbell Scientific, Logan, UT, USA), which was located inside a temperature-controlled cabin. The CH_4 flux data were fit using linear regression. The data were quality-checked using regression diagnostics where CH_4 fluxes outside of significance thresholds at 95 % and 90 % confidence levels were filtered out (Snedecor and Cochran, 1989), as well as manual quality flags that were used to filter out data points affected by known instrumental issues.

We aggregated the higher frequency CH_4 flux data to daily scale by taking the daily CH_4 flux median. Median was chosen to estimate the central tendency of CH_4 fluxes due to skewed and non-normal flux data distributions, and to avoid the disproportionate influence of short-lived high CH_4 flux events that may not be related to belowground plant-mediated CH_4 cycling processes that were the main perspective of this study. Then, we subset the daily-aggregated chamber CH_4 flux data to contain the dates of the productive season in 2023. We defined the productive season as the period between the first and last passing of daily median net ecosystem CO_2 exchange (NEE) past zero, as this can be considered as the plant active season relevant for plant-mediated CH_4 fluxes (Körner et al., 2023). For NEE, we utilized the half-hourly gap-filled NEE (NEE_VUT: estimated across 40 friction velocity threshold realizations for each year according to FLUXNET data processing protocols; quality flags = 3 filtered out) from the ICOS Abisko-Stordalen Palsa Bog (SE-Sto) eddy covariance data processed with FLUXNET standards (Lundin et al., 2023; Pastorello et al., 2020). The resulting productive season used for CH_4 flux data subsetting was 19 May 2023 to 30 August 2023 (Fig. B1). As a background proxy for potential plant carbon substrate provision and plant-mediated gas transport (Knox et al., 2021), we also utilized the half-hourly gap-filled gross primary production (GPP; GPP_NT_VUT: nighttime partitioning at the daily scale and GPP_DT_VUT: daytime partitioning with light response curves at the hourly scale, with variable friction velocity thresholds implemented as an ensemble of 40 friction velocity thresholds by the FLUXNET team; see Lundin et al., 2023 and Pastorello et al., 2020 for details) data from Lundin et al. (2023). However, it is important to note that the EC tower footprint covers only intact and partly thawed stages and does not estimate the NEE and GPP for the fully thawed stage (Łakomiec et al., 2021). To explore the possible diurnal-scale plant-mediated CH_4 transport as a supporting analysis, we also aggregated CH_4 fluxes to the hourly scale using means and medians (Fig. B1).

To explore the variation in the trait-CH_4 flux relationships during the productive season, we calculated CH_4 flux period values (early, middle and peak CH_4 flux) by fitting Gaussian generalized additive models (GAM) with identity link function for daily median CH_4 flux data per chamber with function gam from package mgcv (Wood, 2011, 2017). In the models used for determining CH_4 flux period values, CH_4 flux (response variable) was transformed to approximate normality using inverse hyperbolic sine and date was included as an explanatory variable in a thin plate regression spline. Following an approach similar to TIMESAT (Eklundh and Jönsson, 2015; Jönsson and Eklundh, 2002) and Delwiche et al.

(2021), CH_4 flux period values were calculated as follows: (1) peak CH_4 flux: the highest predicted CH_4 flux value during the productive season, (2) early CH_4 flux: the point where the predicted daily CH_4 flux reached 10 % of the peak CH_4 flux for the first time, and (3) middle CH_4 flux: the point where the predicted daily CH_4 flux reached 50 % of the peak CH_4 flux for the first time. We also calculated the whole season median to represent the whole productive season CH_4 flux estimate per chamber. Since one chamber at intact permafrost thaw stage had GAM $R^2 < 0.1$, we used a moving 7 d median to estimate the early, middle and peak CH_4 season values. See details of GAM fit in Table C6.

2.7 Porewater CH_4 concentration and isotopic measurements

Data of porewater CH_4 and CO_2 concentrations, $\delta^{13}CH_4$ and $\delta^{13}CO_2$ were obtained from Wilson et al. (2026). The porewater samples were collected from the field near the automated flux chambers using stainless steel sippers on 25 and 26 July 2023. The bottom of the sippers is perforated, and a syringe is attached to the top of the sipper via a stopcock. The sipper was inserted in the peat to the desired depth (0–4, 10–14, 20–24, 30–34, 40–44, 50–54, 60–64, 70–74, and 80–84 cm below peat surface) and the syringe was used to carefully draw up 30 mL of porewater. The porewater was then injected into pre-evacuated sealed glass serum vials. Phosphoric acid (1 mL, 10 %) was added to each vial to preserve the samples and ensure that all dissolved inorganic carbon was in the form of dissolved CO_2 in equilibrium with gaseous CO_2. Porewater CO_2 and CH_4 concentrations and isotopes were analyzed simultaneously via headspace analysis, corrected for solubility using Henry's Law, on a Finnigan Mat Delta V Isotope Ratio Mass Spectrometer coupled to a gas chromatograph (Merritt et al., 1995). The analytical uncertainty based on repeated measurements of a standard was < 0.15 ‰ for $\delta^{13}CO_2$ and $\delta^{13}CH_4$ and <5 % for CO_2 and CH_4 concentrations. To obtain a robust estimate of the isotopic fractionation between CO_2 and CH_4, we calculated the isotope fractionation factor (α_C) (e.g., Hodgkins et al., 2014; McCalley et al., 2014) with the following formula:

$$\alpha_C = \frac{\delta^{13}CO_2 + 1000}{\delta^{13}CH_4 + 1000} \quad (1)$$

2.8 Statistical analysis

To confirm the similarity of the peat core ($n = 9$) and CH_4 flux plots ($n = 9$), we used principal component analyses (function PCA from package FactoMineR; Lê et al., 2008), PERMANOVA (function adonis2 from package vegan; Oksanen et al., 2025), and Euclidean distances between plots within thaw stages, using normalized plot herbaceous and shrub plant cover and GA, mean peat temperature and pH (see Fig. B2).

For assessing general differences in daily median CH_4 flux between thaw stages across the productive season, we built linear mixed effects models where CH_4 flux was the response variable and thaw stage (factor) was the explanatory variable, and chamber ($n = 3$ per thaw stage) was the random effect. To account for the normality of residuals and chamber-dependent temporal autocorrelation, we applied inverse hyperbolic sine transformation to CH_4 fluxes, and modeled temporal autocorrelation with autoregressive autocorrelation structure of order 1 (corAR1). We built three different models, where each had either intact, partly or fully thawed permafrost stage as the reference level and fit the model with restricted maximum likelihood and obtained p-values ($\alpha = 0.05$) from Wald t-test. Linear mixed effects models were built with function lme from package nlme (Pinheiro and Bates, 2000; Pinheiro et al., 2023).

Due to the small sample size ($n = 3$ per thaw stage), we were unable to test for statistical differences in belowground traits between thaw stages and sampling depths (traits, porewater CH_4 concentration and isotopic data) and relied on descriptive methods. However, to explore the general direction and strength of the relationships between root and rhizome traits and CH_4 fluxes (early, middle, peak, and season median) across the thaw stages, we used linear regressions with centered and scaled trait and CH_4 flux values. Only models which did not violate assumptions of homoscedasticity, linearity and normality of residuals were included in the analyses. In cases with little trait variation within each thaw stage, pseudoreplication was considered too severe for reliable model estimates, and these model results were not reported. We focused on model R^2, slopes, and model p-values. In cases where linear regressions were unreliable or violated the model assumptions, we explored the relationship strength with Kendall τ correlation coefficients. We acknowledge that the model and correlation estimates can be unstable with small sample size and thus use them as descriptive exploratory tools for estimating the changes in the general directions of the trait-CH_4 flux relationships across thaw stages during the productive season. All data processing and statistical analyses were conducted in R v4.5.1 (R Core Team, 2025).

3 Results

3.1 More herbaceous roots with decreasing tissue density

Belowground traits varied between thaw stages, and the biomass-weighted traits followed shifts from shrub- to herbaceous-dominated plant communities (Fig. 2, Table C1). Summed root biomass and surface area (SA) were 22.2× and 17.0× lower, respectively, at the fully thawed than intact stage, but herbaceous root biomass (mean: 238.3 ± 172 g m^{-2}) and SA (mean: 19.9 ± 13 m^2 m^{-2}) were highest at partly thawed stage. Total shrub root length reached a very high mean of 178.62 $km\,m^{-2}$ and a maximum of 199.7 $km\,m^{-2}$ in the intact stage, substantially higher values than for herbaceous roots (mean: 19.79 $km\,m^{-2}$ and max 33.33 $km\,m^{-2}$ in the partly thawed stage) (Fig. B4). While shrub rhizome biomass and SA decreased from intact to partly thawed stage, herbaceous rhizomes showed an opposite trend (e.g., mean SA 0.13 ± 0 to $3.41 \pm 0.08\,m^2\,m^{-2}$, 26-fold increase). Notably, herbaceous root and rhizome tissue density (TD) were 1.5× and 2.4× lower in fully thawed than in intact permafrost, respectively (mean ± standard deviation root 0.004 ± 0.0008 to $0.003 \pm 0.0002\,g\,cm^{-3}$; rhizome $0.2\,g\,cm^{-3} \pm 0$ to $0.08 \pm 0.01\,g\,cm^{-3}$), and these decreases were reflected in the biomass-weighted values (root: 1.5× lower, rhizome: 7.4× lower). While specific root length (SRL) was highest at partly thawed stage (mean shrub $193.6 \pm 32\,m\,g^{-1}$, 1.4× higher than at intact; mean herbaceous $71.6 \pm 35\,m\,g^{-1}$, 2.3× and 1.2× higher than at intact and fully thawed, respectively), the biomass-weighted means showed a 2.2-fold decrease from intact to fully thawed stage.

Most of the root biomass was found in the top 10 cm for shrub (coefficient of variation CV and mean for intact: 69 %, $766.0 \pm 155\,g\,m^{-2}$; partly thawed: 67 %, $65.1 \pm 28\,g\,m^{-2}$) and herbaceous PFTs (CV and mean intact: 56 %, $17.5 \pm 9\,g\,m^{-2}$, partly thawed: 45 %, $86.4 \pm 89\,g\,m^{-2}$, fully thawed: 73 %, $27.7 \pm 20\,g\,m^{-2}$) (Fig. B3). Shrub roots reached the maximum total length of 167.3 $km\,m^{-2}$ at top 10 cm at the intact stage (Fig. B4). SRL and root TD varied less with depth across thaw stages (max CV SRL: 51 %, TD: 31 %; partly thawed herbaceous). All herbaceous rhizomes were present in the top 10 cm (mean biomass intact: $11.5 \pm 0\,g\,m^{-2}$, partly thawed: $101.9 \pm 109\,g\,m^{-2}$, fully thawed: $107.8 \pm 12\,g\,m^{-2}$, Fig. B5). Most of the shrub rhizomes were located in the top 10 cm (CV and mean biomass intact: 78.5 %, $392.4 \pm 227\,g\,m^{-2}$; partly thawed: 66.7 %, $93.9 \pm 15\,g\,m^{-2}$), but they were also found in 10–20 cm depth (mean intact: $109.4 \pm 154\,g\,m^{-2}$, partly thawed: $28.9 \pm 0\,g\,m^{-2}$).

3.2 Root tissue density, specific root length and diameter correlated best with CH_4 fluxes

The relationships between root traits and CH_4 fluxes (CH_4 flux difference between intact, partly and fully thawed $p<0.01$, fully and partly thawed $p>0.05$, Sect. A2) differed between PFTs but with little temporal variation. Increasing root TD was associated with decreasing CH_4 flux for herbaceous (min standardized regression beta coefficient, β at peak CH_4, max β at middle CH_4) and shrub PFTs (min β at middle CH_4, max β at CH_4 season median) (Fig. 3). Shrub root diameter had negative (min β at early CH_4, max β at CH_4 season median) and SRL positive (min β at peak CH_4, max β at CH_4 season median) associations with CH_4 fluxes. In general, the direction and strength of the relationships between root traits and CH_4 fluxes did not vary strongly across CH_4 flux season values (Figs. 3, B6).

PFTs combined, all root traits except diameter showed negative trends, where the strongest relationships were for root TD (min β at early and peak CH_4, max β at middle CH_4) (Fig. 3). In addition, summed root biomass and SA showed relatively strong negative relationships, with biomass showing slightly stronger negative relationships than SA (biomass: min Kendall's τ at early CH_4, max τ at middle CH_4; SA: min τ at early CH_4, max τ at peak CH_4) (Fig. B6).

Herbaceous and shrub rhizome traits showed contrasting relationships with CH_4 fluxes (Figs. 4, B7). Herbaceous rhizome biomass and SA showed positive relationships with CH_4 fluxes, with stronger trends for SA (SA: min β at peak CH_4, max β at CH_4 season median). Increases in herbaceous rhizome diameter were also associated with slightly higher CH_4 fluxes (min τ at early to peak CH_4, max τ at CH_4 season median). In contrast, shrubs had negative trends between rhizome biomass and CH_4 fluxes (min τ at early, middle and season median CH_4, max τ at peak CH_4; Fig. B7). While summed rhizome SA did not show clear trends (Fig. 4), higher summed rhizome biomass was associated with lower CH_4 fluxes (nonsignificant β at early CH_4, max β at peak CH_4; Fig. B7), while the relationship between rhizome diameter and CH_4 flux was positive (min τ at early and middle CH_4, max τ at peak and season median CH_4) (Fig. 4).

In comparison with belowground trait relationships, CH_4 fluxes were weakly and positively correlated with plant green area (GA) and peat temperature (Fig. B8). GA, which also did not show clear trends with permafrost thaw (Fig. B9), showed no clear relationships with CH_4 fluxes (max τ for shrub at peak CH_4; Fig. B8). Peat temperature did not show clear relationships with CH_4 fluxes (max τ at middle CH_4; Fig. B8). However, increases in peat moisture were generally associated with higher CH_4 fluxes ($\tau = 0.73$ at early, middle and season median CH_4; Fig. B8), with the highest CH_4 fluxes occurring in the wettest plots in the fully thawed stage (median VWC = 100 %), and lowest CH_4 fluxes in the drier intact stage (median VWC = 43.4 %).

4 Discussion

Permafrost thaw in subarctic peatlands can lead to substantial alterations in peatland hydrology, vegetation composition and carbon cycling, and higher CH_4 emissions with higher water table level and more anoxic conditions belowground (Johnston et al., 2014; Knoblauch et al., 2018; Turetsky et al., 2014; Varner et al., 2022). These trends were visible in the Stordalen Mire where CH_4 fluxes increased significantly from intact to fully thawed permafrost stage with maximum CH_4 fluxes in August (Sect. A2 and Fig. B10), and porewater CH_4 concentrations increased with depth and CH_4 production slightly shifted from hydrogenotrophic to acetoclastic methanogenesis (Fig. B11), as has been observed pre-

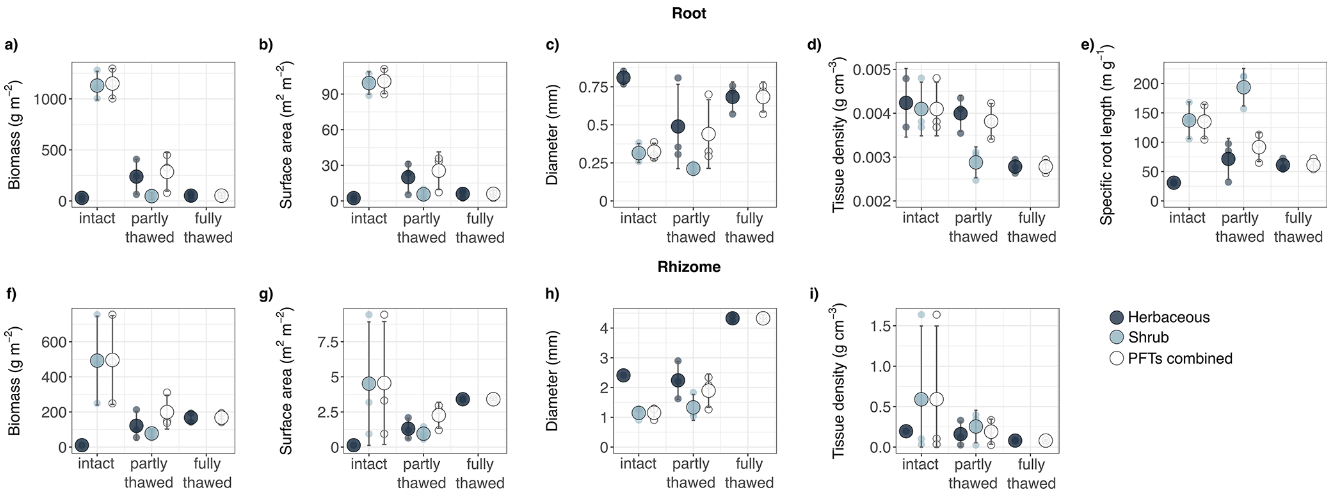

Figure 2. Belowground traits varied between thaw stages. Root traits **(a–e)** are shown in the top row and rhizome traits **(f–i)** in the bottom row. Large points represent group means, small points plot-scale measurements, and error bars ±1 standard deviation of the mean. The colors represent plant functional types (PFT; dark grey: herbaceous, light grey: shrub, white: PFTs combined). Trait values for combined PFTs were summed herbaceous and shrub values **(a, b, f, g)** or biomass-weighted means between herbaceous and shrub PFTs **(c–e, h, i)**.

viously at Stordalen (Hodgkins et al., 2014; Holmes et al., 2022; McCalley et al., 2014; Perryman et al., 2020; Varner et al., 2022). Shifts from hydrogenotrophic to acetoclastic methanogenesis can indicate increased root exudate-driven CH_4 production (see Sect. 4.2) (Saarnio et al., 2004; Ström et al., 2003).

The increased CH_4 fluxes with permafrost thaw in Stordalen are driven by a complex network consisting of drivers such as higher water table level and increased anoxia (Holmes et al., 2022; Malhotra and Roulet, 2015), higher peat temperatures at the end of growing season (Mollenkopf et al., 2026), increased labile carbon availability (Hodgkins et al., 2014; Holmes et al., 2022; Hough et al., 2022), shifts in microbial communities from hydrogenotrophic to acetoclastic methanogens (McCalley et al., 2014), and increasing dominance and productivity of graminoid vegetation (Christensen et al., 2004; Johansson et al., 2006; Malhotra and Roulet, 2015; Öquist and Svensson, 2002; Varner et al., 2022). For the first time in Stordalen and, to our knowledge, in other thawing permafrost peatlands, we explored the effect of belowground plant traits on CH_4 fluxes. In general, root and rhizome traits reflected plant community transitions and were consistent with an increase in plant-mediated transport of acetoclastically-produced CH_4.

4.1 Root and rhizome traits reflect plant community shifts along permafrost thaw gradient

The vegetation composition in Stordalen follows the changing hydrology and soil nutrient availability. The vegetation shifts from shrub-dominated (intact stage; e.g., *R. chamaemorus*, *B. nana*, and *E. nigrum*) palsas to increasingly more graminoid- and *Sphagnum*-dominated semi-wet bogs (partly thawed; e.g., *V. oxycoccos*, *C. rotundata*, and *S. capillifolium*) and wet fens (fully thawed; *E. angustifolium*, *E. fluviatile*, and *S. riparium*; Tables C1 and C2) (Hough et al., 2022; Johansson et al., 2006; Malhotra and Roulet, 2015; Varner et al., 2022). Following these vegetation transitions, plant traits reflect plant adaptation to the changing environmental conditions (Dong et al., 2020; Moor et al., 2017; Pan et al., 2019). While studying plant trait variation and its influence on ecosystem functioning often requires species-specificity to capture changes in diversity (Kichenin et al., 2013; Violle et al., 2014) and separation into fine and coarse root fractions (Freschet et al., 2021b; McCormack et al., 2015), CH_4 flux models often utilize PFTs which have been found to adequately represent the collective trait effects on CH_4 fluxes in peatlands (Gray et al., 2013; Laine et al., 2022). Thus, we here focused on root and rhizome traits at the PFT (herbaceous and shrub) level. This approach provides empirical constraints on plant-mediated carbon substrate provision and CH_4 transport that can inform parameterization and sensitivity analyses in process-based wetland CH_4 models, such as LPJ-GUESS (Smith et al., 2001, 2014), and HIMMELI (Raivonen et al., 2017).

Following vegetation community shifts, most belowground shrub biomass and total length were found in the intact stage while herbaceous biomass increased from intact to fully thawed stage. The shrub root biomass values were lower than previous estimates for *R. chamaemorus*, *E. nigrum* and *A. polifolia* (total $> 2000\,g\,m^{-2}$) in Stordalen (Wallén, 1986), but are much higher than recent belowground biomass estimates ($\sim 280\,g\,m^{-2}$; Hough et al., 2022). In addition, Hough et al. (2022) reported higher total root biomass at the fully thawed ($\sim 218\,g\,m^{-2}$) than partly thawed stage ($\sim 146\,g\,m^{-2}$), whereas this study showed the oppo-

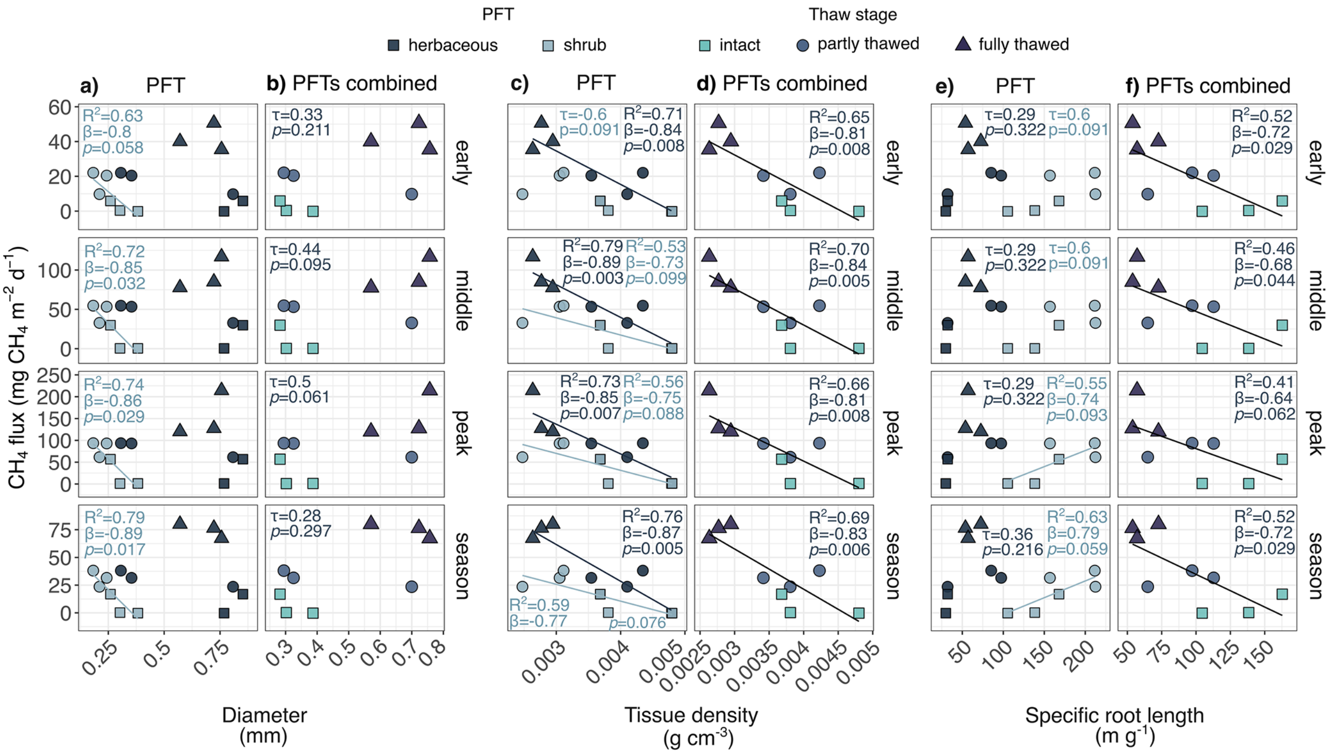

Figure 3. Root tissue density, diameter, and specific length showed strongest relationships with CH_4 fluxes. **(a–b)** Relationships between root diameter and CH_4 fluxes (early, middle, peak and season) per plant functional type (PFT; **a**) and across PFTs (biomass-weighted means; **b**). **(c–d)** Relationships between root tissue density and CH_4 fluxes per PFT **(c)** and across PFTs (biomass-weighted means; **d**). **(e–f)** Relationships between specific root length and CH_4 fluxes per PFT (e) and across PFTs (biomass-weighted means; **f**). In **(a)**, **(c)** and **(e)**, dark gray: herbaceous plants, light gray: shrubs. In **(b)**, **(d)** and **(f)**, light blue rectangle: intact, grey circle: partly thawed, dark purple triangle: fully thawed stage. In all plots **(a–f)**, lines represent linear regression for visualization, while R^2 and standardized effect size/slope (β) are based on linear regressions with centered and scaled trait and CH_4 flux values (lines, R^2 and β are only shown when $R^2 > 0.2$, model $p < 0.1$, and the linear regression model assumptions were met). Kendall's τ is shown for relationships where linear regression model assumptions were not met and $\tau \geq 0.2$ (note that due to the low sample size, p-values should be interpreted with caution). See relationships between root biomass, surface area and CH_4 fluxes in Fig. B6.

site (Fig. 2). These differences could arise from different root biomass standardization and sampling methods, a problem highlighted in root ecology (Freschet et al., 2021a): Wallén (1986) calculated fine root biomass based on ^{14}C activity which can lead to overestimations (Wallén, 1986), while Hough et al. (2022) sampled a larger area (625 cm^2) than in our study ($\sim$ 79 cm^2), leading to differences particularly at the fully thawed stage, where graminoids root more vertically than laterally. In addition, our root samples may have consisted of a different mix of species than in Hough et al. (2022), which together with the low sample size, may have influenced these results. Nonetheless, root biomass decreased by depth, as is common particularly for shrubs (Iversen et al., 2015; Wallén, 1986). As we observed *R. chamaemorus* roots up to 30 cm depth, similar to Wallén (1986) and Keuper et al. (2017) in Stordalen and by Metsävainio (1931) in Finnish peatlands, and as *E. angustifolium* and *E. fluviatile* roots have been found at 40 cm depth (Iversen et al., 2015; Metsävainio, 1931; Shaver and Billings, 1975), the maximum rooting may occur deeper than our sampling depth (ca. 30 cm). In general, these findings, and particularly the remarkably high total shrub root length values, showed that permafrost-affected peat soils are rich in plant roots and likely contribute to the carbon cycling of these ecosystems (Bardgett et al., 2014; Iversen et al., 2015).

Variation in tissue density (TD) and specific root length (SRL) (Fig. 2) with thaw suggest changes in plant gas transport and resource acquisition. Increasing soil moisture with thaw (via higher water table level; Table 2 and Fig. B8) and subsequent aerenchyma formation (e.g., Jackson and Armstrong, 1999) may have decreased TD. The increase in herbaceous rhizome SA may reflect greater aerenchyma proportion, confirming rhizome SA as a proxy for plant gas transport capacity. SRL was highest and root diameter lowest at the partly thawed stage, which could reflect increased resource acquisition particularly for shrubs (Bergmann et al., 2020), but further research with larger sample sizes is needed to investigate the potential changes in shrub resource acqui-

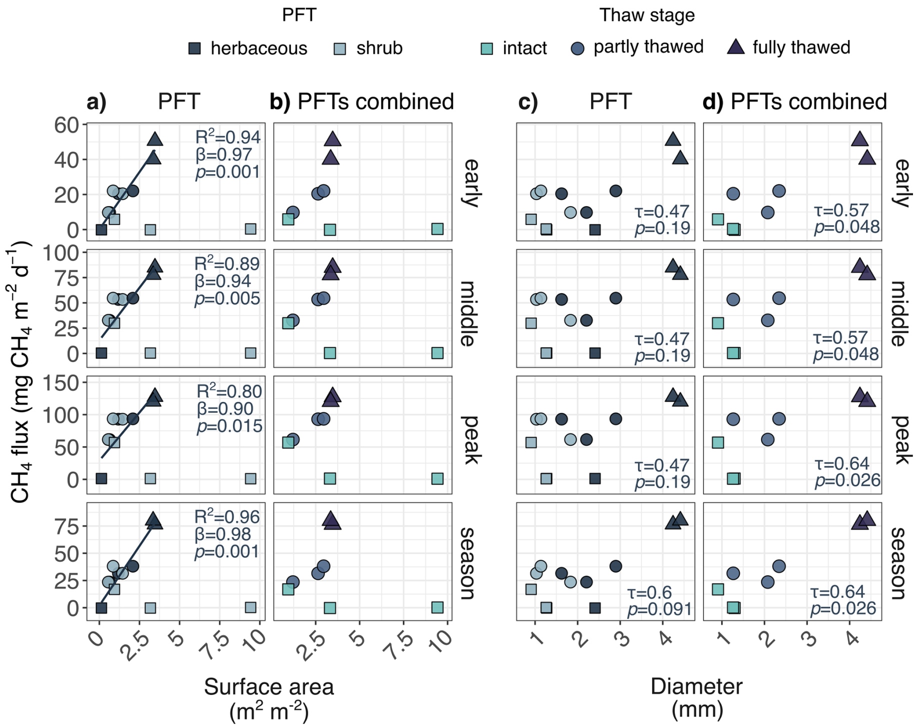

Figure 4. Relationships between rhizome traits and CH_4 fluxes were strongest for surface area and diameter. Columns **(a–b)** Relationships between rhizome surface area and CH_4 fluxes (early, middle, peak and season; rows) per plant functional type (PFT; **a**) and across PFTs (summed; **b**). Columns **(c–d)** Relationships between rhizome diameter and CH_4 fluxes per PFT **(c)** and across PFTs (biomass-weighted means; **(d)**. In **(a)** and **(c)**, dark gray color represents herbaceous plants while light gray represents shrubs. In **(b)** and **(d)**, light blue rectangles represent the intact permafrost, dark blue circles represent the partly thawed stage, and dark purple triangles represent the fully thawed stage. Lines represent linear regressions for visualization, while R^2 and standardized effect size/slope (β) are based on linear regressions with centered and scaled trait and CH_4 flux values (lines, R^2 and β are only shown when R^2>0.2, model p<0.1, and the linear regression model assumptions were met). Kendall's τ is shown for relationships where linear regression model assumptions were not met and τ>0.2. See relationships between rhizome biomass, tissue density and CH_4 fluxes in Fig. B7.

sition . As the peat C / N ratio is highest in the partly thawed stage (Hodgkins et al., 2014), the high SRL may reflect low N availability, shifts in species and species-specific resource acquisition (Hewitt et al., 2019; Keuper et al., 2017). However, as fine root SRL is more meaningful for resource acquisition (Bergmann et al., 2020; McCormack et al., 2015), our results based on the whole root system provide only a rough estimate. Nonetheless, 99% of total shrub root length was < 2 mm in diameter (vs. 31 %, 75 %, and 63 % in intact to fully thawed stages, respectively, for herbaceous), and thus within the traditional fine root definition (McCormack et al., 2015).

4.2 Belowground traits reflect increasing plant-mediated CH_4 transport

The increasing peat moisture and associated changes in belowground plant traits contributed to the increasing CH_4 fluxes along the permafrost thaw gradient. Given our exploratory results (see Sect. 3.2 and Fig. B8) and earlier studies conducted at Stordalen (Holmes et al., 2022; Malhotra and Roulet, 2015), the increasing peat moisture was likely one of the primary drivers of the increasing CH_4 fluxes along the thaw gradient. However, due to the low sample size we were unable to separate the effects of plant traits and peat moisture in multivariate models, and larger sample sizes are recommended to analyze the interactions between peat moisture and plant belowground traits in future studies. Nonetheless, the univariate relationships between plant belowground traits and CH_4 fluxes indicated (1) maintained carbon substrate provision and (2) increasing plant-mediated CH_4 transport across the permafrost thaw gradient. In Stordalen, permafrost thaw has led to increasing plant-derived labile carbon availability and acetoclastic methanogenesis (Hodgkins et al., 2014; Holmes et al., 2022; McCalley et al., 2014; Ström and Christensen, 2007), but plant-mediated CH_4 transport has so far been mostly assumed based on literature and plant aboveground characteristics and activity, such as number of shoots and gross photosynthetic rates (Öquist and Svensson, 2002).

Shrub roots suggested increasing carbon substrate provision. The higher CH_4 fluxes with increasing shrub SRL (and smaller diameter; Bergmann et al., 2020) may be related to increased root exudation (Guyonnet et al., 2018; Wen et al., 2022). The negative root TD-CH_4 flux relationships support this, as higher root TD may be associated with lower root exudation (Wen et al., 2022). In contrast, herbaceous SRL was weakly associated with CH_4 fluxes, possibly due to decoupling of root exudation and SRL in some Cyperaceae species in nutrient-limited environments (Wen et al., 2022), and the SRL also including coarse roots (Picon-Cochard et al., 2012). However, based on the ^{13}C-depleted $\delta^{13}CH_4$ and high α_C, hydrogenotrophic methanogenesis may have dominated in the topmost peat, and most of the dissolved, less bioavailable organic carbon possibly originated from *Sphagnum* in the partly thawed stage (Hodgkins et al., 2014; McCalley et al., 2014; Mondav et al., 2014; Wilson et al., 2022). Nonetheless, the lower α_C, more enriched $\delta^{13}CH_4$, and higher CH_4 concentrations below the root sampling depth (30–44 cm) indicated acetoclastic methanogenesis (Fig. B11) (e.g., by *Methanosarcina*; McCalley et al., 2014), possibly fueled by root exudates (Saarnio et al., 2004; Ström et al., 2003; Ström and Christensen, 2007). Indeed, based on photosynthetic rates, the partly thawed stage has been estimated to have more labile carbon for methanogenesis (Öquist and Svensson, 2002), and *E. angustifolium* and *E. vaginatum* have high potential root exudation rates in Stordalen (Ström and Christensen, 2007) and graminoid root exudation rates can exceed that of shrubs in the partly and fully thawed stages (Mollenkopf et al., 2026). Based on these previous studies, it is possible that the SRL based on the whole heterogeneous root system did not represent the potential root exudation accurately for herbaceous plants. Thus, roots (including herbaceous) may have exuded labile carbon, but with shrubs having a lesser effect on the net CH_4 flux.

Herbaceous plant coverage increased with thaw, which was reflected in traits indicating plant-mediated CH_4 transport (Fig. 2, Table C1). Higher herbaceous rhizome SA was positively associated with greater CH_4 fluxes, which, together with the positive diameter-CH_4 flux trends, could indicate enhanced CH_4 transport via larger and more porous rhizomes (Määttä and Malhotra, 2024). Rhizome-mediated CH_4 transport could be particularly relevant for plants with pressurized gas transport, such as *Equisetum* spp., where pressure gradients between the atmosphere, leaves, and rhizomes can drive CH_4 emission via old leaves and broken stems (Vroom et al., 2022). As shrub rhizomes were not associated with CH_4 fluxes (Figs. 4, B8), they may not drive plant–mediated CH_4 cycling in Stordalen, though standardized measurements of, e.g., rhizome length and biomass are needed to confirm this (e.g., Freschet et al., 2021a).

Plant-mediated CH_4 transport may have been pronounced in the fully thawed stage with high peat moisture, herbaceous plant coverage, and low porewater CH_4 concentrations (Table C1 and Figs. B8, B11), indicating plant CH_4 uptake. As low root and rhizome TD indicates higher porosity (Ye and Ryser, 2022), the negative relationships between root TD and CH_4 flux suggest increased plant-mediated CH_4 transport in response to increasing peat moisture. The isotopic evidence (heavier $\delta^{13}CH_4$ and lower α_C) may further suggest plant-mediated transport of acetoclastically-produced CH_4 at the fully thawed stage (Chanton, 2005). This supports previous findings of higher herbaceous shoot numbers increasing CH_4 flux in the fully thawed stage (Öquist and Svensson, 2002). However, a recent study conducted in the same productive season found that 30 % of the CH_4 flux in the fully thawed stage consisted of graminoid plant-mediated CH_4 transport and the rest of CH_4 production stimulated by graminoid root exudation, while in the partly thawed stage plant-mediated CH_4 transport dominated the CH_4 flux (80 %) (Mollenkopf et al., 2026). Nonetheless, both this and the study by Mollenkopf et al. (2026) together suggest increased herbaceous plant-mediated CH_4 transport and carbon substrate provision in the fully thawed stage. In Stordalen, most of the plant-mediated CH_4 transport likely occurs via diffusion, typical for *Carex* spp., *E. angustifolium*, and *E. vaginatum* (e.g., Ge et al., 2025; Noyce et al., 2014; Bhullar et al., 2013). CH_4 diffusion may be more efficient through *E. angustifolium* with low root branching in the fully thawed than at partly thawed stage with more densely rooted *Carex* species (Schimel, 1995; Shaver and Billings, 1975; Table C1). However, pressurized CH_4 transport via *Equisetum fluviatile* (in fully thawed stage) could be negligible and requires further investigation as we did not separate the belowground material into species (Hyvönen et al., 1998; Kankaala and Bergström, 2004). As graminoid (e.g., *E. angustifolium*) roots have low bioavailability in the fully thawed stage (Hough et al., 2022), and root porosity and decomposability may be decoupled (Pan et al., 2019; Ye and Ryser, 2022), the low root and rhizome TD were unlikely to lead to increased decomposition and carbon substrate provision.

Simultaneously to plant-mediated CH_4 transport, herbaceous roots may have enhanced rhizospheric CH_4 oxidation. Previous studies at Stordalen have reported shifts in methanotroph communities with thaw as well as an increase in CH_4 consumption, which may result from greater plant-mediated rhizospheric oxidation (i.e., more O_2 transport with lower root TD) and acetoclastic methanogenesis (Perryman et al., 2020; Singleton et al., 2018). In addition, *Sphagnum* spp. can host methanotrophic CH_4-consuming bacteria (e.g., Larmola et al., 2010; Putkinen et al., 2014), which may have increased CH_4 consumption in the more O_2-rich intact and partly thawed stages dominated by *S. balticum* and *S. capillifolium*, with intact stage chambers possibly having higher CH_4 consumption rates than peat cores with no *S. balticum* (Table 1). However, the average $\delta^{13}CH_4$ emitted from the partly thawed chamber plots was -79.6 ± 0.9 ‰ in 2011, similar to or ^{13}C-depleted relative to the porewater CH_4 at the same sites, indicating little CH_4 oxidation (McCalley et al., 2014). Thus, the heavier $\delta^{13}CH_4$ in the fully and partly thawed stages could also indicate increased CH_4 oxidation close to O_2-rich air at the topmost peat or in the oxidized rhizosphere at ca. 20–44 cm depth (Perryman et al., 2020; Singleton et al., 2018). In addition, during CH_4 oxidation, methanotrophs preferentially consume lighter $^{12}CH_4$, enriching the remaining CH_4 pool in ^{13}C while producing isotopically light CO_2 (Whiticar, 1999). However, isotopically light CO_2 could also indicate less methanogenesis instead of increased methanotrophy, and rhizospheric $\delta^{13}CH_4$ enrichment can also result from faster plant $^{12}CH_4$ uptake and increased plant-mediated CH_4 transport (Chanton, 2005). Thus, based on the lower α_C (i.e., maintained acetoclastic methanogenesis) at 20–44 cm depth, and the strongly negative relationships between root TD and CH_4 fluxes (i.e., decreasing amount of aerenchyma is related with lower CH_4 fluxes and vice versa), it seems that the CH_4-oxidizing effect of herbaceous plants particularly in the fully thawed stage is overshadowed by increased carbon provision for methanogenesis and enhanced plant-mediated CH_4 transport.

4.3 Belowground trait relationships with CH_4 fluxes did not vary within the productive season

The relationships between the static belowground traits and CH_4 fluxes (early, middle, peak, and season median) did not vary strongly within the productive season. This may result from the lack of temporal root and rhizome sampling within the productive season. However, as an exploratory analysis, our results may indicate higher herbaceous plant-mediated CH_4 transport at the middle CH_4 flux period (Fig. 3). In contrast to our hypotheses, shrub root traits were more strongly related (i.e., higher linear regression β and R^2) with peak and season median CH_4 fluxes whereas herbaceous root (TD) and rhizome (SA) traits were strongly related with CH_4 fluxes throughout the season. This could result from the lack of temporal sampling, but also from low temporal variation in coarse root diameter (diameter is used for determining root TD; see Sect. 2.5) (Picon-Cochard et al., 2012), possibly contributing to the lack of temporal trends between root diameter and CH_4 fluxes. The root TD-CH_4 flux relationships may have reflected higher CH_4-transporting herbaceous root biomass at the middle and peak CH_4 flux period (July–September; Shaver and Billings, 1977) instead of temporal TD and diameter variation. Indeed, diffusive plant-mediated CH_4 transport via *Carex* spp. could be high during the mid- and peak-growing season, as for example *Carex rostrata* (present at the partly and fully thawed stages but not captured by our aboveground measurements; see Table C1 and e.g., Hough et al., 2022) has been found to transport most CH_4 at high summer and early autumn (Ge et al., 2025; Noyce et al., 2014). Furthermore, a study conducted in Stordalen during the same productive season found that plant-mediated CH_4 transport and carbon substrate provision via graminoids was highest in August and September, further confirming these results (Mollenkopf et al., 2026). In addition, gross primary production (GPP), a proxy for plant-mediated gas transport (Knox et al., 2021), peaked in July and August (max monthly medians: 3.87 and 2.79 µmol CO_2 m^{-2} s^{-1}, respectively; Fig. B1). Concurrently, CH_4 fluxes at the partly and fully thawed stages were slightly higher during nighttime (Fig. B1). Both of these GPP and CH_4 flux trends could further indicate seasonally (via higher herbaceous plant biomass) and diurnally- (via stomatal opening and closure) varying plant-mediated CH_4 transport . However, as GPP and CH_4 flux peaks did not coincide in the same hourly time periods, further research into diel CH_4 fluxes and plant-mediated CH_4 transport is needed (Fig. B1) (Knox et al., 2021). As *Carex*, *Eriophorum* and *Equisetum* rhizomes are perennial (Husby, 2013; Shaver, 1976), the pre-existing rhizomes may have contributed to CH_4 transport particularly in the beginning of the productive season with active root growth (esp. *E. angustifolium*; Shaver and Billings, 1975), resulting in strong rhizome-CH_4 flux relationships (Figs. 4, B7).

Our exploratory analyses suggested stronger shrub carbon substrate provision (SRL and diameter) at peak CH_4 flux period and across the season (season median; Fig. 3). While uncertain due to the static trait values, these results could be supported by the greater GPP at the intact and partly thawed stages (Łakomiec et al., 2021) in July and August (Fig. B1), as GPP can also be a proxy for root exudation and correlates with increased wetland CH_4 emissions (Knox et al., 2021). In addition, in a separate study within the same productive season, shrubs and graminoids were found to release more root-derived carbon at the end of the season (Mollenkopf et al., 2026). However, the biomass-weighted SRL trends were negative, which could result from species-specific SRL variation and the heterogeneous herbaceous root system (Gao et al., 2024; Picon-Cochard et al., 2012). The stronger negative trends in the beginning of the productive season may arise from increased plant carbon investment into herbaceous root growth in comparison with shrubs (Billings et al., 1978; Kummerow and Russell, 1980; Wang et al., 2016). However, within the intact and partly thawed stages and in a mixture of herbaceous and shrub plants, the SRL-CH_4 flux trends could in fact be positive (Fig. 3), but inferential statistics with larger sample sizes per thaw stage are required to investigate this further. As temporal variation in SRL and its relationship with root exudation can be negligible throughout growing season (Gao et al., 2024) and studies in (sub)arctic peatlands are lacking (Iversen et al., 2015), the negative trends between biomass-weighted SRL and CH_4 fluxes across the thaw gradient remain uncertain.

Taken together, the temporal variation in root and rhizome traits may have contributed to CH_4 fluxes but belowground trait sampling with larger sample sizes throughout the productive season is needed to investigate these relationships further. Given the uncertain herbaceous SRL and root diameter relationships, future studies could benefit from separating the roots into coarse and fine fractions, measuring the associated root exudation rates, and utilizing minirhizotrons (Iversen et al., 2012; Phillips et al., 2008) to disentangle the temporal variation in root carbon substrate provision and CH_4 transport across the permafrost thaw gradient.

5 Conclusions

Permafrost thaw alters peatland methane (CH_4) fluxes through changes in soil anoxia, nutrient and labile carbon availability, and vegetation composition. Here, we explored the relationships between plant root and rhizome traits and CH_4 fluxes along a permafrost thaw gradient in a subarctic peatland. The belowground traits reflected vegetation community shifts along the thaw gradient from shrub- to herbaceous-dominated, with decreasing shrub belowground biomass and root tissue density with increasing thaw. Root tissue density showed a strong negative correlation with CH_4 fluxes, and increasing herbaceous rhizome surface area was associated with higher CH_4 fluxes. These relationships indicated increasing plant-mediated CH_4 transport with thaw, which was supported by lower pore water CH_4 concentrations in the fully thawed stage. Simultaneously, shrub specific root length (SRL) was positively, and root diameter negatively related with CH_4 fluxes, suggesting increased labile carbon substrate provision for acetoclastic methanogenesis. The relationships did not vary strongly during the productive season, but this was likely a result of the static belowground trait data, warranting further temporal trait sampling.

We encourage further observational and experimental research particularly into the relationships between root and rhizome tissue density, SRL and CH_4 fluxes. The observed relationships could be further investigated with larger sample sizes and by combining temporal root trait sampling, root separation into fine and coarse fractions, and root exudation measurements to especially quantify the relationship between SRL and root exudation. Nonetheless, as root and rhizome trait data are scarce particularly from permafrost peatlands, and as the contribution of roots and rhizomes on plant-mediated CH_4 fluxes is understudied, this study provided valuable belowground proxies for plant-mediated CH_4 transport and fluxes. These proxies can inform future observational and experimental studies, as well as process-based wetland models by improving parameterization particularly related to plant-mediated CH_4 transport and helping fill gaps in our understanding of plant-mediated CH_4 cycling.

Appendix A: Texts

A1 Vegetation surveys

To evaluate the similarity between the CH_4 flux chamber plots and peat core plots, we conducted vegetation surveys using the point-intercept method on 19–23 July 2023. We used a $1.01\,m^2$ survey grid divided into 36 subquadrats ($16.8\,cm \times 16.8\,cm = 0.03\,m^2$) and 25 intercept points. We lowered a dowel (60 cm long, 0.5 cm diameter) at each intercept point and noted the presence (i.e., "hit") of each vascular plant and moss species that the dowel touched. At the peat core plots, the grid was always positioned towards northeast from the measurer and with the core in the middle of the grid. At the chamber plots, the grid was positioned so that the chamber collar was approximately in the middle of the northeast edge of the grid (due to the chamber structure, we were unable to set the collar perfectly in the middle of the grid). The ground cover (e.g., litter and water), plant and moss species were surveyed separately. For ground cover data, if the measuring dowel hit multiple classes, only the class that touched the dowel first was recorded. Species and ground cover percentages were obtained by dividing the sum of hits for a species, vegetation (herbaceous, shrub and moss) or ground cover class by the total number of intercepts ($n = 25$), multiplied by 100.

A2 Chamber CH_4 flux analyses

The fully thawed permafrost stage had the highest CH_4 flux (season median = 75.2 mg $CH_4\,m^{-2}\,d^{-1}$, IQR = 60.6 mg $CH_4\,m^{-2}\,d^{-1}$), followed by partly thawed stage (season median = 30.0 mg $CH_4\,m^{-2}\,d^{-1}$, IQR = 33.6 mg $CH_4\,m^{-2}\,d^{-1}$) but CH_4 fluxes at partly and fully thawed stages did not differ significantly ($p>0.05$). Intact stage had the lowest CH_4 fluxes (season median = 0.3 mg $CH_4\,m^{-2}\,d^{-1}$, IQR = 2.1 mg $CH_4\,m^{-2}\,d^{-1}$, $p<0.01$). At all thaw stages, CH_4 flux increased from the beginning to the end of the productive season: the maximum monthly median CH_4 fluxes were observed in August (max CH_4 flux: fully thawed 375.9 mg $CH_4\,m^{-2}\,d^{-1}$, partly thawed 160.4 mg $CH_4\,m^{-2}\,d^{-1}$, intact 96.4 mg $CH_4\,m^{-2}\,d^{-1}$), while minima were reached in June at intact (−1.9 mg $CH_4\,m^{-2}\,d^{-1}$) and fully thawed (10.3 mg $CH_4\,m^{-2}\,d^{-1}$) stages, and in May at the partly thawed stage (2.0 mg $CH_4\,m^{-2}\,d^{-1}$). In general, variation in CH_4 flux (coefficient of variation, CV) was larger between thaw stages (94 %; May: 109 %, August: 79 %) than within them but the intact stage had large within-stage CH_4 flux variation (148 %) which increased from May and June (125 % and 124 %, respectively) to August (165 %), while the other stages had relatively low variation (partly thawed: 37 %, fully thawed: 29 %).

Appendix B: Figures

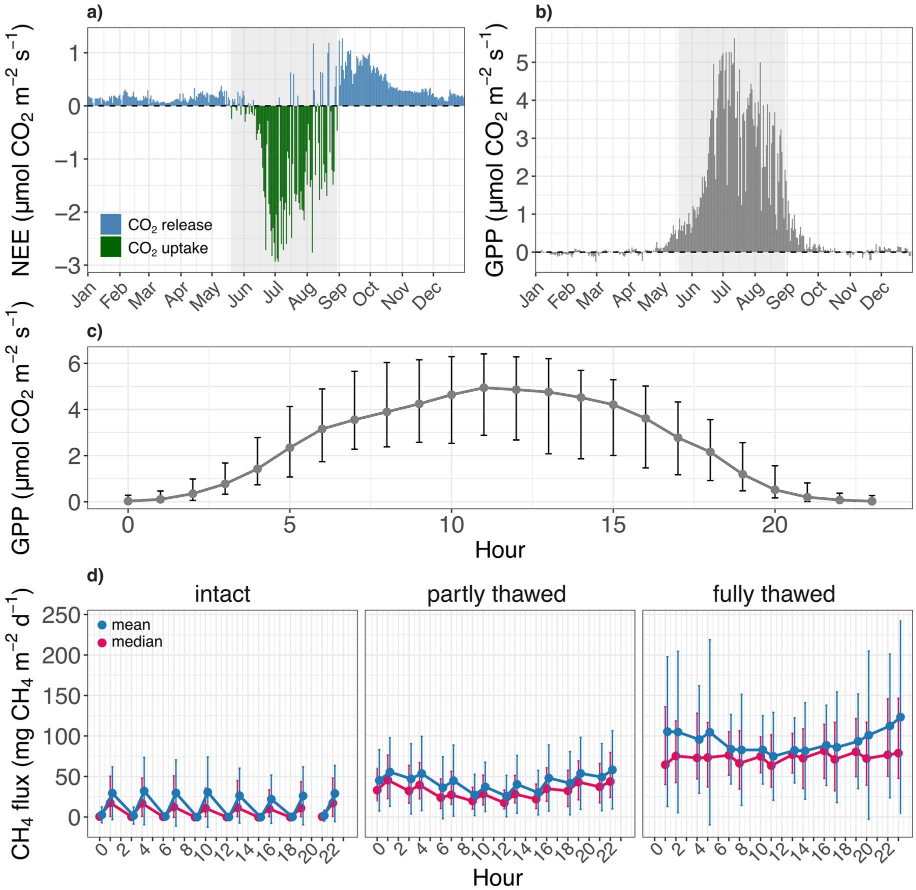

Figure B1. Daily net ecosystem CO_2 exchange (NEE; µmol CO_2 m^{-2} s^{-1}) **(a)** and gross primary production (GPP; µmol CO_2 m^{-2} s^{-1}) **(b)**, and hourly GPP and CH_4 fluxes during the productive season in 2023. **(a)** The productive season was defined as the period between the first and last passing of daily median NEE past zero (highlighted in gray; 19 May 2023 to 30 August 2023) (Körner et al., 2023). **(b)** Daily median GPP (based on nighttime partitioning) is shown for reference as a proxy for plant-mediated carbon substrate provision at the ecosystem scale (Knox et al., 2021). **(c)** Hourly GPP medians (based on daytime partitioning with light response curves for better estimation of diurnal trends). The error bars represent the ranges between 25th and 75th percentiles around the hourly medians. **(d)** Hourly CH_4 flux medians (in red) and means (in blue) at each permafrost thaw stage. The error bars represent the ranges between 25th and 75th percentiles around the hourly medians. Hourly means are shown in addition to medians to reflect short-term CH_4 pulses at the diurnal scale. NEE and GPP data: Lundin et al. (2023). Note that the NEE and GPP data likely mostly originate from intact and partly thawed permafrost stages and do not cover the fully thawed stage (Łakomiec et al., 2021).

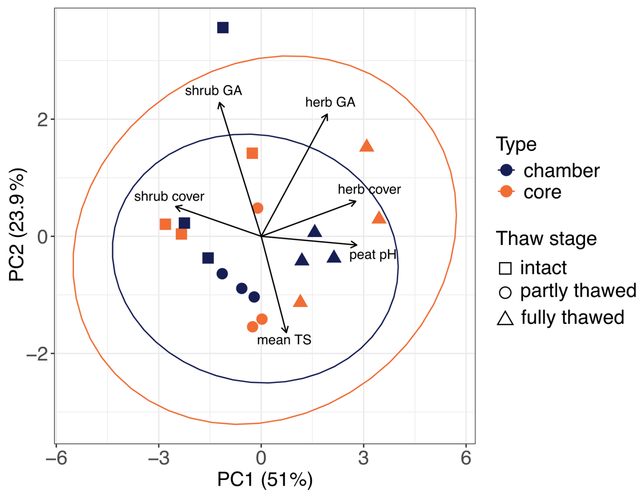

Figure B2. The similarity of peat core ($n = 9$) and automated chamber CH_4 flux measurement ($n = 9$) plots based on principal component analysis (PCA). In the figure, chamber and core plots are represented by dark purple and orange points, respectively, while thaw stages are shown in different shapes (rectangle = intact permafrost, circle = partly thawed permafrost, triangle = fully thawed permafrost). The ellipses represent 95 % data ellipses for the chamber and core plots within the multivariate space defined by the first two principal components (chamber = dark purple, orange = core). The PCA was based on normalized plot herbaceous and shrub plant cover and green area (GA), mean peat temperature (mean TS) and peat or porewater pH (here, referred to as peat pH), using function PCA from package FactoMineR (Lê et al., 2008) (results shown in the figure). In addition, we used PERMANOVA with function adonis2 from package vegan (Oksanen et al., 2025) and Euclidean distances between plots within thaw stages to estimate the similarity between core and chamber plots based on the same environmental variables. Based on these assessments, the peat core plots had a larger spread in multivariate space than CH_4 flux plots mostly due to slightly higher shrub or herbaceous plant cover in one plot within each thaw stage, but the differences were not significant with the sample size $n = 9$ ($p = 0.94$). Thus, the root and rhizome measurements could be used to roughly represent belowground traits in the CH_4 flux measurement plots. However, we acknowledge that the measured root and rhizome traits do not exactly correspond to those within the CH_4 flux plots and took this into account in the result interpretation.

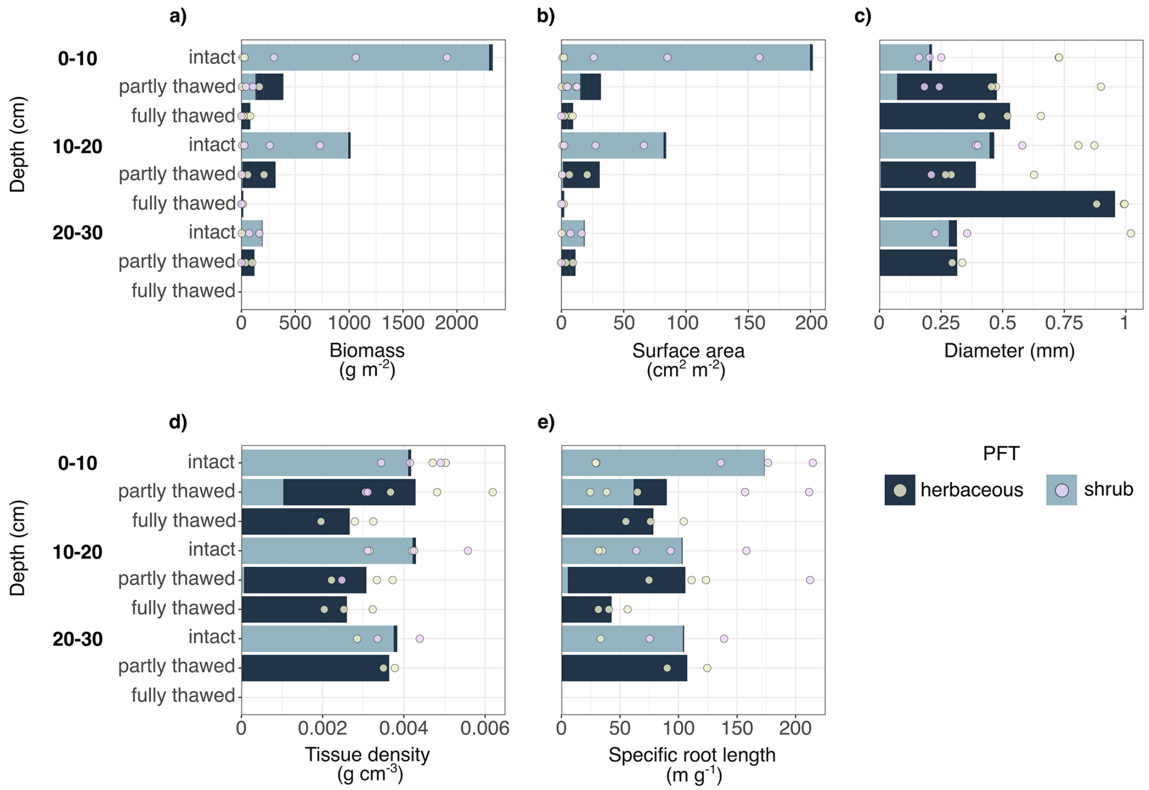

Figure B3. Root traits across the depth profile (0–10, 10–20, 20–30 cm) per thaw stage and plant functional type (PFT). The stacked bar colors (dark blue: herbaceous, light blue: shrub) represent the proportion of the PFT on the total biomass **(a)** or surface area **(b)**, or the contribution of each PFT on the biomass-weighted trait mean **(c–e)**. The points (light green: herbaceous, light purple: shrub) represent depth-per-plot measurements. **(a–b)** and **(e)** Root biomass, surface area and length were standardized to 10 cm depth increments. **(c)–(e)** Biomass-weighted trait means.

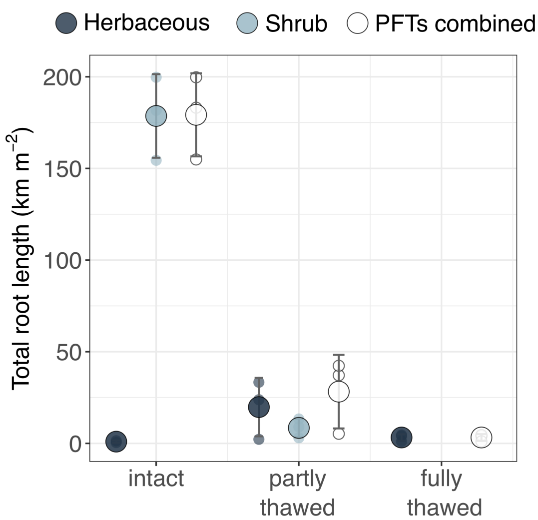

Figure B4. Root total length (km m^{-2}) across thaw stages per and across plant functional types (PFT). Large points indicate thaw stage mean and small points plot-scale measurements. Colors indicate PFTs (dark grey: herbaceous, light grey: shrub, white: PFTs summed). Error bars represent 1 standard deviation of the mean. Root total length was standardized to 30 cm depth in all plots.

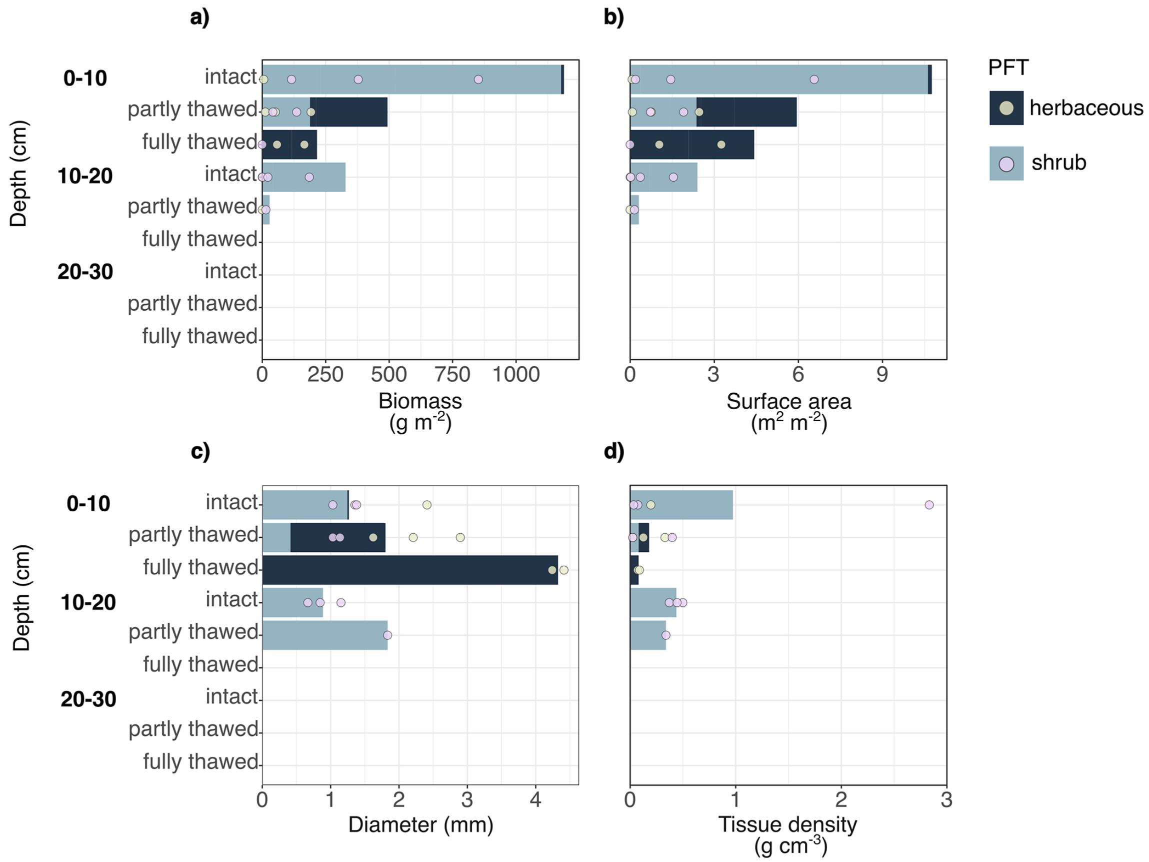

Figure B5. Rhizome traits across the depth profile (0–10, 10–20, 20–30 cm) per thaw stage and plant functional type (PFT). The stacked bar colors (dark blue: herbaceous, light blue: shrub) represent the proportion of the PFT on the total biomass **(a)** or surface area **(b)**, or the contribution of each PFT on the biomass-weighted trait mean **(c–d)**. The points (light green: herbaceous, light purple: shrub) represent depth-per-plot measurements. **(a–b)** and **(e)** Root biomass, surface area and length were standardized to 10 cm depth increments. **(c–d)** Biomass-weighted trait means.

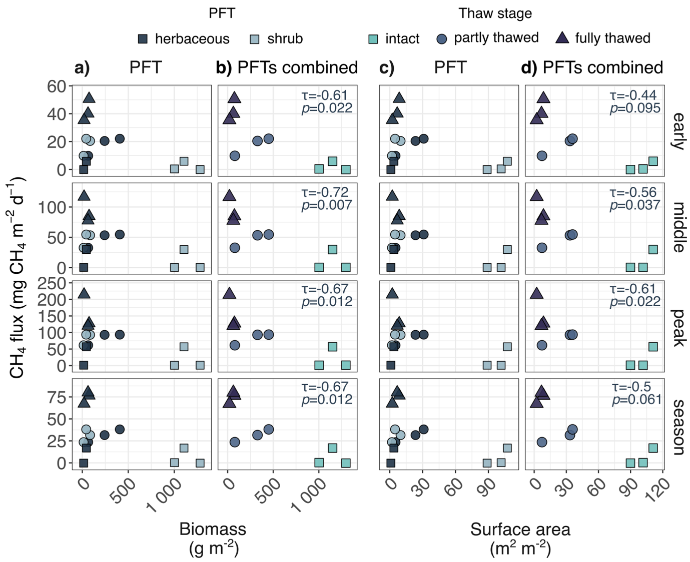

Figure B6. Relationship between root biomass (columns **a–b**), surface area (columns **c–d**) and CH_4 fluxes (early, middle, peak and season; rows). **(a, c)** Relationships between root traits and CH_4 fluxes per plant functional type (PFT), where dark gray: herbaceous plants, light gray: shrubs. **(b, d)** Relationships between root traits and CH_4 fluxes across PFTs (biomass and surface area summed), where light blue rectangle: intact, gray circle: partly thawed, and dark purple triangle: fully thawed stage. Kendall's τ is shown for relationships where $\tau \geq 0.2$ (note that due to the low sample size, p-values should be interpreted with caution). Linear regression model assumptions were not met for any of the relationships.

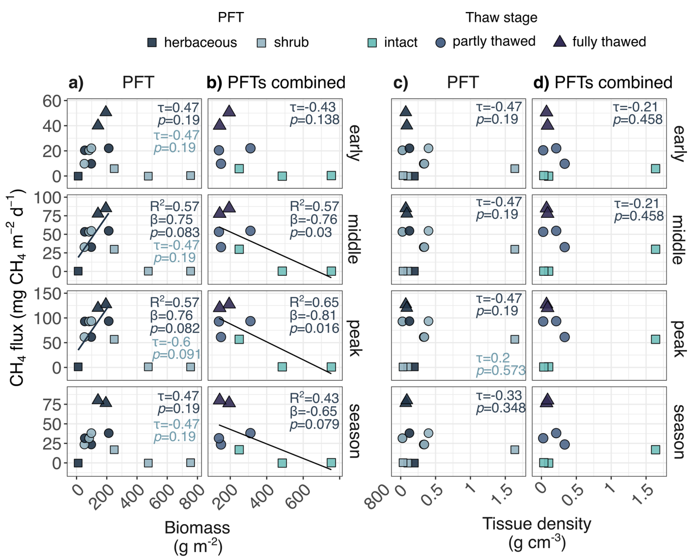

Figure B7. Relationship between rhizome biomass (columns **a–b**), tissue density (columns **c–d**) and CH_4 fluxes (early, middle, peak and season; rows). **(a, c)** Relationships between rhizome traits and CH_4 fluxes per plant functional type (PFT), where dark gray: herbaceous plants, light gray: shrubs. **(b, d)** Relationships between rhizome traits and CH_4 fluxes across PFTs (summed biomass, biomass-weighted tissue density), where light blue rectangle: intact, gray circle: partly thawed, and dark purple triangle: fully thawed stage. The lines represent linear regression fit used for visualization, while R^2 and effect size (β) are reported for linear regressions with centered and scaled CH_4 flux and trait values (when R^2>0.2, model p<0.1, and linear regression model assumptions were met). Kendall's τ is shown for relationships where $\tau \geq 0.2$ (note that due to the low sample size, p-values should be interpreted with caution).

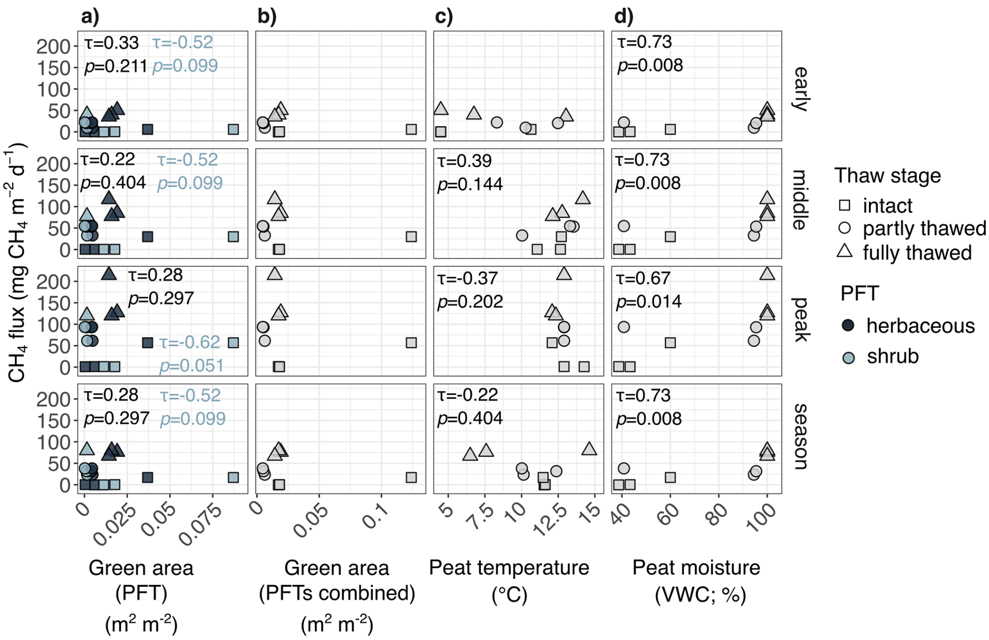

Figure B8. Relationship between plant functional type (PFT)-specific plant green area (column **a**), plant green area summed across PFTs (column **b**), peat temperature (column **c**), peat moisture (volumetric water content VWC; column **d**), and CH_4 flux season values (rows). Kendall τ correlation coefficient (τ) is reported for the relationship when $\tau > 0.2$ (note that due to sample $n = 9$, the correlation p-values should be interpreted with caution). The different point shapes represent thaw stages (rectangle = intact permafrost, circle = partly thawed permafrost, and triangle = fully thawed permafrost). **(a)** Colors represent different PFTs (dark blue = herbaceous plants, light blue = shrubs).

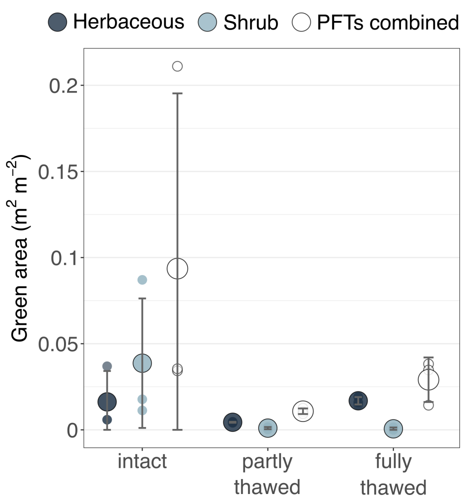

Figure B9. The plant green area (GA; $m^2\ m^{-2}$) varied slightly between thaw stages. Large points represent group means, small points plot-scale measurements, and error bars ±1 standard deviation. The colors represent plant functional type (PFT) groups: dark grey is herbaceous, light grey is shrub, and white is the sum of PFT GAs. Herbaceous GA coefficient of variation (CV) was highest within intact permafrost (137 %), while shrub GA varied most within intact permafrost (109 %). Note that shrubs (*Betula nana*) were only found in one plot and were only 3 % of the total GA in the fully thawed permafrost stage.

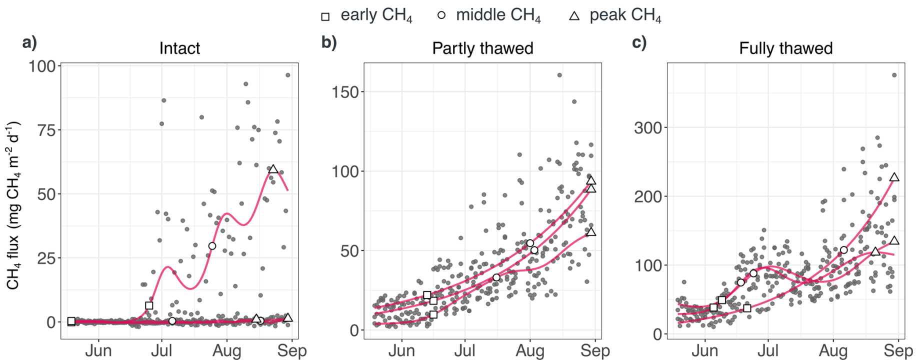

Figure B10. Daily median CH_4 flux with CH_4 flux period values over the productive season at intact **(a)**, partly thawed **(b)** and fully thawed **(c)** stages. **(a–c)** Red lines represent chamber-specific GAM fit ($R^2 \geq 0.3$), except for one chamber in a) where GAM $R^2 < 0.1$, and the line represents the moving 7 d median CH_4 flux. Squares represent early, circles middle and triangles peak CH_4 flux season. See chamber GAM R^2 in Table C5.

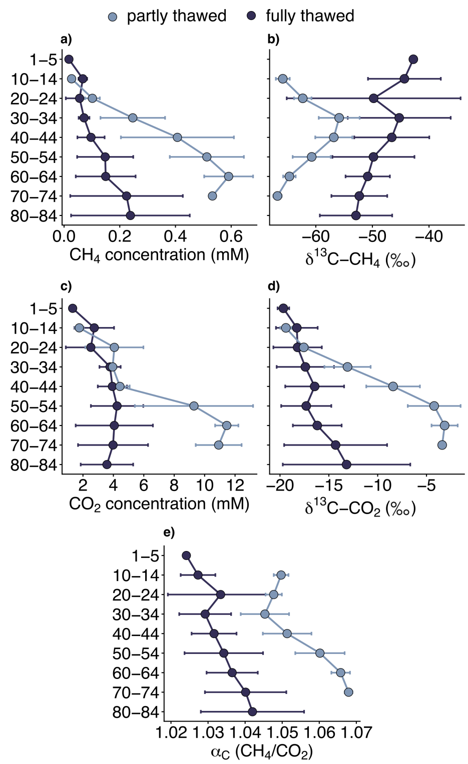

Figure B11. Porewater CH_4 concentration (mM) **(a)**, δ^{13}C-CH_4 (‰) **(b)**, CO_2 concentration **(c)**, δ^{13}C-CO_2 (‰) **(d)**, and carbon isotope fractionation factor (α_C CO_2 / CH_4) **(e)** from peat surface to 84 cm depth at partly and fully thawed permafrost stages. Line and point colors represent thaw stages. **(c)** α_C: higher values indicate larger fractionation (i.e., more hydrogenotrophy) and vice versa (i.e., more acetoclasty). Briefly, mean CH_4 concentrations increased from 0.027 ± 0.004 (standard deviation) mM to 0.533 ± 0.0007 mM at 70–74 cm depth at the partly thawed stage and from 0.017 ± 0.007 mM to 0.238 ± 0.213 mM at 80–84 cm depth at the fully thawed stage. δ^{13}C-CH_4 values became enriched at ca. 30–44 cm (partly thawed ca. −56.4 ‰, fully thawed ca. −46 ‰), and this enrichment was associated with a decrease in α_C (ca. 1.048 partly thawed, ca. 1.03 fully thawed). Mean CO_2 concentrations increased from 1.758 ± 0.284 mM to 11.454 ± 0.766 at 60–64 cm depth and 10.923 ± 1.51 at 70–74 cm depth at the partly thawed stage (with a decrease at 30–44 cm depth, with means of 3.951 and 4.430 mM), and from 1.322 ± 0.089 to 3.576 ± 1.725 mM at 80–84 cm at the fully thawed stage. δ^{13}C-CO_2 became more enriched with depth particularly at the partly thawed stage (from −19.398 ‰ to −3.394 ‰).

Appendix C: Tables

Table C1. Plant cover (%) by species and herbaceous and shrub vegetation classes, litter and water surface cover (%), and peat characteristics in each chamber and peat coring ("core") plot (as peat cores were selected to represent each individual chamber, the core and chamber plots have the same ID number). Note that the intact 1 chamber plot was on a collapsing palsa. Chamber plot WTD is the mean annual WTD across the 2007–2017 period per thaw stage (Crill et al., 2023). Values after "±" are one standard deviation of the mean. WTD = water table depth (cm; from the peat surface).

Plot	Species	Plant cover (%)		Litter and water cover (%)		Mean soil temp (°C)		pH		WTD (cm)		Active layer depth (cm)	
		Chamber	Core	Chamber	Core	Chamber	Core	Chamber	Core	Chamber	Core	Chamber	Core
Intact 1	*Eriophorum vaginatum*	48	28	Litter: 20	Litter: 16	9.5 ± 0.9	9.3 ± 1.5	3.1	3.0	–	–	47	37.5
	Vaccinium uliginosum	48	28		Water: 0	Water: 0							
	Andromeda polifolia	32	24										
	Empetrum nigrum	24	56										
	Rubus chamaemorus	0	8										
	Vaccinium vitis-idaea	0	4										
	Dicranum sp.	8	52										
	Polytrichum sp.	4	0										
	Shrub	104	120										
	Herbaceous	48	28										
Intact 2	*A. polifolia*	52	48	Litter: 28	Litter: 16	7.7 ± 0.6	7.7 ± 1.1	3.1	3.0	–	–	41.5	39
	E. nigrum	16	16	Water: 0	Water: 0								
	R. chamaemorus	4	32										
	V. uliginosum	4	0										
	Carex rotundata	4	0										
	Betula nana	0	28										
	V. vitis-idaea	0	4										
	E. vaginatum	0	4										
	Ptilidium ciliare	48	20										
	Dicranum sp.	8	20										
	Shrub	76	128										
	Herbaceous	4	4										
Intact 3	*E. vaginatum*	84	92	Litter: 0	Litter: 4	8.7 ± 0.8	8.3 ± 1.9	2.8	3.2	–	–	–	85
	V. uliginosum	24	20	Water: 12	Water: 0								
	R. chamaemorus	16	4										
	E. nigrum	12	20										
	A. polifolia	8	8										
	B. nana	8	12										
	Sphagnum balticum	32	0										
	Dicranum sp.	0	8										
	Herbaceous	84	92										
	Shrub	68	64										
Partly thawed 1	*C. rotundata*	52	0	Litter: 0	Litter: 0	9.5 ± 0.6	7.0 ± 1.2	3.3	3.2	−9.1 ± 4.6	−14.7	>85	>85
	E. vaginatum	0	80	Water: 0	Water: 0								
	S. capillifolium	100	100										
	Herbaceous	52	80										
	Shrub	0	0										
Partly thawed 2	*C. rotundata*	52	60	Litter: 16	Litter: 20	9.1 ± 0.5	10.9 ± 1.0	3.2	3.8	−9.1 ± 4.6	−21	>85	>85
	V. oxycoccos	48	20	Water: 0	Water: 0								
	A. polifolia	28	24										
	E. angustifolium	0	8										
	E. vaginatum	0	4										
	Drosera rotundifolia	0	4										
	S. capillifolium	100	72										
	P. ciliare	0	16										
	Herbaceous	52	76										
	Shrub	76	44										
Partly thawed 3	*V. oxycoccos*	16	36	Litter: 44	Litter: 8	9.1 ± 0.6	10.9 ± 0.7	3.3	3.4	−9.1 ± 4.6	−27	>85	>85
	C. rotundata	40	36	Water: 0	Water: 0								
	E. angustifolium	0	24										
	S. capillifolium	88	96										
	Herbaceous	40	60										
	Shrub	40	36										
Fully thawed 1	*E. angustifolium*	96	100	Litter: 0	Litter: 4	9.7 ± 0.3	8.7 ± 0.4	5.1	5.7	2.1 ± 4.4	0	>85	>85
	Equisetum fluviatile	40	20	Water: 12	Water: 0								
	Herbaceous	136	120										
	Shrub	0	0										
Fully thawed 2	*E. angustifolium*	88	100	Litter: 0	Litter: 0	8.4 ± 1.0	9.6 ± 0.3	5.0	6.0	2.1 ± 4.4	0	>85	>85
	E. fluviatile	24	68	Water: 0	Water: 0								
	Comarum palustre	4	12										
	S. riparium	12	0										
	Herbaceous	116	180										
	Shrub	0	0										
Fully thawed 3	*E. angustifolium*	92	84	Litter: 0	Litter: 24	9.1 ± 0.3	10.1 ± 0.4	4.7	4.8	2.1 ± 4.4	0	>85	>85
	S. riparium	40	96	Water: 0	Water: 0								
	Herbaceous	92	84										
	Shrub	0	0										

Table C2. Species included in the vegetation green area (GA) measurements per thaw stage. Mean GA (with standard deviation) is reported for each species across the three plots per thaw stage, and comprises the sum of stem and leaf green area ($m^2\ m^{-2}$).

Thaw stage	Species	Mean GA ($m^2\ m^{-2}$)
Intact	*Andromeda polifolia*	0.108 ± 0.06
	Betula nana	0.024 ± 0.02
	Carex rotundata	0.009 ± 0
	Empetrum nigrum	0.083 ± 0.07
	Eriophorum vaginatum	0.479 ± 0.54
	Rubus chamaemorus	0.160 ± 22.34
	Vaccinium uliginosum	0.190 ± 0.25
	Vaccinium vitis-idaea	0.005 ± 0.004
Partly thawed	*Andromeda polifolia*	0.035 ± 0.04
	Betula nana	0.016 ± 0.02
	Carex rotundata	0.163 ± 0.07
	Drosera rotundifolia	0.001 ± 0
	Empetrum nigrum	0.029 ± 0
	Eriophorum angustifolium	0.054 ± 0
	Eriophorum vaginatum	0.316 ± 0.16
	Rubus chamaemorus	0.026 ± 0
	Vaccinium oxycoccos	0.011 ± 0.01
	Vaccinium uliginosum	0.001 ± 0
Fully thawed	*Betula nana*	0.010 ± 0
	Carex canescens	0.003 ± 0
	Comarum palustre	0.086 ± 0.06
	Equisetum fluviatile	0.896 ± 0.63
	Eriophorum angustifolium	0.651 ± 0.64
	Galium palustre	0.012 ± 0

Table C3. Peat moisture data aggregated to daily medians from May–August periods in 2024 and 2025. Peat moisture was measured as volumetric water content (VWC, %) at each chamber. Date is expressed as YYYY-MM-DD.

date	chamber	thaw_stage	VWC
2024-05-14	1	intact	41.0605101
2024-05-15	1	intact	41.1284652
2024-05-16	1	intact	41.6925529
2024-05-17	1	intact	42.2016153
2024-05-18	1	intact	42.5223202
2024-05-19	1	intact	44.8038062
2024-05-20	1	intact	43.6937476
2024-05-21	1	intact	43.3301476
2024-05-22	1	intact	43.5006552
2024-05-23	1	intact	43.2403591
2024-05-24	1	intact	43.1114018
2024-05-25	1	intact	42.9779908
2024-05-26	1	intact	39.4578292
2024-05-27	1	intact	39.9465683
2024-05-28	1	intact	45.9747075
2024-05-29	1	intact	43.6734942
2024-05-30	1	intact	42.9068318
2024-05-31	1	intact	42.739248
2024-06-01	1	intact	42.9200879
2024-06-02	1	intact	42.697045
2024-06-03	1	intact	42.7556407
2024-06-04	1	intact	45.5608004
2024-06-05	1	intact	42.9458915
2024-06-06	1	intact	42.46882
2024-06-07	1	intact	42.2993965
2024-06-08	1	intact	42.3057493
2024-06-09	1	intact	42.229999
2024-06-10	1	intact	42.2858368
2024-06-11	1	intact	42.5450621
2024-06-12	1	intact	42.5045112
2024-06-13	1	intact	42.2792988
2024-06-14	1	intact	41.7452371
2024-06-15	1	intact	41.72232
2024-06-16	1	intact	41.6654059
2024-06-17	1	intact	41.7218161
2024-06-18	1	intact	42.1474714
2024-06-19	1	intact	42.1628706
2024-06-20	1	intact	41.5623153
2024-06-21	1	intact	42.1571109
2024-06-22	1	intact	41.7464336
2024-06-23	1	intact	41.3910747
2024-06-24	1	intact	42.0146809
2024-06-25	1	intact	42.2219108
2024-06-26	1	intact	41.7569689
2024-06-27	1	intact	41.5048579
2024-06-28	1	intact	41.4076303
2024-06-29	1	intact	41.558936
2024-06-30	1	intact	41.6865289
2024-07-01	1	intact	41.5572918
2024-07-02	1	intact	41.6468828
2024-07-03	1	intact	41.4396179
2024-07-04	1	intact	41.1977082
2024-07-05	1	intact	41.0962093
2024-07-06	1	intact	40.8885064

Table C3. Continued.

date	chamber	thaw_stage	VWC
2024-07-07	1	intact	40.6928102
2024-07-08	1	intact	40.7722413
2024-07-09	1	intact	40.9942864
2024-07-10	1	intact	40.9023587
2024-07-11	1	intact	41.4654589
2024-07-12	1	intact	41.2064899
2024-07-13	1	intact	41.0474941
2024-07-14	1	intact	35.7947273
2024-07-15	1	intact	34.8900478
2024-07-16	1	intact	35.0700105
2024-07-17	1	intact	35.3165857
2024-07-18	1	intact	35.2525265
2024-07-19	1	intact	35.2496995
2024-07-20	1	intact	35.3519407
2024-07-21	1	intact	35.3741362
2024-07-22	1	intact	35.3358996
2024-07-23	1	intact	35.5018052
2024-07-24	1	intact	35.5543534
2024-07-25	1	intact	35.5738091
2024-07-26	1	intact	36.8698854
2024-07-27	1	intact	36.3863743
2024-07-28	1	intact	36.3465022
2024-07-29	1	intact	36.3155981
2024-07-30	1	intact	36.3269812
2024-07-31	1	intact	36.3614147
2024-08-01	1	intact	36.4497978
2024-08-02	1	intact	36.5660007
2024-08-03	1	intact	36.6090859
2024-08-04	1	intact	36.4899768
2024-08-05	1	intact	36.4324907
2024-08-06	1	intact	36.3707506
2024-08-07	1	intact	36.2436739
2024-08-08	1	intact	36.0350938
2024-08-09	1	intact	36.1075603
2024-08-10	1	intact	38.7570375
2024-08-11	1	intact	39.9771353
2024-08-12	1	intact	39.129402
2024-08-13	1	intact	38.0886619
2024-08-14	1	intact	37.7621626
2024-08-15	1	intact	37.7590662
2024-08-16	1	intact	37.7339249
2024-08-17	1	intact	38.1100251
2024-08-18	1	intact	37.7571963
2024-08-19	1	intact	38.5992006
2024-08-20	1	intact	38.0145145
2024-08-21	1	intact	37.72617
2024-08-22	1	intact	37.6849787
2024-08-23	1	intact	37.6408093
2024-08-24	1	intact	40.6025472
2024-08-25	1	intact	39.7633976
2024-08-26	1	intact	38.8518066
2024-08-27	1	intact	38.4906671
2024-08-28	1	intact	38.4274347
2024-08-29	1	intact	38.4430851
2024-08-30	1	intact	38.4820275
2024-08-31	1	intact	38.5266596

Table C3. Continued.

date	chamber	thaw_stage	VWC
2025-05-19	1	intact	34.3399304
2025-05-20	1	intact	34.3668885
2025-05-21	1	intact	34.9092957
2025-05-22	1	intact	34.6029418
2025-05-23	1	intact	35.1063053
2025-05-24	1	intact	35.4680888
2025-05-25	1	intact	35.798061
2025-05-26	1	intact	36.4221714
2025-05-27	1	intact	36.7283591
2025-05-28	1	intact	36.484788
2025-05-29	1	intact	36.762761
2025-05-30	1	intact	36.5908181
2025-05-31	1	intact	36.4515043
2025-06-01	1	intact	36.3192213
2025-06-02	1	intact	36.878365
2025-06-03	1	intact	36.6368608
2025-06-04	1	intact	36.5252457
2025-06-05	1	intact	36.5697882
2025-06-06	1	intact	36.734546
2025-06-07	1	intact	36.9713132
2025-06-08	1	intact	39.0109161
2025-06-09	1	intact	37.7733121
2025-06-10	1	intact	37.8248662
2025-06-11	1	intact	37.4616858
2025-06-12	1	intact	37.3653948
2025-06-13	1	intact	37.350499
2025-06-14	1	intact	37.2339994
2025-06-15	1	intact	37.1396519
2025-06-16	1	intact	37.2104127
2025-06-17	1	intact	38.601145
2025-06-18	1	intact	37.9801786
2025-06-19	1	intact	37.517413
2025-06-20	1	intact	37.3551307
2025-06-21	1	intact	37.287688
2025-06-22	1	intact	37.3709688
2025-06-23	1	intact	37.4600688
2025-06-24	1	intact	37.5701231
2025-06-25	1	intact	37.7202259
2025-06-26	1	intact	37.7349142
2025-06-27	1	intact	37.5863211
2025-06-28	1	intact	37.667158
2025-06-29	1	intact	37.8840823
2025-06-30	1	intact	37.9937577
2025-07-01	1	intact	37.8382746
2025-07-02	1	intact	37.932973
2025-07-03	1	intact	37.8885515
2025-07-04	1	intact	37.8500175
2025-07-05	1	intact	37.8558833
2025-07-06	1	intact	37.9269764
2025-07-07	1	intact	38.0312946
2025-07-08	1	intact	38.1466912
2025-07-09	1	intact	38.1095332
2025-07-10	1	intact	38.0234441
2025-07-11	1	intact	38.1531378
2025-07-12	1	intact	38.3718072

Table C3. Continued.

date	chamber	thaw_stage	VWC
2025-07-13	1	intact	38.5394924
2025-07-14	1	intact	38.6891127
2025-07-15	1	intact	38.819535
2025-07-16	1	intact	38.8414596
2025-07-17	1	intact	38.908572
2025-07-18	1	intact	38.998773
2025-07-19	1	intact	39.0516733
2025-07-20	1	intact	39.1832985
2025-07-21	1	intact	39.3484182
2025-07-22	1	intact	39.4353804
2025-07-23	1	intact	39.5367167
2025-07-24	1	intact	39.6149027
2025-07-25	1	intact	39.6217029
2025-07-26	1	intact	39.704586
2025-07-27	1	intact	39.7596666
2025-07-28	1	intact	40.6316854
2025-07-29	1	intact	42.0448957
2025-07-30	1	intact	42.8866136
2025-07-31	1	intact	42.5227909
2025-08-01	1	intact	43.0241339
2025-08-02	1	intact	42.956997
2025-08-03	1	intact	42.901445
2025-08-04	1	intact	42.7549333
2025-08-05	1	intact	43.6937008
2025-08-06	1	intact	43.4992494
2025-08-07	1	intact	43.4129464
2025-08-08	1	intact	43.2022341
2025-08-09	1	intact	43.2466535
2025-08-10	1	intact	43.3382094
2025-08-11	1	intact	43.8715466
2025-08-12	1	intact	43.7305426
2025-08-13	1	intact	43.9782491
2024-05-11	2	intact	58.2969594
2024-05-12	2	intact	64.1062899
2024-05-13	2	intact	72.0318297
2024-05-14	2	intact	80.170228
2024-05-15	2	intact	89.7283065
2024-05-16	2	intact	96.2713834
2024-07-22	2	intact	94.8884625
2024-07-23	2	intact	94.8096798
2024-07-24	2	intact	94.4829199
2024-07-25	2	intact	94.531827
2024-07-26	2	intact	95.126923
2024-07-27	2	intact	94.7515675
2024-07-28	2	intact	94.4436875
2024-07-29	2	intact	93.9859819
2024-07-30	2	intact	93.8746628
2024-07-31	2	intact	93.5588625
2024-08-01	2	intact	93.2904957
2024-08-02	2	intact	93.2791925
2024-08-03	2	intact	93.3097479
2024-08-04	2	intact	92.9387846
2024-08-05	2	intact	92.6046859
2024-08-06	2	intact	92.1410661

Table C3. Continued.

date	chamber	thaw_stage	VWC
2024-08-07	2	intact	91.4638475
2024-08-08	2	intact	90.4810847
2024-08-09	2	intact	90.238477
2024-08-10	2	intact	90.293199
2024-08-11	2	intact	98.2432935
2024-08-12	2	intact	98.3081471
2024-08-13	2	intact	97.7041068
2024-08-14	2	intact	96.9494125
2024-08-15	2	intact	95.9790598
2024-08-16	2	intact	95.71334
2024-08-17	2	intact	97.0265295
2024-08-18	2	intact	96.5236913
2024-08-19	2	intact	96.1387949
2024-08-20	2	intact	96.6065714
2024-08-21	2	intact	95.7736692
2024-08-22	2	intact	95.2951666
2024-08-23	2	intact	94.935956
2024-08-24	2	intact	94.5526047
2025-05-14	2	intact	88.4097374
2025-05-15	2	intact	90.0687188
2025-05-16	2	intact	92.8086446
2025-05-17	2	intact	96.9311225
2025-05-18	2	intact	98.6169481
2024-05-10	3	intact	38.9609525
2024-05-11	3	intact	39.0881217
2024-05-12	3	intact	39.6648636
2024-05-13	3	intact	42.1605271
2024-05-14	3	intact	43.3112574
2024-05-15	3	intact	44.6099838
2024-05-16	3	intact	45.5385825
2024-05-17	3	intact	47.3084808
2024-05-18	3	intact	48.5035132
2024-05-19	3	intact	50.4007523
2024-05-20	3	intact	48.8658716
2024-05-21	3	intact	48.9658485
2024-05-22	3	intact	49.0844925
2024-05-23	3	intact	48.3587129
2024-05-24	3	intact	48.0686103
2024-05-25	3	intact	48.2605121
2024-05-26	3	intact	48.1289526
2024-05-27	3	intact	47.7895886
2024-05-28	3	intact	51.0075133
2024-05-29	3	intact	49.7429248
2024-05-30	3	intact	48.7647746
2024-05-31	3	intact	48.2659168
2024-06-01	3	intact	48.4430927
2024-06-02	3	intact	48.2907268
2024-06-03	3	intact	48.0020249
2024-06-04	3	intact	50.0020459
2024-06-05	3	intact	48.3963745
2024-06-06	3	intact	47.4932016
2024-06-07	3	intact	47.1561349
2024-06-08	3	intact	47.1254357

Table C3. Continued.

date	chamber	thaw_stage	VWC
2024-06-09	3	intact	46.9239771
2024-06-10	3	intact	46.9932759
2024-06-11	3	intact	47.4347461
2024-06-12	3	intact	47.1513389
2024-06-13	3	intact	46.8688216
2024-06-14	3	intact	46.6469283
2024-06-15	3	intact	46.1604873
2024-06-16	3	intact	46.2152407
2024-06-17	3	intact	45.7201649
2024-06-18	3	intact	46.1929062
2024-06-19	3	intact	46.9220416
2024-06-20	3	intact	45.8938354
2024-06-21	3	intact	46.6408514
2024-06-22	3	intact	46.5725281
2024-06-23	3	intact	46.2489897
2024-06-24	3	intact	46.494786
2024-06-25	3	intact	46.7193126
2024-06-26	3	intact	46.3026069
2024-06-27	3	intact	46.3027376
2024-06-28	3	intact	46.0341589
2024-06-29	3	intact	45.8313789
2024-06-30	3	intact	45.7578394
2024-07-01	3	intact	45.5795378
2024-07-02	3	intact	45.7009313
2024-07-03	3	intact	45.6072897
2024-07-04	3	intact	45.1725268
2024-07-05	3	intact	45.0066554
2024-07-06	3	intact	44.882393
2024-07-07	3	intact	44.8080611
2024-07-08	3	intact	45.016208
2024-07-09	3	intact	45.1913102
2024-07-10	3	intact	45.1876413
2024-07-11	3	intact	45.1514322
2024-07-12	3	intact	44.8994898
2024-07-13	3	intact	45.0352276
2024-07-14	3	intact	45.0179801
2024-07-15	3	intact	44.8791047
2024-07-16	3	intact	44.3087749
2024-07-17	3	intact	44.5601726
2024-07-18	3	intact	44.3087749
2024-07-19	3	intact	44.2573307
2024-07-20	3	intact	44.3212085
2024-07-21	3	intact	43.854425
2024-07-22	3	intact	43.548669
2024-07-23	3	intact	43.4062449
2024-07-24	3	intact	43.6958188
2024-07-25	3	intact	43.7022027
2024-07-26	3	intact	44.1455961
2024-07-27	3	intact	43.7387816
2024-07-28	3	intact	43.6565068
2024-07-29	3	intact	43.4274296
2024-07-30	3	intact	43.1971473
2024-07-31	3	intact	43.3772167
2024-08-01	3	intact	43.4211504

Table C3. Continued.

date	chamber	thaw_stage	VWC
2024-08-02	3	intact	43.6283881
2024-08-03	3	intact	43.5999975
2024-08-04	3	intact	43.5209945
2024-08-05	3	intact	43.5849323
2024-08-06	3	intact	43.4944053
2024-08-07	3	intact	43.2090827
2024-08-08	3	intact	42.878589
2024-08-09	3	intact	43.2093403
2024-08-10	3	intact	44.8511958
2024-08-11	3	intact	45.3509339
2024-08-12	3	intact	45.2068126
2024-08-13	3	intact	44.1643231
2024-08-14	3	intact	43.467851
2024-08-15	3	intact	43.2065352
2024-08-16	3	intact	43.0769688
2024-08-17	3	intact	43.2165965
2024-08-18	3	intact	42.9047879
2024-08-19	3	intact	43.4107359
2024-08-20	3	intact	43.2152303
2024-08-21	3	intact	42.715058
2024-08-22	3	intact	42.7575573
2024-08-23	3	intact	42.6199075
2024-08-24	3	intact	44.4155087
2024-08-25	3	intact	44.0640803
2024-08-26	3	intact	43.0309649
2024-08-27	3	intact	42.7854592
2024-08-28	3	intact	42.712697
2024-08-29	3	intact	42.7105229
2024-08-30	3	intact	42.7590007
2024-08-31	3	intact	43.0005141
2025-05-10	3	intact	43.1915684
2025-05-11	3	intact	42.7998532
2025-05-12	3	intact	42.1991242
2025-05-13	3	intact	41.9407254
2025-05-14	3	intact	43.3775363
2025-05-15	3	intact	43.0588883
2025-05-16	3	intact	43.1160897
2025-05-17	3	intact	43.6800364
2025-05-18	3	intact	44.0230023
2025-05-19	3	intact	44.5942203
2025-05-20	3	intact	44.4439276
2025-05-21	3	intact	44.5878499
2025-05-22	3	intact	43.8925075
2025-05-23	3	intact	43.9340232
2025-05-24	3	intact	43.785213
2025-05-25	3	intact	43.4232237
2025-05-26	3	intact	43.0124782
2025-05-27	3	intact	42.9246662
2025-05-28	3	intact	42.6452924
2025-05-29	3	intact	43.4086194
2025-05-30	3	intact	43.1477091
2025-05-31	3	intact	42.8682916
2025-06-01	3	intact	42.1642552
2025-06-02	3	intact	42.7060202

Table C3. Continued.

date	chamber	thaw_stage	VWC
2025-06-03	3	intact	42.7013343
2025-06-04	3	intact	42.2288585
2025-06-05	3	intact	41.8312875
2025-06-06	3	intact	41.7994214
2025-06-07	3	intact	42.0386097
2025-06-08	3	intact	45.2235757
2025-06-09	3	intact	44.0488206
2025-06-10	3	intact	44.0912301
2025-06-11	3	intact	43.2897209
2025-06-12	3	intact	42.5613302
2025-06-13	3	intact	42.1633269
2025-06-14	3	intact	41.7650138
2025-06-15	3	intact	41.9829822
2025-06-16	3	intact	41.6085659
2025-06-17	3	intact	43.6170852
2025-06-18	3	intact	43.1037754
2025-06-19	3	intact	42.6057504
2025-06-20	3	intact	42.3459775
2025-06-21	3	intact	41.6919751
2025-06-22	3	intact	41.7310206
2025-06-23	3	intact	41.451628
2025-06-24	3	intact	41.2798991
2025-06-25	3	intact	41.2927876
2025-06-26	3	intact	41.6079502
2025-06-27	3	intact	41.1320714
2025-06-28	3	intact	40.8731877
2025-06-29	3	intact	41.3697209
2025-06-30	3	intact	41.5705543
2025-07-01	3	intact	41.1176543
2025-07-02	3	intact	41.4167392
2025-07-03	3	intact	41.1890307
2025-07-04	3	intact	40.9631061
2025-07-05	3	intact	40.889521
2025-07-06	3	intact	41.0306014
2025-07-07	3	intact	41.0255442
2025-07-08	3	intact	40.7040801
2025-07-09	3	intact	40.8150369
2025-07-10	3	intact	40.7177419
2025-07-11	3	intact	40.5862457
2025-07-12	3	intact	40.7300375
2025-07-13	3	intact	40.9086849
2025-07-14	3	intact	41.0026501
2025-07-15	3	intact	40.9160923
2025-07-16	3	intact	40.6999667
2025-07-17	3	intact	40.6562788
2025-07-18	3	intact	40.8571483
2025-07-19	3	intact	40.7952451
2025-07-20	3	intact	40.6227576
2025-07-21	3	intact	40.7410779
2025-07-22	3	intact	40.7651646
2025-07-23	3	intact	40.6394092
2025-07-24	3	intact	40.5174144
2025-07-25	3	intact	40.1996569
2025-07-26	3	intact	40.1924119
2025-07-27	3	intact	39.891316
2025-07-28	3	intact	40.331905

Table C3. Continued.

date	chamber	thaw_stage	VWC
2025-07-29	3	intact	41.0565073
2025-07-30	3	intact	41.1144106
2025-07-31	3	intact	40.8637635
2025-08-01	3	intact	41.211406
2025-08-02	3	intact	40.8657144
2025-08-03	3	intact	40.5790127
2025-08-04	3	intact	40.0207215
2025-08-05	3	intact	40.6474824
2025-08-06	3	intact	40.2552052
2025-08-07	3	intact	40.0146965
2025-08-08	3	intact	39.7854033
2025-08-09	3	intact	39.7559042
2025-08-10	3	intact	39.7748234
2025-08-11	3	intact	40.6312473
2025-08-12	3	intact	40.8534005
2025-08-13	3	intact	41.1519138
2024-05-11	4	partly_thawed	49.8555574
2024-05-12	4	partly_thawed	52.720588
2024-05-13	4	partly_thawed	60.1632906
2024-05-14	4	partly_thawed	67.3829149
2024-05-15	4	partly_thawed	74.9544639
2024-05-16	4	partly_thawed	79.3564756
2024-05-17	4	partly_thawed	84.4267739
2024-05-18	4	partly_thawed	87.9392211
2024-05-19	4	partly_thawed	89.8230249
2024-05-20	4	partly_thawed	90.7456008
2024-05-21	4	partly_thawed	90.7514573
2024-05-22	4	partly_thawed	90.7700186
2024-05-23	4	partly_thawed	90.8305783
2024-05-24	4	partly_thawed	90.6490025
2024-05-25	4	partly_thawed	90.9123117
2024-05-26	4	partly_thawed	91.0683036
2024-05-27	4	partly_thawed	90.9908622
2024-05-28	4	partly_thawed	97.8901781
2024-05-29	4	partly_thawed	96.6787814
2024-05-30	4	partly_thawed	96.3073014
2024-05-31	4	partly_thawed	96.0391499
2024-06-01	4	partly_thawed	96.0253428
2024-06-02	4	partly_thawed	95.9662291
2024-06-03	4	partly_thawed	96.0034197
2024-06-04	4	partly_thawed	97.633573
2024-06-05	4	partly_thawed	97.0808634
2024-06-06	4	partly_thawed	96.9252714
2024-06-07	4	partly_thawed	96.6937816
2024-06-08	4	partly_thawed	96.7012293
2024-06-09	4	partly_thawed	96.5853374
2024-06-10	4	partly_thawed	96.6848543
2024-06-11	4	partly_thawed	96.8017914
2024-06-12	4	partly_thawed	96.7196811
2024-06-13	4	partly_thawed	96.4263166
2024-06-14	4	partly_thawed	96.197365
2024-06-15	4	partly_thawed	95.8823663
2024-06-16	4	partly_thawed	95.7998048
2024-06-17	4	partly_thawed	95.571752
2024-06-18	4	partly_thawed	95.6953318
2024-06-19	4	partly_thawed	96.141151

Table C3. Continued.

date	chamber	thaw_stage	VWC
2024-06-20	4	partly_thawed	95.8549733
2024-06-21	4	partly_thawed	96.1738493
2024-06-22	4	partly_thawed	95.9189169
2024-06-23	4	partly_thawed	95.8892168
2024-06-24	4	partly_thawed	95.9277184
2024-06-25	4	partly_thawed	96.157378
2024-06-26	4	partly_thawed	95.931844
2024-06-27	4	partly_thawed	96.0160702
2024-06-28	4	partly_thawed	96.0577923
2024-06-29	4	partly_thawed	95.8067448
2024-06-30	4	partly_thawed	95.7805466
2024-07-01	4	partly_thawed	95.754433
2024-07-02	4	partly_thawed	95.5755981
2024-07-03	4	partly_thawed	95.547198
2024-07-04	4	partly_thawed	95.1979659
2024-07-05	4	partly_thawed	95.0919664
2024-07-06	4	partly_thawed	94.9632617
2024-07-07	4	partly_thawed	95.0192704
2024-07-08	4	partly_thawed	94.7005146
2024-07-09	4	partly_thawed	94.812145
2024-07-10	4	partly_thawed	94.9084249
2024-07-11	4	partly_thawed	94.6809057
2024-07-12	4	partly_thawed	94.7479106
2024-07-13	4	partly_thawed	94.7520933
2024-07-14	4	partly_thawed	94.8235013
2024-07-15	4	partly_thawed	94.6031397
2024-07-16	4	partly_thawed	94.1086335
2024-07-17	4	partly_thawed	94.2020805
2024-07-18	4	partly_thawed	94.0135469
2024-07-19	4	partly_thawed	93.8938157
2024-07-20	4	partly_thawed	93.9394041
2024-07-21	4	partly_thawed	94.1266095
2024-07-22	4	partly_thawed	93.7251959
2024-07-23	4	partly_thawed	93.64881
2024-07-24	4	partly_thawed	93.435231
2024-07-25	4	partly_thawed	93.5608663
2024-07-26	4	partly_thawed	94.2662339
2024-07-27	4	partly_thawed	94.0360828
2024-07-28	4	partly_thawed	93.6973702
2024-07-29	4	partly_thawed	93.5104338
2024-07-30	4	partly_thawed	93.5188966
2024-07-31	4	partly_thawed	93.4610766
2024-08-01	4	partly_thawed	93.2407645
2024-08-02	4	partly_thawed	93.3501502
2024-08-03	4	partly_thawed	93.5090234
2024-08-04	4	partly_thawed	93.4681266
2024-08-05	4	partly_thawed	93.0862044
2024-08-06	4	partly_thawed	92.754536
2024-08-07	4	partly_thawed	92.0861392
2024-08-08	4	partly_thawed	89.8600281
2024-08-09	4	partly_thawed	88.6083247
2024-08-10	4	partly_thawed	93.7429076
2024-08-11	4	partly_thawed	96.3971978
2024-08-12	4	partly_thawed	96.7714379
2024-08-13	4	partly_thawed	96.1790046

Table C3. Continued.

date	chamber	thaw_stage	VWC
2024-08-14	4	partly_thawed	95.4805294
2024-08-15	4	partly_thawed	95.1901602
2024-08-16	4	partly_thawed	94.7954764
2024-08-17	4	partly_thawed	95.7007873
2024-08-18	4	partly_thawed	95.6622121
2024-08-19	4	partly_thawed	95.5452766
2024-08-20	4	partly_thawed	95.9823236
2024-08-21	4	partly_thawed	95.1376063
2024-08-22	4	partly_thawed	94.9095823
2024-08-23	4	partly_thawed	94.7849225
2024-08-24	4	partly_thawed	95.3699361
2024-08-25	4	partly_thawed	99.1667085
2024-08-26	4	partly_thawed	98.4730024
2024-08-27	4	partly_thawed	97.2801962
2024-08-28	4	partly_thawed	97.2244829
2024-08-29	4	partly_thawed	96.7999412
2024-08-30	4	partly_thawed	96.5548128
2024-08-31	4	partly_thawed	96.9843542
2025-05-13	4	partly_thawed	71.496324
2025-05-14	4	partly_thawed	74.9113323
2025-05-15	4	partly_thawed	77.6893555
2025-05-16	4	partly_thawed	80.592722
2025-05-17	4	partly_thawed	80.463519
2025-05-18	4	partly_thawed	82.6095588
2025-05-19	4	partly_thawed	86.4048325
2025-05-20	4	partly_thawed	89.6868677
2025-05-21	4	partly_thawed	93.5725108
2025-05-22	4	partly_thawed	94.2503613
2025-05-23	4	partly_thawed	96.2295083
2025-05-24	4	partly_thawed	96.217765
2025-05-25	4	partly_thawed	96.2646855
2025-05-26	4	partly_thawed	96.2658443
2025-05-27	4	partly_thawed	96.2844174
2025-05-28	4	partly_thawed	96.4855902
2025-05-29	4	partly_thawed	96.7289162
2025-05-30	4	partly_thawed	96.4630284
2025-05-31	4	partly_thawed	96.1093504
2025-06-01	4	partly_thawed	95.7849465
2025-06-02	4	partly_thawed	96.1520364
2025-06-03	4	partly_thawed	95.9476813
2025-06-04	4	partly_thawed	95.6877689
2025-06-05	4	partly_thawed	95.208279
2025-06-06	4	partly_thawed	95.0508549
2025-06-07	4	partly_thawed	95.2461146
2025-06-08	4	partly_thawed	97.9819325
2025-06-09	4	partly_thawed	96.8970755
2025-06-10	4	partly_thawed	97.0834652
2025-06-11	4	partly_thawed	96.329234
2025-06-12	4	partly_thawed	95.9417918
2025-06-13	4	partly_thawed	96.0068997
2025-06-14	4	partly_thawed	95.7263162
2025-06-15	4	partly_thawed	95.5543196
2025-06-16	4	partly_thawed	95.4265164
2025-06-17	4	partly_thawed	97.2987303
2025-06-18	4	partly_thawed	96.88346

Table C3. Continued.

date	chamber	thaw_stage	VWC
2025-06-19	4	partly_thawed	96.725795
2025-06-20	4	partly_thawed	96.4336452
2025-06-21	4	partly_thawed	96.2851528
2025-06-22	4	partly_thawed	96.1339363
2025-06-23	4	partly_thawed	96.2604577
2025-06-24	4	partly_thawed	96.0523123
2025-06-25	4	partly_thawed	96.4545533
2025-06-26	4	partly_thawed	96.4344473
2025-06-27	4	partly_thawed	96.2206789
2025-06-28	4	partly_thawed	96.3551756
2025-06-29	4	partly_thawed	96.4344472
2025-06-30	4	partly_thawed	96.4692007
2025-07-01	4	partly_thawed	96.5289479
2025-07-02	4	partly_thawed	96.6357391
2025-07-03	4	partly_thawed	96.639549
2025-07-04	4	partly_thawed	96.3970268
2025-07-05	4	partly_thawed	96.5443384
2025-07-06	4	partly_thawed	96.5654405
2025-07-07	4	partly_thawed	96.3633743
2025-07-08	4	partly_thawed	96.3053746
2025-07-09	4	partly_thawed	96.0762436
2025-07-10	4	partly_thawed	96.222341
2025-07-11	4	partly_thawed	96.0062162
2025-07-12	4	partly_thawed	95.9708977
2025-07-13	4	partly_thawed	96.054812
2025-07-14	4	partly_thawed	95.8118747
2025-07-15	4	partly_thawed	95.7380507
2025-07-16	4	partly_thawed	95.4185404
2025-07-17	4	partly_thawed	95.1656292
2025-07-18	4	partly_thawed	95.1214574
2025-07-19	4	partly_thawed	94.622206
2025-07-20	4	partly_thawed	94.6179325
2025-07-21	4	partly_thawed	94.50871
2025-07-22	4	partly_thawed	94.2020436
2025-07-23	4	partly_thawed	93.7199007
2025-07-24	4	partly_thawed	93.0349775
2025-07-25	4	partly_thawed	91.7738109
2025-07-26	4	partly_thawed	91.7289513
2025-07-27	4	partly_thawed	90.4664931
2025-07-28	4	partly_thawed	90.6529878
2025-07-29	4	partly_thawed	92.771468
2025-07-30	4	partly_thawed	93.4510911
2025-07-31	4	partly_thawed	93.3233611
2025-08-01	4	partly_thawed	93.5678513
2025-08-02	4	partly_thawed	93.4685838
2025-08-03	4	partly_thawed	93.120213
2025-08-04	4	partly_thawed	92.2252436
2025-08-05	4	partly_thawed	92.5999005
2025-08-06	4	partly_thawed	93.2104271
2025-08-07	4	partly_thawed	93.1780287
2025-08-08	4	partly_thawed	92.2174486
2025-08-09	4	partly_thawed	91.6998141
2025-08-10	4	partly_thawed	91.9301454
2025-08-11	4	partly_thawed	92.0904443
2025-08-12	4	partly_thawed	91.8020685

Table C3. Continued.

date	chamber	thaw_stage	VWC
2025-08-13	4	partly_thawed	91.9201142
2024-05-13	5	partly_thawed	43.6271539
2024-05-14	5	partly_thawed	41.1262654
2024-05-15	5	partly_thawed	39.1855372
2024-05-16	5	partly_thawed	38.5595344
2024-05-17	5	partly_thawed	39.4838125
2024-05-18	5	partly_thawed	40.6286496
2024-05-19	5	partly_thawed	43.3719364
2024-05-20	5	partly_thawed	43.6168255
2024-05-21	5	partly_thawed	43.0391455
2024-05-22	5	partly_thawed	43.207343
2024-05-23	5	partly_thawed	43.5525757
2024-05-24	5	partly_thawed	43.7533626
2024-05-25	5	partly_thawed	43.759915
2024-05-26	5	partly_thawed	43.7196326
2024-05-27	5	partly_thawed	43.8000808
2024-05-28	5	partly_thawed	54.565258
2024-05-29	5	partly_thawed	52.2328619
2024-05-30	5	partly_thawed	51.5634301
2024-05-31	5	partly_thawed	50.9334974
2024-06-01	5	partly_thawed	51.4731797
2024-06-02	5	partly_thawed	50.9844084
2024-06-03	5	partly_thawed	50.936304
2024-06-04	5	partly_thawed	59.0139599
2024-06-05	5	partly_thawed	56.240896
2024-06-06	5	partly_thawed	55.3317567
2024-06-07	5	partly_thawed	54.9625267
2024-06-08	5	partly_thawed	55.0411954
2024-06-09	5	partly_thawed	54.8697666
2024-06-10	5	partly_thawed	55.3186776
2024-06-11	5	partly_thawed	55.5078531
2024-06-12	5	partly_thawed	55.4910497
2024-06-13	5	partly_thawed	55.387109
2024-06-14	5	partly_thawed	55.5918932
2024-06-15	5	partly_thawed	55.3887655
2024-06-16	5	partly_thawed	55.6576457
2024-06-17	5	partly_thawed	55.5702034
2024-06-18	5	partly_thawed	56.0221005
2024-06-19	5	partly_thawed	57.1484839
2024-06-20	5	partly_thawed	57.0582744
2024-06-21	5	partly_thawed	58.0357923
2024-06-22	5	partly_thawed	57.8572105
2024-06-23	5	partly_thawed	57.5190066
2024-06-24	5	partly_thawed	57.8458735
2024-06-25	5	partly_thawed	58.4081
2024-06-26	5	partly_thawed	58.1315272
2024-06-27	5	partly_thawed	58.3822003
2024-06-28	5	partly_thawed	58.5260321
2024-06-29	5	partly_thawed	58.3259377
2024-06-30	5	partly_thawed	58.8411691
2024-07-01	5	partly_thawed	58.9237247
2024-07-02	5	partly_thawed	59.1475116
2024-07-03	5	partly_thawed	59.4189022
2024-07-04	5	partly_thawed	59.1835291

Table C3. Continued.

date	chamber	thaw_stage	VWC
2024-07-05	5	partly_thawed	59.0081939
2024-07-06	5	partly_thawed	59.0622164
2024-07-07	5	partly_thawed	59.2836356
2024-07-08	5	partly_thawed	59.3734011
2024-07-09	5	partly_thawed	59.8642332
2024-07-10	5	partly_thawed	59.8344147
2024-07-11	5	partly_thawed	59.6311553
2024-07-12	5	partly_thawed	59.6848401
2024-07-13	5	partly_thawed	59.7857659
2024-07-14	5	partly_thawed	59.880565
2024-07-15	5	partly_thawed	59.9523808
2024-07-16	5	partly_thawed	59.503146
2024-07-17	5	partly_thawed	59.9060002
2024-07-18	5	partly_thawed	59.7320359
2024-07-19	5	partly_thawed	59.7234287
2024-07-20	5	partly_thawed	60.0002417
2024-07-21	5	partly_thawed	60.3017455
2024-07-22	5	partly_thawed	60.0036096
2024-07-23	5	partly_thawed	60.0871876
2024-07-24	5	partly_thawed	60.4146503
2024-07-25	5	partly_thawed	60.6491829
2024-07-26	5	partly_thawed	60.5549467
2024-07-27	5	partly_thawed	59.6898149
2024-07-28	5	partly_thawed	59.702604
2024-07-29	5	partly_thawed	59.5495159
2024-07-30	5	partly_thawed	59.8029993
2024-07-31	5	partly_thawed	60.2394121
2024-08-01	5	partly_thawed	59.7300429
2024-08-02	5	partly_thawed	59.9953061
2024-08-03	5	partly_thawed	60.2579258
2024-08-04	5	partly_thawed	60.006602
2024-08-05	5	partly_thawed	60.1649661
2024-08-06	5	partly_thawed	60.2899706
2024-08-07	5	partly_thawed	59.8389596
2024-08-08	5	partly_thawed	59.3323731
2024-08-09	5	partly_thawed	59.4766911
2024-08-10	5	partly_thawed	68.6746909
2024-08-11	5	partly_thawed	73.5995464
2024-08-12	5	partly_thawed	71.7301359
2024-08-13	5	partly_thawed	69.5603349
2024-08-14	5	partly_thawed	68.3717665
2024-08-15	5	partly_thawed	67.9561468
2024-08-16	5	partly_thawed	67.9076812
2024-08-17	5	partly_thawed	69.6611548
2024-08-18	5	partly_thawed	68.8981548
2024-08-19	5	partly_thawed	69.3707555
2024-08-20	5	partly_thawed	69.2499663
2024-08-21	5	partly_thawed	68.5214302
2024-08-22	5	partly_thawed	68.5151396
2024-08-23	5	partly_thawed	68.3995995
2024-08-24	5	partly_thawed	70.4124213
2024-08-25	5	partly_thawed	77.2365622
2024-08-26	5	partly_thawed	73.9295076
2024-08-27	5	partly_thawed	72.4702136

Table C3. Continued.

date	chamber	thaw_stage	VWC
2024-08-28	5	partly_thawed	72.1735294
2024-08-29	5	partly_thawed	72.195875
2024-08-30	5	partly_thawed	72.1454834
2024-08-31	5	partly_thawed	72.2044971
2025-05-16	5	partly_thawed	38.8703123
2025-05-17	5	partly_thawed	42.6859796
2025-05-18	5	partly_thawed	45.9623006
2025-05-19	5	partly_thawed	47.3897238
2025-05-20	5	partly_thawed	48.8084877
2025-05-21	5	partly_thawed	50.2713509
2025-05-22	5	partly_thawed	49.7731398
2025-05-23	5	partly_thawed	50.3692614
2025-05-24	5	partly_thawed	51.7716447
2025-05-25	5	partly_thawed	54.2216691
2025-05-26	5	partly_thawed	55.2552748
2025-05-27	5	partly_thawed	55.9196644
2025-05-28	5	partly_thawed	56.2619085
2025-05-29	5	partly_thawed	57.2534429
2025-05-30	5	partly_thawed	57.0787485
2025-05-31	5	partly_thawed	57.0124728
2025-06-01	5	partly_thawed	56.9163938
2025-06-02	5	partly_thawed	59.6102572
2025-06-03	5	partly_thawed	57.7415809
2025-06-04	5	partly_thawed	57.740284
2025-06-05	5	partly_thawed	57.8346803
2025-06-06	5	partly_thawed	58.0532865
2025-06-07	5	partly_thawed	58.6667034
2025-06-08	5	partly_thawed	68.2655768
2025-06-09	5	partly_thawed	66.1097746
2025-06-10	5	partly_thawed	67.2836741
2025-06-11	5	partly_thawed	67.0146094
2025-06-12	5	partly_thawed	67.0965537
2025-06-13	5	partly_thawed	67.905056
2025-06-14	5	partly_thawed	68.576366
2025-06-15	5	partly_thawed	68.3105105
2025-06-16	5	partly_thawed	68.6090593
2025-06-17	5	partly_thawed	72.1929534
2025-06-18	5	partly_thawed	71.5965323
2025-06-19	5	partly_thawed	71.028011
2025-06-20	5	partly_thawed	70.4813804
2025-06-21	5	partly_thawed	70.767944
2025-06-22	5	partly_thawed	70.7834957
2025-06-23	5	partly_thawed	71.2576672
2025-06-24	5	partly_thawed	71.9317509
2025-06-25	5	partly_thawed	71.8738903
2025-06-26	5	partly_thawed	71.7151122
2025-06-27	5	partly_thawed	71.695347
2025-06-28	5	partly_thawed	72.0337285
2025-06-29	5	partly_thawed	72.9613079
2025-06-30	5	partly_thawed	72.4493385
2025-07-01	5	partly_thawed	72.4260203
2025-07-02	5	partly_thawed	72.3779499
2025-07-03	5	partly_thawed	72.573169
2025-07-04	5	partly_thawed	72.3221643
2025-07-05	5	partly_thawed	72.506088

Table C3. Continued.

date	chamber	thaw_stage	VWC
2025-07-06	5	partly_thawed	72.6390257
2025-07-07	5	partly_thawed	72.4699037
2025-07-08	5	partly_thawed	72.4251401
2025-07-09	5	partly_thawed	72.4098445
2025-07-10	5	partly_thawed	72.8531183
2025-07-11	5	partly_thawed	72.7644185
2025-07-12	5	partly_thawed	72.9727688
2025-07-13	5	partly_thawed	73.3946316
2025-07-14	5	partly_thawed	73.2657621
2025-07-15	5	partly_thawed	73.2707867
2025-07-16	5	partly_thawed	73.2046517
2025-07-17	5	partly_thawed	73.2303215
2025-07-18	5	partly_thawed	73.5544391
2025-07-19	5	partly_thawed	73.2307043
2025-07-20	5	partly_thawed	73.6010232
2025-07-21	5	partly_thawed	73.5439315
2025-07-22	5	partly_thawed	69.2146213
2025-07-23	5	partly_thawed	69.1599561
2025-07-24	5	partly_thawed	68.8324611
2025-07-25	5	partly_thawed	68.8059575
2025-07-26	5	partly_thawed	68.5905469
2025-07-27	5	partly_thawed	68.050301
2025-07-28	5	partly_thawed	68.8661191
2025-07-29	5	partly_thawed	73.6819074
2025-07-30	5	partly_thawed	72.7756391
2025-07-31	5	partly_thawed	72.4939806
2025-08-01	5	partly_thawed	72.9695913
2025-08-02	5	partly_thawed	72.8938286
2025-08-03	5	partly_thawed	72.6904782
2025-08-04	5	partly_thawed	72.0246217
2025-08-05	5	partly_thawed	73.4605355
2025-08-06	5	partly_thawed	72.908535
2025-08-07	5	partly_thawed	72.7084488
2025-08-08	5	partly_thawed	72.7447147
2025-08-09	5	partly_thawed	72.6186498
2025-08-10	5	partly_thawed	72.671094
2025-08-11	5	partly_thawed	73.885777
2025-08-12	5	partly_thawed	73.7526503
2025-08-13	5	partly_thawed	73.6563077
2024-05-13	6	partly_thawed	24.4257762
2024-05-14	6	partly_thawed	24.5878508
2024-05-15	6	partly_thawed	24.4448328
2024-05-16	6	partly_thawed	24.6131899
2024-05-17	6	partly_thawed	25.1848029
2024-05-18	6	partly_thawed	25.7065827
2024-05-19	6	partly_thawed	26.9261162
2024-05-20	6	partly_thawed	27.1569068
2024-05-21	6	partly_thawed	27.4096662
2024-05-22	6	partly_thawed	28.6730808
2024-05-23	6	partly_thawed	31.7494113
2024-05-24	6	partly_thawed	34.3640755
2024-05-25	6	partly_thawed	34.8143188
2024-05-26	6	partly_thawed	35.1932261
2024-05-27	6	partly_thawed	35.2205199
2024-05-28	6	partly_thawed	40.3704005
2024-05-29	6	partly_thawed	39.3222946
2024-05-30	6	partly_thawed	38.9569375

Table C3. Continued.

date	chamber	thaw_stage	VWC
2024-05-31	6	partly_thawed	38.7289791
2024-06-01	6	partly_thawed	38.5680946
2024-06-02	6	partly_thawed	38.4359373
2024-06-03	6	partly_thawed	38.468677
2024-06-04	6	partly_thawed	39.9270505
2024-06-05	6	partly_thawed	39.4915139
2024-06-06	6	partly_thawed	39.3634539
2024-06-07	6	partly_thawed	39.193098
2024-06-08	6	partly_thawed	38.9769612
2024-06-09	6	partly_thawed	38.867746
2024-06-10	6	partly_thawed	38.9599343
2024-06-11	6	partly_thawed	38.9346689
2024-06-12	6	partly_thawed	38.8985419
2024-06-13	6	partly_thawed	38.7634826
2024-06-14	6	partly_thawed	38.8436028
2024-06-15	6	partly_thawed	38.6154244
2024-06-16	6	partly_thawed	38.804368
2024-06-17	6	partly_thawed	38.5831637
2024-06-18	6	partly_thawed	38.6851732
2024-06-19	6	partly_thawed	38.9858723
2024-06-20	6	partly_thawed	38.794138
2024-06-21	6	partly_thawed	39.0802944
2024-06-22	6	partly_thawed	39.0107282
2024-06-23	6	partly_thawed	39.1201403
2024-06-24	6	partly_thawed	39.0338005
2024-06-25	6	partly_thawed	39.2721773
2024-06-26	6	partly_thawed	38.9670597
2024-06-27	6	partly_thawed	39.170119
2024-06-28	6	partly_thawed	39.4639095
2024-06-29	6	partly_thawed	38.857074
2024-06-30	6	partly_thawed	38.7898457
2024-07-01	6	partly_thawed	38.8410381
2024-07-02	6	partly_thawed	38.7564236
2024-07-03	6	partly_thawed	38.7739319
2024-07-04	6	partly_thawed	38.5030175
2024-07-05	6	partly_thawed	38.4387787
2024-07-06	6	partly_thawed	38.3715087
2024-07-07	6	partly_thawed	38.55256
2024-07-08	6	partly_thawed	38.3652913
2024-07-09	6	partly_thawed	38.5583632
2024-07-10	6	partly_thawed	38.5734034
2024-07-11	6	partly_thawed	38.4609223
2024-07-12	6	partly_thawed	38.4398337
2024-07-13	6	partly_thawed	38.5383508
2024-07-14	6	partly_thawed	38.6874423
2024-07-15	6	partly_thawed	38.5478282
2024-07-16	6	partly_thawed	38.2795836
2024-07-17	6	partly_thawed	38.3958645
2024-07-18	6	partly_thawed	38.2736595
2024-07-19	6	partly_thawed	38.0218329
2024-07-20	6	partly_thawed	38.0112551
2024-07-21	6	partly_thawed	38.2432593
2024-07-22	6	partly_thawed	37.9671464
2024-07-23	6	partly_thawed	37.8202884
2024-07-24	6	partly_thawed	37.5676232
2024-07-25	6	partly_thawed	37.6501921
2024-07-26	6	partly_thawed	38.2144615

Table C3. Continued.

date	chamber	thaw_stage	VWC
2024-07-27	6	partly_thawed	38.082619
2024-07-28	6	partly_thawed	37.8939965
2024-07-29	6	partly_thawed	37.8951742
2024-07-30	6	partly_thawed	37.9486412
2024-07-31	6	partly_thawed	38.1121711
2024-08-01	6	partly_thawed	38.0540679
2024-08-02	6	partly_thawed	38.2045299
2024-08-03	6	partly_thawed	38.4097386
2024-08-04	6	partly_thawed	38.6414599
2024-08-05	6	partly_thawed	38.7234181
2024-08-06	6	partly_thawed	38.7263984
2024-08-07	6	partly_thawed	38.4778017
2024-08-08	6	partly_thawed	37.7829221
2024-08-09	6	partly_thawed	37.4793786
2024-08-10	6	partly_thawed	40.0600839
2024-08-11	6	partly_thawed	42.8598558
2024-08-12	6	partly_thawed	43.4056764
2024-08-13	6	partly_thawed	41.7240635
2024-08-14	6	partly_thawed	41.2876133
2024-08-15	6	partly_thawed	40.9155542
2024-08-16	6	partly_thawed	40.7254592
2024-08-17	6	partly_thawed	41.6914071
2024-08-18	6	partly_thawed	41.2872277
2024-08-19	6	partly_thawed	41.0267432
2024-08-20	6	partly_thawed	41.6657965
2024-08-21	6	partly_thawed	40.6937557
2024-08-22	6	partly_thawed	40.4246475
2024-08-23	6	partly_thawed	40.2649337
2024-08-24	6	partly_thawed	41.0073861
2024-08-25	6	partly_thawed	46.6533004
2024-08-26	6	partly_thawed	44.5352978
2024-08-27	6	partly_thawed	42.8553482
2024-08-28	6	partly_thawed	42.5901719
2024-08-29	6	partly_thawed	42.1719278
2024-08-30	6	partly_thawed	42.0296061
2024-08-31	6	partly_thawed	42.2743034
2025-05-13	6	partly_thawed	33.6914625
2025-05-14	6	partly_thawed	34.6572765
2025-05-15	6	partly_thawed	34.5047943
2025-05-16	6	partly_thawed	34.9622638
2025-05-17	6	partly_thawed	35.0442179
2025-05-18	6	partly_thawed	35.3933297
2025-05-19	6	partly_thawed	36.9535508
2025-05-20	6	partly_thawed	39.0550498
2025-05-21	6	partly_thawed	41.3061747
2025-05-22	6	partly_thawed	41.3072513
2025-05-23	6	partly_thawed	42.6545269
2025-05-24	6	partly_thawed	46.8812843
2025-05-25	6	partly_thawed	47.0938394
2025-05-26	6	partly_thawed	47.1728971
2025-05-27	6	partly_thawed	46.8862849
2025-05-28	6	partly_thawed	47.0602668
2025-05-29	6	partly_thawed	47.1322004
2025-05-30	6	partly_thawed	46.1384207
2025-05-31	6	partly_thawed	45.705344
2025-06-01	6	partly_thawed	45.3410932
2025-06-02	6	partly_thawed	45.6964165

Table C3. Continued.

date	chamber	thaw_stage	VWC
2025-06-03	6	partly_thawed	45.4275321
2025-06-04	6	partly_thawed	45.267919
2025-06-05	6	partly_thawed	44.5548535
2025-06-06	6	partly_thawed	44.2060022
2025-06-07	6	partly_thawed	44.4907426
2025-06-08	6	partly_thawed	46.8087832
2025-06-09	6	partly_thawed	45.4119553
2025-06-10	6	partly_thawed	45.637654
2025-06-11	6	partly_thawed	44.9481593
2025-06-12	6	partly_thawed	44.7019053
2025-06-13	6	partly_thawed	44.9276393
2025-06-14	6	partly_thawed	44.6392618
2025-06-15	6	partly_thawed	44.3114437
2025-06-16	6	partly_thawed	44.2760487
2025-06-17	6	partly_thawed	46.1654783
2025-06-18	6	partly_thawed	45.5111733
2025-06-19	6	partly_thawed	45.3859792
2025-06-20	6	partly_thawed	45.1341576
2025-06-21	6	partly_thawed	44.9835225
2025-06-22	6	partly_thawed	44.8388617
2025-06-23	6	partly_thawed	45.0161311
2025-06-24	6	partly_thawed	44.7029506
2025-06-25	6	partly_thawed	45.0839704
2025-06-26	6	partly_thawed	45.0759162
2025-06-27	6	partly_thawed	44.7520846
2025-06-28	6	partly_thawed	45.0520049
2025-06-29	6	partly_thawed	45.316209
2025-06-30	6	partly_thawed	45.1326679
2025-07-01	6	partly_thawed	45.1610061
2025-07-02	6	partly_thawed	45.2237421
2025-07-03	6	partly_thawed	45.4152113
2025-07-04	6	partly_thawed	45.4158629
2025-07-05	6	partly_thawed	45.3657303
2025-07-06	6	partly_thawed	45.4587191
2025-07-07	6	partly_thawed	45.2364246
2025-07-08	6	partly_thawed	45.5403905
2025-07-09	6	partly_thawed	45.2469878
2025-07-10	6	partly_thawed	45.3723966
2025-07-11	6	partly_thawed	45.2759769
2025-07-12	6	partly_thawed	45.0351748
2025-07-13	6	partly_thawed	44.9947346
2025-07-14	6	partly_thawed	45.0673527
2025-07-15	6	partly_thawed	45.040618
2025-07-16	6	partly_thawed	44.7554142
2025-07-17	6	partly_thawed	44.504684
2025-07-18	6	partly_thawed	44.6625771
2025-07-19	6	partly_thawed	44.3800746
2025-07-20	6	partly_thawed	44.1760304
2025-07-21	6	partly_thawed	44.060276
2025-07-22	6	partly_thawed	44.0071614
2025-07-23	6	partly_thawed	43.4985294
2025-07-24	6	partly_thawed	42.9361388
2025-07-25	6	partly_thawed	42.3050128
2025-07-26	6	partly_thawed	42.3236148
2025-07-27	6	partly_thawed	41.686167
2025-07-28	6	partly_thawed	42.1187001
2025-07-29	6	partly_thawed	43.6492636

Table C3. Continued.

date	chamber	thaw_stage	VWC
2025-07-30	6	partly_thawed	44.3789372
2025-07-31	6	partly_thawed	44.134676
2025-08-01	6	partly_thawed	44.788446
2025-08-02	6	partly_thawed	44.2818034
2025-08-03	6	partly_thawed	43.8155932
2025-08-04	6	partly_thawed	43.0293282
2025-08-05	6	partly_thawed	43.6913037
2025-08-06	6	partly_thawed	44.3824709
2025-08-07	6	partly_thawed	44.4156602
2025-08-08	6	partly_thawed	43.8285302
2025-08-09	6	partly_thawed	42.9554348
2025-08-10	6	partly_thawed	43.5089903
2025-08-11	6	partly_thawed	43.4041283
2025-08-12	6	partly_thawed	43.2266381
2025-08-13	6	partly_thawed	44.0843055
2024-05-10	7	fully_thawed	100
2024-05-11	7	fully_thawed	100
2024-05-12	7	fully_thawed	100
2024-05-13	7	fully_thawed	100
2024-05-14	7	fully_thawed	100
2024-05-15	7	fully_thawed	100
2024-05-16	7	fully_thawed	100
2024-05-17	7	fully_thawed	100
2024-05-18	7	fully_thawed	100
2024-05-19	7	fully_thawed	100
2024-05-20	7	fully_thawed	100
2024-05-21	7	fully_thawed	100
2024-05-22	7	fully_thawed	100
2024-05-23	7	fully_thawed	100
2024-05-24	7	fully_thawed	100
2024-05-25	7	fully_thawed	100
2024-05-26	7	fully_thawed	100
2024-05-27	7	fully_thawed	100
2024-05-28	7	fully_thawed	100
2024-05-29	7	fully_thawed	100
2024-05-30	7	fully_thawed	100
2024-05-31	7	fully_thawed	100
2024-06-01	7	fully_thawed	100
2024-06-02	7	fully_thawed	100
2024-06-03	7	fully_thawed	100
2024-06-04	7	fully_thawed	100
2024-06-05	7	fully_thawed	100
2024-06-06	7	fully_thawed	100
2024-06-07	7	fully_thawed	100
2024-06-08	7	fully_thawed	100
2024-06-09	7	fully_thawed	100
2024-06-10	7	fully_thawed	100
2024-06-11	7	fully_thawed	100
2024-06-12	7	fully_thawed	100
2024-06-13	7	fully_thawed	100
2024-06-14	7	fully_thawed	100
2024-06-15	7	fully_thawed	100
2024-06-16	7	fully_thawed	100
2024-06-17	7	fully_thawed	100
2024-06-18	7	fully_thawed	100
2024-06-19	7	fully_thawed	100
2024-06-20	7	fully_thawed	100
2024-06-21	7	fully_thawed	100
2024-06-22	7	fully_thawed	100

Table C3. Continued.

date	chamber	thaw_stage	VWC
2024-06-23	7	fully_thawed	100
2024-06-24	7	fully_thawed	100
2024-06-25	7	fully_thawed	100
2024-06-26	7	fully_thawed	100
2024-06-27	7	fully_thawed	100
2024-06-28	7	fully_thawed	100
2024-06-29	7	fully_thawed	100
2024-06-30	7	fully_thawed	100
2024-07-01	7	fully_thawed	100
2024-07-02	7	fully_thawed	100
2024-07-03	7	fully_thawed	100
2024-07-04	7	fully_thawed	100
2024-07-05	7	fully_thawed	100
2024-07-06	7	fully_thawed	100
2024-07-07	7	fully_thawed	100
2024-07-08	7	fully_thawed	100
2024-07-09	7	fully_thawed	100
2024-07-10	7	fully_thawed	100
2024-07-11	7	fully_thawed	100
2024-07-12	7	fully_thawed	100
2024-07-13	7	fully_thawed	100
2024-07-14	7	fully_thawed	100
2024-07-15	7	fully_thawed	100
2024-07-16	7	fully_thawed	100
2024-07-17	7	fully_thawed	100
2024-07-18	7	fully_thawed	100
2024-07-19	7	fully_thawed	100
2024-07-20	7	fully_thawed	100
2024-07-21	7	fully_thawed	100
2024-07-22	7	fully_thawed	100
2024-07-23	7	fully_thawed	100
2024-07-24	7	fully_thawed	100
2024-07-25	7	fully_thawed	100
2024-07-26	7	fully_thawed	100
2024-07-27	7	fully_thawed	100
2024-07-28	7	fully_thawed	100
2024-07-29	7	fully_thawed	100
2024-07-30	7	fully_thawed	100
2024-07-31	7	fully_thawed	100
2024-08-01	7	fully_thawed	100
2024-08-02	7	fully_thawed	100
2024-08-03	7	fully_thawed	100
2024-08-04	7	fully_thawed	100
2024-08-05	7	fully_thawed	100
2024-08-06	7	fully_thawed	100
2024-08-07	7	fully_thawed	100
2024-08-08	7	fully_thawed	100
2024-08-09	7	fully_thawed	100
2024-08-10	7	fully_thawed	100
2024-08-11	7	fully_thawed	100
2024-08-12	7	fully_thawed	100
2024-08-13	7	fully_thawed	100
2024-08-14	7	fully_thawed	100
2024-08-15	7	fully_thawed	100
2024-08-16	7	fully_thawed	100
2024-08-17	7	fully_thawed	100
2024-08-18	7	fully_thawed	100
2024-08-19	7	fully_thawed	100
2024-08-20	7	fully_thawed	100

Table C3. Continued.

date	chamber	thaw_stage	VWC
2024-08-21	7	fully_thawed	100
2024-08-22	7	fully_thawed	100
2024-08-23	7	fully_thawed	100
2024-08-24	7	fully_thawed	100
2024-08-25	7	fully_thawed	100
2024-08-26	7	fully_thawed	100
2024-08-27	7	fully_thawed	100
2024-08-28	7	fully_thawed	100
2024-08-29	7	fully_thawed	100
2024-08-30	7	fully_thawed	100
2024-08-31	7	fully_thawed	100
2025-05-29	7	fully_thawed	100
2025-05-30	7	fully_thawed	100
2025-05-31	7	fully_thawed	100
2025-06-01	7	fully_thawed	100
2025-06-02	7	fully_thawed	100
2025-06-03	7	fully_thawed	100
2025-06-04	7	fully_thawed	100
2025-06-05	7	fully_thawed	100
2025-06-06	7	fully_thawed	100
2025-06-07	7	fully_thawed	100
2025-06-08	7	fully_thawed	100
2025-06-09	7	fully_thawed	100
2025-06-10	7	fully_thawed	100
2025-06-11	7	fully_thawed	100
2025-06-12	7	fully_thawed	100
2025-06-13	7	fully_thawed	100
2025-06-14	7	fully_thawed	100
2025-06-15	7	fully_thawed	100
2025-06-16	7	fully_thawed	100
2025-06-17	7	fully_thawed	100
2025-06-18	7	fully_thawed	100
2025-06-19	7	fully_thawed	100
2025-06-20	7	fully_thawed	100
2025-06-21	7	fully_thawed	100
2025-06-22	7	fully_thawed	100
2025-06-23	7	fully_thawed	100
2025-06-24	7	fully_thawed	100
2025-06-25	7	fully_thawed	100
2025-06-26	7	fully_thawed	100
2025-06-27	7	fully_thawed	100
2025-06-28	7	fully_thawed	100
2025-06-29	7	fully_thawed	100
2025-06-30	7	fully_thawed	100
2025-07-01	7	fully_thawed	100
2025-07-02	7	fully_thawed	100
2025-07-03	7	fully_thawed	100
2025-07-04	7	fully_thawed	100
2025-07-05	7	fully_thawed	100
2025-07-06	7	fully_thawed	100
2025-07-07	7	fully_thawed	100
2025-07-08	7	fully_thawed	100
2025-07-09	7	fully_thawed	100
2025-07-10	7	fully_thawed	100
2025-07-11	7	fully_thawed	100
2025-07-12	7	fully_thawed	100
2025-07-13	7	fully_thawed	100
2025-07-14	7	fully_thawed	100
2025-07-15	7	fully_thawed	100

Table C3. Continued.

date	chamber	thaw_stage	VWC
2025-07-16	7	fully_thawed	100
2025-07-17	7	fully_thawed	100
2025-07-18	7	fully_thawed	100
2025-07-19	7	fully_thawed	100
2025-07-20	7	fully_thawed	100
2025-07-21	7	fully_thawed	100
2025-07-22	7	fully_thawed	100
2025-07-23	7	fully_thawed	100
2025-07-24	7	fully_thawed	100
2025-07-25	7	fully_thawed	100
2025-07-26	7	fully_thawed	100
2025-07-27	7	fully_thawed	100
2025-07-28	7	fully_thawed	100
2025-07-29	7	fully_thawed	100
2025-07-30	7	fully_thawed	100
2025-07-31	7	fully_thawed	100
2025-08-01	7	fully_thawed	100
2025-08-02	7	fully_thawed	100
2025-08-03	7	fully_thawed	100
2025-08-04	7	fully_thawed	100
2025-08-05	7	fully_thawed	100
2025-08-06	7	fully_thawed	100
2025-08-07	7	fully_thawed	100
2025-08-08	7	fully_thawed	100
2025-08-09	7	fully_thawed	100
2025-08-10	7	fully_thawed	100
2025-08-11	7	fully_thawed	100
2025-08-12	7	fully_thawed	100
2025-08-13	7	fully_thawed	100
2024-05-18	8	fully_thawed	100
2024-05-22	8	fully_thawed	100
2024-05-23	8	fully_thawed	100
2024-05-24	8	fully_thawed	100
2024-05-25	8	fully_thawed	100
2024-05-26	8	fully_thawed	100
2024-05-27	8	fully_thawed	100
2024-05-28	8	fully_thawed	100
2024-05-29	8	fully_thawed	100
2024-05-30	8	fully_thawed	100
2024-05-31	8	fully_thawed	100
2024-06-01	8	fully_thawed	100
2024-06-02	8	fully_thawed	100
2024-06-03	8	fully_thawed	100
2024-06-04	8	fully_thawed	100
2024-06-05	8	fully_thawed	100
2024-06-06	8	fully_thawed	100
2024-06-07	8	fully_thawed	100
2024-06-08	8	fully_thawed	100
2024-06-09	8	fully_thawed	100
2024-06-10	8	fully_thawed	100
2024-06-11	8	fully_thawed	100
2024-06-12	8	fully_thawed	100
2024-06-13	8	fully_thawed	100
2024-06-14	8	fully_thawed	100
2024-06-15	8	fully_thawed	100
2024-06-16	8	fully_thawed	100

Table C3. Continued.

date	chamber	thaw_stage	VWC
2024-06-17	8	fully_thawed	100
2024-06-18	8	fully_thawed	100
2024-06-19	8	fully_thawed	100
2024-06-20	8	fully_thawed	100
2024-06-21	8	fully_thawed	100
2024-06-22	8	fully_thawed	100
2024-06-23	8	fully_thawed	100
2024-06-24	8	fully_thawed	100
2024-06-25	8	fully_thawed	100
2024-06-26	8	fully_thawed	100
2024-06-27	8	fully_thawed	100
2024-06-28	8	fully_thawed	100
2024-06-29	8	fully_thawed	100
2024-06-30	8	fully_thawed	100
2024-07-01	8	fully_thawed	100
2024-07-02	8	fully_thawed	100
2024-07-03	8	fully_thawed	100
2024-07-04	8	fully_thawed	100
2024-07-05	8	fully_thawed	100
2024-07-06	8	fully_thawed	100
2024-07-07	8	fully_thawed	100
2024-07-08	8	fully_thawed	100
2024-07-09	8	fully_thawed	100
2024-07-10	8	fully_thawed	100
2024-07-11	8	fully_thawed	100
2024-07-12	8	fully_thawed	100
2024-07-13	8	fully_thawed	100
2024-07-14	8	fully_thawed	100
2024-07-15	8	fully_thawed	100
2024-07-16	8	fully_thawed	100
2024-07-17	8	fully_thawed	100
2024-07-18	8	fully_thawed	100
2024-07-19	8	fully_thawed	100
2024-07-20	8	fully_thawed	100
2024-07-21	8	fully_thawed	100
2024-07-22	8	fully_thawed	100
2024-07-23	8	fully_thawed	100
2024-07-24	8	fully_thawed	100
2024-07-25	8	fully_thawed	100
2024-07-26	8	fully_thawed	100
2024-07-27	8	fully_thawed	100
2024-07-28	8	fully_thawed	100
2024-07-29	8	fully_thawed	100
2024-07-30	8	fully_thawed	100
2024-07-31	8	fully_thawed	100
2024-08-01	8	fully_thawed	100
2024-08-02	8	fully_thawed	100
2024-08-03	8	fully_thawed	100
2024-08-04	8	fully_thawed	100
2024-08-05	8	fully_thawed	100
2024-08-06	8	fully_thawed	100
2024-08-07	8	fully_thawed	100
2024-08-08	8	fully_thawed	100
2024-08-09	8	fully_thawed	100
2024-08-10	8	fully_thawed	100
2024-08-11	8	fully_thawed	100
2024-08-12	8	fully_thawed	100

Table C3. Continued.

date	chamber	thaw_stage	VWC
2024-08-13	8	fully_thawed	100
2024-08-14	8	fully_thawed	100
2024-08-15	8	fully_thawed	100
2024-08-16	8	fully_thawed	100
2024-08-17	8	fully_thawed	100
2024-08-18	8	fully_thawed	100
2024-08-19	8	fully_thawed	100
2024-08-20	8	fully_thawed	100
2024-08-21	8	fully_thawed	100
2024-08-22	8	fully_thawed	100
2024-08-23	8	fully_thawed	100
2024-08-24	8	fully_thawed	100
2024-08-25	8	fully_thawed	100
2024-08-26	8	fully_thawed	100
2024-08-27	8	fully_thawed	100
2024-08-28	8	fully_thawed	100
2024-08-29	8	fully_thawed	100
2024-08-30	8	fully_thawed	100
2024-08-31	8	fully_thawed	100
2025-05-29	8	fully_thawed	100
2025-05-30	8	fully_thawed	100
2025-05-31	8	fully_thawed	100
2025-06-01	8	fully_thawed	100
2025-06-02	8	fully_thawed	100
2025-06-03	8	fully_thawed	100
2025-06-04	8	fully_thawed	100
2025-06-05	8	fully_thawed	100
2025-06-06	8	fully_thawed	100
2025-06-07	8	fully_thawed	100
2025-06-08	8	fully_thawed	100
2025-06-09	8	fully_thawed	100
2025-06-10	8	fully_thawed	100
2025-06-11	8	fully_thawed	100
2025-06-12	8	fully_thawed	100
2025-06-13	8	fully_thawed	100
2025-06-14	8	fully_thawed	100
2025-06-15	8	fully_thawed	100
2025-06-16	8	fully_thawed	100
2025-06-17	8	fully_thawed	100
2025-06-18	8	fully_thawed	100
2025-06-19	8	fully_thawed	100
2025-06-20	8	fully_thawed	100
2025-06-21	8	fully_thawed	100
2025-06-22	8	fully_thawed	100
2025-06-23	8	fully_thawed	100
2025-06-24	8	fully_thawed	100
2025-06-25	8	fully_thawed	100
2025-06-26	8	fully_thawed	100
2025-06-27	8	fully_thawed	100
2025-06-28	8	fully_thawed	100
2025-06-29	8	fully_thawed	100
2025-06-30	8	fully_thawed	100
2025-07-01	8	fully_thawed	100
2025-07-02	8	fully_thawed	100
2025-07-03	8	fully_thawed	100
2025-07-04	8	fully_thawed	100
2025-07-05	8	fully_thawed	100

Table C3. Continued.

date	chamber	thaw_stage	VWC
2025-07-06	8	fully_thawed	100
2025-07-07	8	fully_thawed	100
2025-07-08	8	fully_thawed	100
2025-07-09	8	fully_thawed	100
2025-07-10	8	fully_thawed	100
2025-07-11	8	fully_thawed	100
2025-07-12	8	fully_thawed	100
2025-07-13	8	fully_thawed	100
2025-07-14	8	fully_thawed	100
2025-07-15	8	fully_thawed	100
2025-07-16	8	fully_thawed	100
2025-07-17	8	fully_thawed	100
2025-07-18	8	fully_thawed	100
2025-07-19	8	fully_thawed	100
2025-07-20	8	fully_thawed	100
2025-07-21	8	fully_thawed	100
2025-07-22	8	fully_thawed	100
2025-07-23	8	fully_thawed	100
2025-07-24	8	fully_thawed	100
2025-07-25	8	fully_thawed	100
2025-07-26	8	fully_thawed	100
2025-07-27	8	fully_thawed	100
2025-07-28	8	fully_thawed	100
2025-07-29	8	fully_thawed	100
2025-07-30	8	fully_thawed	100
2025-07-31	8	fully_thawed	100
2025-08-01	8	fully_thawed	100
2025-08-02	8	fully_thawed	100
2025-08-03	8	fully_thawed	100
2025-08-04	8	fully_thawed	100
2025-08-05	8	fully_thawed	100
2025-08-06	8	fully_thawed	100
2025-08-07	8	fully_thawed	100
2025-08-08	8	fully_thawed	100
2025-08-09	8	fully_thawed	100
2025-08-10	8	fully_thawed	100
2025-08-11	8	fully_thawed	100
2025-08-12	8	fully_thawed	100
2025-08-13	8	fully_thawed	100
2024-05-25	9	fully_thawed	98.6794751
2024-05-26	9	fully_thawed	100
2024-05-27	9	fully_thawed	100
2024-05-28	9	fully_thawed	100
2024-05-29	9	fully_thawed	100
2024-05-30	9	fully_thawed	100
2024-05-31	9	fully_thawed	100
2024-06-01	9	fully_thawed	100
2024-06-02	9	fully_thawed	100
2024-06-03	9	fully_thawed	100
2024-06-04	9	fully_thawed	100
2024-06-05	9	fully_thawed	100
2024-06-06	9	fully_thawed	100
2024-06-07	9	fully_thawed	100
2024-06-08	9	fully_thawed	100
2024-06-09	9	fully_thawed	100
2024-06-10	9	fully_thawed	100
2024-06-11	9	fully_thawed	100

Table C3. Continued.

date	chamber	thaw_stage	VWC
2024-06-12	9	fully_thawed	100
2024-06-13	9	fully_thawed	100
2024-06-14	9	fully_thawed	100
2024-06-15	9	fully_thawed	100
2024-06-16	9	fully_thawed	100
2024-06-17	9	fully_thawed	100
2024-06-18	9	fully_thawed	100
2024-06-19	9	fully_thawed	100
2024-06-20	9	fully_thawed	100
2024-06-21	9	fully_thawed	100
2024-06-22	9	fully_thawed	100
2024-06-23	9	fully_thawed	100
2024-06-24	9	fully_thawed	100
2024-06-25	9	fully_thawed	100
2024-06-26	9	fully_thawed	100
2024-06-27	9	fully_thawed	100
2024-06-28	9	fully_thawed	100
2024-06-29	9	fully_thawed	100
2024-06-30	9	fully_thawed	100
2024-07-01	9	fully_thawed	100
2024-07-02	9	fully_thawed	100
2024-07-03	9	fully_thawed	100
2024-07-04	9	fully_thawed	100
2024-07-05	9	fully_thawed	100
2024-07-06	9	fully_thawed	100
2024-07-07	9	fully_thawed	100
2024-07-08	9	fully_thawed	100
2024-07-09	9	fully_thawed	100
2024-07-10	9	fully_thawed	100
2024-07-11	9	fully_thawed	100
2024-07-12	9	fully_thawed	100
2024-07-13	9	fully_thawed	100
2024-07-14	9	fully_thawed	100
2024-07-15	9	fully_thawed	100
2024-07-16	9	fully_thawed	100
2024-07-17	9	fully_thawed	100
2024-07-18	9	fully_thawed	100
2024-07-19	9	fully_thawed	100
2024-07-20	9	fully_thawed	100
2024-07-21	9	fully_thawed	100
2024-07-22	9	fully_thawed	100
2024-07-23	9	fully_thawed	100
2024-07-24	9	fully_thawed	100
2024-07-25	9	fully_thawed	100
2024-07-26	9	fully_thawed	100
2024-07-27	9	fully_thawed	100
2024-07-28	9	fully_thawed	100
2024-07-29	9	fully_thawed	100
2024-07-30	9	fully_thawed	100
2024-07-31	9	fully_thawed	100
2024-08-01	9	fully_thawed	100
2024-08-02	9	fully_thawed	100
2024-08-03	9	fully_thawed	100
2024-08-04	9	fully_thawed	100
2024-08-05	9	fully_thawed	100
2024-08-06	9	fully_thawed	100
2024-08-07	9	fully_thawed	100

Table C3. Continued.

date	chamber	thaw_stage	VWC
2024-08-08	9	fully_thawed	100
2024-08-09	9	fully_thawed	100
2024-08-10	9	fully_thawed	100
2024-08-11	9	fully_thawed	100
2024-08-12	9	fully_thawed	100
2024-08-13	9	fully_thawed	100
2024-08-14	9	fully_thawed	100
2024-08-15	9	fully_thawed	100
2024-08-16	9	fully_thawed	100
2024-08-17	9	fully_thawed	100
2024-08-18	9	fully_thawed	100
2024-08-19	9	fully_thawed	100
2024-08-20	9	fully_thawed	100
2024-08-21	9	fully_thawed	100
2024-08-22	9	fully_thawed	100
2024-08-23	9	fully_thawed	100
2024-08-24	9	fully_thawed	100
2024-08-25	9	fully_thawed	100
2024-08-26	9	fully_thawed	100
2024-08-27	9	fully_thawed	100
2024-08-28	9	fully_thawed	100
2024-08-29	9	fully_thawed	100
2024-08-30	9	fully_thawed	100
2024-08-31	9	fully_thawed	100
2025-05-30	9	fully_thawed	100
2025-05-31	9	fully_thawed	100
2025-06-01	9	fully_thawed	100
2025-06-02	9	fully_thawed	100
2025-06-03	9	fully_thawed	100
2025-06-04	9	fully_thawed	100
2025-06-05	9	fully_thawed	100
2025-06-06	9	fully_thawed	100
2025-06-07	9	fully_thawed	100
2025-06-08	9	fully_thawed	100
2025-06-09	9	fully_thawed	100
2025-06-10	9	fully_thawed	100
2025-06-11	9	fully_thawed	100
2025-06-12	9	fully_thawed	100
2025-06-13	9	fully_thawed	100
2025-06-14	9	fully_thawed	100
2025-06-15	9	fully_thawed	100
2025-06-16	9	fully_thawed	100
2025-06-17	9	fully_thawed	100
2025-06-18	9	fully_thawed	100
2025-06-19	9	fully_thawed	100
2025-06-20	9	fully_thawed	100
2025-06-21	9	fully_thawed	100
2025-06-22	9	fully_thawed	100
2025-06-23	9	fully_thawed	100
2025-06-24	9	fully_thawed	100

Table C3. Continued.

date	chamber	thaw_stage	VWC
2025-06-25	9	fully_thawed	100
2025-06-26	9	fully_thawed	100
2025-06-27	9	fully_thawed	100
2025-06-28	9	fully_thawed	100
2025-06-29	9	fully_thawed	100
2025-06-30	9	fully_thawed	100
2025-07-01	9	fully_thawed	100
2025-07-02	9	fully_thawed	100
2025-07-03	9	fully_thawed	100
2025-07-04	9	fully_thawed	100
2025-07-05	9	fully_thawed	100
2025-07-06	9	fully_thawed	100
2025-07-07	9	fully_thawed	100
2025-07-08	9	fully_thawed	100
2025-07-09	9	fully_thawed	100
2025-07-10	9	fully_thawed	100
2025-07-11	9	fully_thawed	100
2025-07-12	9	fully_thawed	100
2025-07-13	9	fully_thawed	100
2025-07-14	9	fully_thawed	100
2025-07-15	9	fully_thawed	100
2025-07-16	9	fully_thawed	100
2025-07-17	9	fully_thawed	100
2025-07-18	9	fully_thawed	100
2025-07-19	9	fully_thawed	100
2025-07-20	9	fully_thawed	100
2025-07-21	9	fully_thawed	100
2025-07-22	9	fully_thawed	100
2025-07-23	9	fully_thawed	100
2025-07-24	9	fully_thawed	100
2025-07-25	9	fully_thawed	100
2025-07-26	9	fully_thawed	100
2025-07-27	9	fully_thawed	100
2025-07-28	9	fully_thawed	100
2025-07-29	9	fully_thawed	100
2025-07-30	9	fully_thawed	100
2025-07-31	9	fully_thawed	100
2025-08-01	9	fully_thawed	100
2025-08-02	9	fully_thawed	100
2025-08-03	9	fully_thawed	100
2025-08-04	9	fully_thawed	100
2025-08-05	9	fully_thawed	100
2025-08-06	9	fully_thawed	100
2025-08-07	9	fully_thawed	100
2025-08-08	9	fully_thawed	100
2025-08-09	9	fully_thawed	100
2025-08-10	9	fully_thawed	100
2025-08-11	9	fully_thawed	100
2025-08-12	9	fully_thawed	100
2025-08-13	9	fully_thawed	100

Table C4. Vascular plant species growing directly on the peat cores and their leaf, stem, and flower biomass. As peat cores were selected to represent each individual chamber, the core and chamber plots have the same ID number. Note that the biomass estimates are likely underestimations due to some plant material being lost in the field. We show this table primarily for the species list. n/a: not applicable.

		Biomass (g)			
Plot	Species	Leaf	Stem	Flower	Total
Intact 1	*E. vaginatum*	0.067	0.003	0	0.071
	V. uliginosum	0.136	0.554	0	0.690
	E. nigrum	0.021	0.023	0	0.044
	A. polifolia	0.071	0.048	0	0.119
	R. chamaemorus	0.032	0.008	0	0.040
Intact 3	*V. uliginosum*	0.016	0.091	0	0.107
	E. nigrum	0.098	0.152	0	0.250
	A. polifolia	0.248	0.333	0	0.582
	E. vaginatum	0.009	0	0	0.009
Intact 5	*E. vaginatum*	0.516	0.045	0	0.562
	A. polifolia	0.100	0.032	0	0.132
	E. nigrum	0.411	0.534	0	0.945
	V. uliginosum	0.096	0.362	0	0.457
	V. oxycoccos	0.018	0.031	0	0.050
Partly thawed 2	*E. vaginatum*	1.192	0.453	0.025	1.670
Partly thawed 4	*E. angustifolium*	0.005	0.112	0	0.117
	V. oxycoccos	0.006	0.009	0	0.016
	A. polifolia	0.047	0.031	0.008	0.086
	C. rotundata	0.068	0.078	0	0.146
Partly thawed 6	*V. oxycoccos*	0.045	0.047	0	0.092
	C. rotundata	0.509	0.100	0.033	0.643
	E. angustifolium	0.113	0.060	0	0.173
Fully thawed 7	*E. angustifolium*	0.005	0.004	0	0.009
Fully thawed 8	n/a (only dead vegetation)	0	0	0	0
Fully thawed 9	*E. angustifolium*	0.010	0	0	0.010

Table C5. Automated chamber CH_4 flux (mg CH_4 m^{-2} d^{-1}) and peat temperature data aggregated to daily scale with medians (CH_4 flux) and means (CH_4 flux and peat temperature). Each thaw stage (intact, partly thawed and fully thawed permafrost) has three chambers, resulting in 9 chambers in total across the gradient. Date is reported as YYYY-MM-DD. Peat temperature was measured at each chamber in °C. NA: not available.

date	chamber_id	ch4_flux_mgch4m2d1_median	ch4_flux_mgch4m2d1_mean	peat_temp	thaw_stage
2023-05-19	1	−0.2219145	−0.3145721	5.1625	intact
2023-05-20	1	0.00574399	−0.066311	7.025	intact
2023-05-21	1	−0.3989296	−0.2403219	8.22857143	intact
2023-05-22	1	−0.7773529	−0.6796529	8.74285714	intact
2023-05-23	1	0.53550176	0.80188001	9.575	intact
2023-05-24	1	0.00458017	0.05634888	6.9875	intact
2023-05-25	1	−0.3354689	−0.2465779	6.175	intact
2023-05-26	1	−0.2424118	−0.2141699	4.64	intact
2023-05-27	1	−0.4223987	−0.5790264	4.53333333	intact
2023-05-28	1	0.31664522	0.13312589	7.91666667	intact
2023-05-29	1	−0.2720298	−0.3088527	6.74	intact
2023-05-30	1	−0.8175203	−0.8096751	6.0625	intact
2023-05-31	1	−0.2975853	−0.2703059	5.41428571	intact
2023-06-01	1	−0.2607799	−0.2098863	4.18571429	intact
2023-06-02	1	−0.0602156	−0.192396	5.975	intact
2023-06-03	1	−0.3074867	−0.1193395	6.6875	intact
2023-06-04	1	−0.2435461	−0.3969697	6.425	intact
2023-06-05	1	−0.1268613	−0.0325668	5.525	intact
2023-06-06	1	−0.2170739	−0.1498328	6.2	intact
2023-06-07	1	−0.1004278	−0.253325	7.05	intact
2023-06-08	1	0.00530328	0.02916815	6.775	intact
2023-06-09	1	0.37509357	0.13051516	8.775	intact
2023-06-10	1	−0.3912885	0.75210652	10.3875	intact
2023-06-11	1	−0.2676505	7.10531651	10.25	intact
2023-06-12	1	−0.1921932	0.00541212	9.91428571	intact
2023-06-13	1	−0.1997423	−0.0672235	9.14285714	intact
2023-06-14	1	−0.2465116	−0.1894103	9.2875	intact
2023-06-15	1	0.05328964	−0.0747067	8.9875	intact
2023-06-16	1	−0.7401661	−0.7508377	11.2375	intact
2023-06-17	1	−1.4492469	−1.9318429	13.275	intact
2023-06-18	1	−1.0694678	0.87740401	14.84	intact
2023-06-19	1	−1.800643	−1.4149338	15.4428571	intact
2023-06-20	1	−0.6641352	−0.8904488	15.325	intact
2023-06-21	1	0.64270481	1.29724865	14.95	intact
2023-06-22	1	−0.4805503	−1.0409474	15.15	intact
2023-06-23	1	−0.6481454	−0.2488546	14.6375	intact
2023-06-24	1	−0.5993958	−0.394253	12.3428571	intact
2023-06-25	1	−0.4903666	−0.2397805	11.6666667	intact
2023-06-26	1	−0.5284011	0.1425571	12.1666667	intact
2023-06-27	1	−0.6145895	−0.5465485	13.8285714	intact
2023-06-28	1	−0.4817611	−0.9907697	15.4428571	intact
2023-06-29	1	−0.5613113	0.09582892	16.5428571	intact
2023-06-30	1	−0.4806346	−0.557347	15.6	intact
2023-07-01	1	−0.2826519	−0.1860474	14.2875	intact
2023-07-02	1	−0.4020796	−0.457094	11.5666667	intact
2023-07-03	1	−0.1175917	−0.1317261	9.725	intact
2023-07-04	1	−0.9511043	5.18601466	11.7428571	intact
2023-07-05	1	−0.0827968	0.50823061	11.8375	intact
2023-07-06	1	−0.6713553	−0.4815579	11.8285714	intact
2023-07-07	1	−0.4162389	−0.4627183	13.7375	intact
2023-07-08	1	−0.6107624	−0.822446	14.62	intact
2023-07-09	1	−0.8287876	−0.2605612	14.0285714	intact
2023-07-10	1	−0.7495102	−0.5675542	14.42	intact
2023-07-11	1	−1.1428114	1.8352124	15.6571429	intact

Table C5. Continued.

date	chamber_id	ch4_flux_mgch4m2d1_median	ch4_flux_mgch4m2d1_mean	peat_temp	thaw_stage
2023-07-12	1	−0.264203	0.62863331	14.725	intact
2023-07-13	1	0.30660979	0.07871734	NA	intact
2023-07-14	1	−0.37722	0.35502003	12.6666667	intact
2023-07-15	1	−0.307862	−0.0255148	13.28	intact
2023-07-16	1	0.87609888	4.27861634	10.3	intact
2023-07-17	1	0.54447304	0.01754673	12.0571429	intact
2023-07-18	1	−0.0222388	−0.0045902	13.12	intact
2023-07-19	1	0.04262962	−0.1162991	11.8125	intact
2023-07-20	1	−0.3077424	0.01642977	11.4375	intact
2023-07-21	1	−0.730497	−0.7647286	11.6625	intact
2023-07-22	1	−0.4557989	−0.2553269	11.175	intact
2023-07-23	1	0.08321685	0.06964423	11.15	intact
2023-07-24	1	−1.0823346	−0.6294407	11.85	intact
2023-07-25	1	0.23061168	0.17592716	NA	intact
2023-07-26	1	0.43042129	0.43546101	NA	intact
2023-07-27	1	−1.1120897	−1.9148722	15.5333333	intact
2023-07-28	1	−1.4984701	−0.7081041	15.6833333	intact
2023-07-29	1	−0.7309139	−0.4819648	16.1625	intact
2023-07-30	1	−0.6813467	−0.5499898	14.375	intact
2023-07-31	1	−0.3995869	−0.0666944	13.9125	intact
2023-08-01	1	0.71797433	0.47320162	14.1	intact
2023-08-02	1	0.5240144	0.40927706	13.125	intact
2023-08-03	1	0.70216274	0.31239212	14.8	intact
2023-08-04	1	−1.0410518	−0.819665	14.5625	intact
2023-08-05	1	−1.1166625	−0.6333762	13.7285714	intact
2023-08-06	1	−0.1846842	2.34459431	12.525	intact
2023-08-07	1	0.64036517	0.62939795	NA	intact
2023-08-08	1	0.56232602	0.57082066	13.65	intact
2023-08-09	1	0.49790533	0.30370317	15.9	intact
2023-08-10	1	1.62976456	1.99928284	13.925	intact
2023-08-11	1	−0.8208423	−0.692715	12.6375	intact
2023-08-12	1	−0.3957228	−0.1429495	12.6875	intact
2023-08-13	1	0.58199905	16.0796192	12.4125	intact
2023-08-14	1	−1.6018361	−1.2600474	13.2	intact
2023-08-15	1	1.96973079	0.60415503	14.5875	intact
2023-08-16	1	1.08742737	2.03264989	12.4625	intact
2023-08-17	1	−1.0586454	−1.801549	12.8571429	intact
2023-08-18	1	0.31386682	10.3882639	12.175	intact
2023-08-19	1	−0.4316554	2.34089622	11.125	intact
2023-08-20	1	0.96403144	0.6801524	12.4166667	intact
2023-08-21	1	1.12343883	1.58686252	12.8375	intact
2023-08-22	1	1.77512416	1.94160349	13.1375	intact
2023-08-23	1	1.85619071	2.24923757	13.2125	intact
2023-08-24	1	−1.6412122	−1.7128361	11.8875	intact
2023-08-25	1	2.44681588	3.7409409	12.1625	intact
2023-08-26	1	0.73525343	5.42349674	NA	intact
2023-08-27	1	1.80610263	7.24959603	NA	intact
2023-08-28	1	1.11419173	1.63513396	NA	intact
2023-08-29	1	2.44297621	3.4181588	NA	intact
2023-08-30	1	1.74860916	0.68099281	NA	intact
2023-05-19	2	4.13109575	5.30438908	3.7125	partly_thawed
2023-05-20	2	2.94946211	4.52922979	4.7625	partly_thawed
2023-05-21	2	3.75940107	3.32820164	5.4125	partly_thawed
2023-05-22	2	9.71601188	11.8834351	5.0125	partly_thawed
2023-05-23	2	8.64402196	8.77209159	5.725	partly_thawed
2023-05-24	2	5.9103027	7.70046925	4.6125	partly_thawed
2023-05-25	2	2.53530721	2.4902531	4.2125	partly_thawed

Table C5. Continued.

date	chamber_id	ch4_flux_mgch4m2d1_median	ch4_flux_mgch4m2d1_mean	peat_temp	thaw_stage
2023-05-26	2	2.21262345	3.92609674	3.6	partly_thawed
2023-05-27	2	3.49860115	4.48461301	3.3625	partly_thawed
2023-05-28	2	3.54034229	4.37367796	4.8875	partly_thawed
2023-05-29	2	2.0143938	3.26080324	4.8875	partly_thawed
2023-05-30	2	7.31216476	5.90158756	4.6375	partly_thawed
2023-05-31	2	6.24483776	10.2935466	4.3375	partly_thawed
2023-06-01	2	4.58040045	6.47404017	3.275	partly_thawed
2023-06-02	2	4.46709781	4.55250207	4.9375	partly_thawed
2023-06-03	2	5.90188832	7.0224574	6.0625	partly_thawed
2023-06-04	2	4.2667141	4.77867334	5.95	partly_thawed
2023-06-05	2	2.83789229	3.29481924	5.15	partly_thawed
2023-06-06	2	4.48985966	5.34541724	5.9625	partly_thawed
2023-06-07	2	10.6005436	9.26890327	6.375	partly_thawed
2023-06-08	2	3.4067355	8.56300614	5.7625	partly_thawed
2023-06-09	2	4.81953768	8.36351233	6.4375	partly_thawed
2023-06-10	2	6.97247438	13.015929	6.6	partly_thawed
2023-06-11	2	6.99941603	10.856649	7.8625	partly_thawed
2023-06-12	2	7.07488065	10.7138892	8.8	partly_thawed
2023-06-13	2	2.36880788	2.25271135	7.9875	partly_thawed
2023-06-14	2	3.69534969	4.09571708	7.7625	partly_thawed
2023-06-15	2	6.35737438	6.05617647	7.8	partly_thawed
2023-06-16	2	8.90876126	10.3740364	8.0375	partly_thawed
2023-06-17	2	13.7418455	25.127661	9.1625	partly_thawed
2023-06-18	2	21.3168396	26.4984381	10.35	partly_thawed
2023-06-19	2	44.1913954	42.7243893	11.6875	partly_thawed
2023-06-20	2	13.9612921	26.1758197	12.325	partly_thawed
2023-06-21	2	17.002752	27.0303765	12.9	partly_thawed
2023-06-22	2	9.881781	10.3891263	11.725	partly_thawed
2023-06-23	2	39.3443563	48.7176035	12.1625	partly_thawed
2023-06-24	2	22.9288347	41.1810605	10.6875	partly_thawed
2023-06-25	2	24.5395551	35.5304197	10.375	partly_thawed
2023-06-26	2	10.3553112	28.0368117	10.2	partly_thawed
2023-06-27	2	12.6763355	32.2712979	11.4125	partly_thawed
2023-06-28	2	26.8731422	38.8797463	12.275	partly_thawed
2023-06-29	2	41.6668303	57.5739375	12.7625	partly_thawed
2023-06-30	2	13.6235424	14.4740752	13.0625	partly_thawed
2023-07-01	2	14.0065013	15.2112271	12.725	partly_thawed
2023-07-02	2	17.7208562	31.5264027	12.2	partly_thawed
2023-07-03	2	12.1039969	18.2924083	10.5125	partly_thawed
2023-07-04	2	39.171177	52.0188426	10.25	partly_thawed
2023-07-05	2	30.2419011	53.8628489	11.5375	partly_thawed
2023-07-06	2	33.2095587	45.1043935	10.6625	partly_thawed
2023-07-07	2	19.3064479	28.9733211	11.275	partly_thawed
2023-07-08	2	27.7635213	53.059753	13.6625	partly_thawed
2023-07-09	2	24.4208601	49.0627616	11.725	partly_thawed
2023-07-10	2	80.350965	97.3248559	11.9625	partly_thawed
2023-07-11	2	23.3612211	52.4062577	12.9875	partly_thawed
2023-07-12	2	16.3920649	21.8967751	12.7375	partly_thawed
2023-07-13	2	26.1858718	26.8513289	13.375	partly_thawed
2023-07-14	2	19.0424557	30.9206373	13.225	partly_thawed
2023-07-15	2	28.6238958	29.9492367	13.25	partly_thawed
2023-07-16	2	24.3665506	52.7666653	10.7125	partly_thawed
2023-07-17	2	66.2401312	72.7004558	10.775	partly_thawed
2023-07-18	2	31.1485143	54.755032	12.1125	partly_thawed
2023-07-19	2	66.1085117	67.4925083	11.3125	partly_thawed
2023-07-20	2	84.775434	96.8885633	10.65	partly_thawed
2023-07-21	2	33.5436586	33.1759336	11.5	partly_thawed

Table C5. Continued.

date	chamber_id	ch4_flux_mgch4m2d1_median	ch4_flux_mgch4m2d1_mean	peat_temp	thaw_stage
2023-07-22	2	21.1983762	25.5808727	11.0875	partly_thawed
2023-07-23	2	22.028071	23.2037045	10.6	partly_thawed
2023-07-24	2	29.6826587	34.0491644	10.625	partly_thawed
2023-07-25	2	23.7492942	27.8349918	10.875	partly_thawed
2023-07-26	2	54.3186128	67.8238034	11.475	partly_thawed
2023-07-27	2	94.2142469	111.266677	12.625	partly_thawed
2023-07-28	2	79.8050552	81.573831	12.425	partly_thawed
2023-07-29	2	51.771095	56.0331814	13.95	partly_thawed
2023-07-30	2	55.6789601	61.591004	13.15	partly_thawed
2023-07-31	2	24.9750167	31.9803513	12.9625	partly_thawed
2023-08-01	2	22.0074125	25.333477	13.3125	partly_thawed
2023-08-02	2	19.9212208	22.9247948	12.175	partly_thawed
2023-08-03	2	22.2636145	29.6652963	12.425	partly_thawed
2023-08-04	2	34.0101748	42.4866362	12.825	partly_thawed
2023-08-05	2	35.7551955	50.5231466	12.35	partly_thawed
2023-08-06	2	75.4574909	90.1113282	10.475	partly_thawed
2023-08-07	2	31.5647914	33.2681439	11.6	partly_thawed
2023-08-08	2	29.7783092	33.5760874	11.475	partly_thawed
2023-08-09	2	21.8526552	35.5465001	13.625	partly_thawed
2023-08-10	2	68.1945167	78.9451332	13.5	partly_thawed
2023-08-11	2	24.4209532	44.3804393	12.575	partly_thawed
2023-08-12	2	43.2268626	54.1392085	12.3125	partly_thawed
2023-08-13	2	22.308178	37.5541739	11.775	partly_thawed
2023-08-14	2	45.2274227	60.1220255	12.7375	partly_thawed
2023-08-15	2	160.398896	124.061429	13.175	partly_thawed
2023-08-16	2	70.8737833	98.6087051	12.2125	partly_thawed
2023-08-17	2	46.837311	68.0622133	12.0875	partly_thawed
2023-08-18	2	54.9761659	77.4073484	10.9125	partly_thawed
2023-08-19	2	47.9671115	80.9321384	10.525	partly_thawed
2023-08-20	2	38.8002323	38.7045713	10.8625	partly_thawed
2023-08-21	2	42.9428792	64.183448	12.35	partly_thawed
2023-08-22	2	143.703647	135.560575	13.075	partly_thawed
2023-08-23	2	117.829983	107.771402	13.1857143	partly_thawed
2023-08-24	2	41.2154506	68.7661472	11.8875	partly_thawed
2023-08-25	2	68.6044776	72.5486917	11.4375	partly_thawed
2023-08-26	2	73.9180198	91.8405196	10.8375	partly_thawed
2023-08-27	2	50.7697585	44.059604	10.1125	partly_thawed
2023-08-28	2	30.4250286	37.2632671	10.725	partly_thawed
2023-08-29	2	47.3675987	53.5110577	12.1125	partly_thawed
2023-08-30	2	65.9836321	69.6352057	11.925	partly_thawed
2023-05-19	3	0.28242124	0.15261538	5.3875	intact
2023-05-20	3	0.65929647	0.83188033	7.175	intact
2023-05-21	3	0.40696228	0.03747182	8.625	intact
2023-05-22	3	−0.6184055	−0.51299	9.2875	intact
2023-05-23	3	0.24514895	−0.2272565	9.575	intact
2023-05-24	3	0.30435326	0.20411986	7.01428571	intact
2023-05-25	3	0.41032638	0.29485431	5.8	intact
2023-05-26	3	−0.6504395	−0.2873725	5.2	intact
2023-05-27	3	0.47876537	0.3438634	4.44	intact
2023-05-28	3	−0.3415914	−0.2238291	NA	intact
2023-05-29	3	−0.0529419	−0.1776445	6.83333333	intact
2023-05-30	3	0.22888423	0.10568133	6.12857143	intact
2023-05-31	3	0.32599017	−0.1156845	5.475	intact
2023-06-01	3	0.42555661	0.45697042	4.18333333	intact
2023-06-02	3	−0.2906701	0.09556482	6.05	intact
2023-06-03	3	0.29584067	0.2031516	6.775	intact
2023-06-04	3	0.2402857	0.17555923	6.4875	intact

Table C5. Continued.

date	chamber_id	ch4_flux_mgch4m2d1_median	ch4_flux_mgch4m2d1_mean	peat_temp	thaw_stage
2023-06-05	3	−0.0897059	−0.07366	5.4875	intact
2023-06-06	3	−0.0252225	0.08601608	6.325	intact
2023-06-07	3	0.58032685	0.19854514	7.2	intact
2023-06-08	3	−0.4394576	−0.4315094	6.85	intact
2023-06-09	3	−0.4314349	−1.3165384	8.9375	intact
2023-06-10	3	0.28334897	0.25267383	10.6142857	intact
2023-06-11	3	−0.2612394	0.89510087	10.25	intact
2023-06-12	3	−0.2946219	−0.5165592	10.0625	intact
2023-06-13	3	−0.0338286	0.3891821	9.1	intact
2023-06-14	3	−0.0907013	−0.1227327	9.3625	intact
2023-06-15	3	0.37245276	0.25697527	9.125	intact
2023-06-16	3	−0.4416667	−0.0272152	11.5	intact
2023-06-17	3	1.0803243	1.31124666	13.35	intact
2023-06-18	3	−0.805758	−1.7893154	15.0625	intact
2023-06-19	3	−0.318924	2.29680327	16.2428571	intact
2023-06-20	3	−0.0642428	1.35758451	15.44	intact
2023-06-21	3	0.7116629	−0.7651908	14.7	intact
2023-06-22	3	−0.133218	−0.0303343	15.2428571	intact
2023-06-23	3	0.89448854	0.70853471	14.7625	intact
2023-06-24	3	0.20661447	0.51858571	12.4333333	intact
2023-06-25	3	0.86352316	0.93431991	10.625	intact
2023-06-26	3	0.24864793	3.13974426	12.6285714	intact
2023-06-27	3	−0.0273573	2.16870067	14.1875	intact
2023-06-28	3	−0.5971706	−1.1064645	15.5125	intact
2023-06-29	3	0.92154582	1.98801112	16.025	intact
2023-06-30	3	0.20754081	0.30538573	15.2375	intact
2023-07-01	3	−0.2894433	−0.1906541	13.9333333	intact
2023-07-02	3	−0.0856144	0.12439697	11.2142857	intact
2023-07-03	3	0.39763121	0.41624183	9.625	intact
2023-07-04	3	0.54802072	10.4729404	12.2571429	intact
2023-07-05	3	−0.0315873	0.59065889	12.2125	intact
2023-07-06	3	0.01004317	−0.1895179	11.9857143	intact
2023-07-07	3	0.10155017	0.06742985	13.45	intact
2023-07-08	3	0.85755443	3.12882287	13.82	intact
2023-07-09	3	0.71818096	0.15651004	14.3	intact
2023-07-10	3	0.90556241	1.57753602	14.68	intact
2023-07-11	3	−0.0662303	3.77381243	15.95	intact
2023-07-12	3	−0.2491408	−0.2563105	14.65	intact
2023-07-13	3	−0.2446549	0.13056121	NA	intact
2023-07-14	3	0.24190531	0.3360966	13.175	intact
2023-07-15	3	−1.1251532	−0.6548019	13.28	intact
2023-07-16	3	0.38496131	5.74970142	10.5	intact
2023-07-17	3	−1.3307463	−1.4488457	12.9	intact
2023-07-18	3	−1.2616284	−0.5680806	12.95	intact
2023-07-19	3	0.77554292	0.76899666	11.85	intact
2023-07-20	3	1.35716245	2.99278933	11.2	intact
2023-07-21	3	−0.1583867	−0.0596001	11.325	intact
2023-07-22	3	0.34193804	0.12411425	11.2125	intact
2023-07-23	3	−0.2813089	−0.109558	11.1375	intact
2023-07-24	3	−0.3406919	0.24243278	12	intact
2023-07-25	3	0.25825101	0.49072928	NA	intact
2023-07-26	3	0.40345057	0.30363802	NA	intact
2023-07-27	3	−0.8741544	−0.2730387	15.7166667	intact
2023-07-28	3	2.32344831	1.97912623	15.4166667	intact
2023-07-29	3	1.03431846	0.05019303	15.975	intact
2023-07-30	3	2.28104972	3.3827716	14.15	intact
2023-07-31	3	0.51588929	0.27541063	13.9375	intact

Table C5. Continued.

date	chamber_id	ch4_flux_mgch4m2d1_median	ch4_flux_mgch4m2d1_mean	peat_temp	thaw_stage
2023-08-01	3	−0.6653183	−0.3017723	13.95	intact
2023-08-02	3	−0.1580113	−0.1861269	13.1375	intact
2023-08-03	3	−0.0312118	0.02398612	14.4375	intact
2023-08-04	3	−0.2318877	−0.3030711	14.825	intact
2023-08-05	3	1.74803945	1.47327998	13.675	intact
2023-08-06	3	3.25164539	5.2593024	12.2428571	intact
2023-08-07	3	−0.6453033	−0.9568866	NA	intact
2023-08-08	3	0.62686935	0.5055592	13.9428571	intact
2023-08-09	3	0.08627569	0.61711875	15.725	intact
2023-08-10	3	0.7454318	3.49928063	13.95	intact
2023-08-11	3	0.68158952	1.02352138	12.7	intact
2023-08-12	3	0.68443802	0.44428649	12.625	intact
2023-08-13	3	0.45153209	6.64623444	12.2	intact
2023-08-14	3	1.26148737	1.70842731	13.3	intact
2023-08-15	3	0.99743126	0.06598729	14.725	intact
2023-08-16	3	−0.2332361	0.84381694	12.5125	intact
2023-08-17	3	1.23112062	0.28531737	12.9	intact
2023-08-18	3	0.96186809	1.33282201	12.3	intact
2023-08-19	3	−0.6037053	2.5732883	11.175	intact
2023-08-20	3	0.4383174	0.39770614	12.5	intact
2023-08-21	3	−0.94329	−1.1745188	12.9375	intact
2023-08-22	3	−0.4447405	−0.4507022	13.15	intact
2023-08-23	3	0.003773	1.36948258	13.2875	intact
2023-08-24	3	−0.4029749	3.39401655	12.225	intact
2023-08-25	3	0.76561396	3.55360633	12.0285714	intact
2023-08-26	3	0.93901561	5.01737693	NA	intact
2023-08-27	3	1.12922045	9.14806285	NA	intact
2023-08-28	3	0.13618351	−0.0469931	NA	intact
2023-08-29	3	0.56588107	3.24386514	NA	intact
2023-08-30	3	−1.1958467	2.78704824	NA	intact
2023-05-19	4	15.3260797	15.3948808	5.65	partly_thawed
2023-05-20	4	15.8434423	15.3772993	5.65	partly_thawed
2023-05-21	4	14.2417932	15.0097768	7.9875	partly_thawed
2023-05-22	4	18.8625876	19.3399555	6.2	partly_thawed
2023-05-23	4	18.642289	17.545261	NA	partly_thawed
2023-05-24	4	21.6231619	17.9463034	NA	partly_thawed
2023-05-25	4	15.3458588	12.6499204	6.325	partly_thawed
2023-05-26	4	7.54260395	8.93673834	4.725	partly_thawed
2023-05-27	4	18.7376978	18.2696356	5.3125	partly_thawed
2023-05-28	4	15.3629006	13.7585135	7.1	partly_thawed
2023-05-29	4	8.01335246	8.20426006	6.7625	partly_thawed
2023-05-30	4	17.2074342	16.7919558	5.9875	partly_thawed
2023-05-31	4	13.6269659	12.4738069	5.4875	partly_thawed
2023-06-01	4	9.6420955	8.78661397	4.35	partly_thawed
2023-06-02	4	16.0230118	16.2797671	7.425	partly_thawed
2023-06-03	4	11.0791401	13.4145906	7.4625	partly_thawed
2023-06-04	4	10.1808821	11.2558409	7.9625	partly_thawed
2023-06-05	4	5.02753368	5.41797059	6.1875	partly_thawed
2023-06-06	4	7.80287108	8.82239757	8.15	partly_thawed
2023-06-07	4	22.8335209	20.9850252	8.8625	partly_thawed
2023-06-08	4	12.5212654	15.7086314	7.6625	partly_thawed
2023-06-09	4	10.1538324	12.6166097	10.0875	partly_thawed
2023-06-10	4	16.8196508	17.9681851	10.6875	partly_thawed
2023-06-11	4	17.1703155	18.5361708	10.0375	partly_thawed
2023-06-12	4	16.6059234	16.2817881	10.1	partly_thawed
2023-06-13	4	4.07412658	4.78916875	9.8625	partly_thawed
2023-06-14	4	9.18142196	10.5433621	10.425	partly_thawed

Table C5. Continued.

date	chamber_id	ch4_flux_mgch4m2d1_median	ch4_flux_mgch4m2d1_mean	peat_temp	thaw_stage
2023-06-15	4	9.95609545	10.8573951	9.85	partly_thawed
2023-06-16	4	19.1560774	18.5344379	13.25	partly_thawed
2023-06-17	4	23.2823381	23.0617603	14.15	partly_thawed
2023-06-18	4	27.1226898	25.7422247	15.6125	partly_thawed
2023-06-19	4	23.6041287	24.2344856	17.225	partly_thawed
2023-06-20	4	21.2917605	21.6602278	14.2	partly_thawed
2023-06-21	4	30.6550238	27.4131775	15.75	partly_thawed
2023-06-22	4	14.1761334	15.6023126	14.6875	partly_thawed
2023-06-23	4	29.6107856	32.0612092	15.475	partly_thawed
2023-06-24	4	26.1851638	25.3115567	13.15	partly_thawed
2023-06-25	4	19.1723247	22.8530436	13.5625	partly_thawed
2023-06-26	4	17.5173585	18.749753	13.1625	partly_thawed
2023-06-27	4	23.2891672	25.0480041	14.8875	partly_thawed
2023-06-28	4	27.026658	27.6241091	14.775	partly_thawed
2023-06-29	4	34.9020762	38.1669749	17.125	partly_thawed
2023-06-30	4	13.4209663	20.4740529	14.3875	partly_thawed
2023-07-01	4	22.8990118	21.8218528	13.125	partly_thawed
2023-07-02	4	30.5293099	28.459866	11.325	partly_thawed
2023-07-03	4	21.5750824	22.1733522	10.2875	partly_thawed
2023-07-04	4	38.6929169	39.0442357	13.075	partly_thawed
2023-07-05	4	28.1062865	30.1459577	11.9125	partly_thawed
2023-07-06	4	35.5901705	34.3911688	14.3875	partly_thawed
2023-07-07	4	26.4246888	28.7979284	13.85	partly_thawed
2023-07-08	4	20.2482046	24.1058125	15.25	partly_thawed
2023-07-09	4	35.9015093	34.5588775	15.625	partly_thawed
2023-07-10	4	41.3976089	40.7314678	16.075	partly_thawed
2023-07-11	4	41.5938532	42.5259194	15.5	partly_thawed
2023-07-12	4	26.1006239	28.7431757	13.3375	partly_thawed
2023-07-13	4	31.041448	30.0550752	13.9375	partly_thawed
2023-07-14	4	40.3052808	43.162112	13.575	partly_thawed
2023-07-15	4	32.1065483	30.2942149	14.2625	partly_thawed
2023-07-16	4	28.8956505	32.3777766	11.325	partly_thawed
2023-07-17	4	48.3482861	46.6741334	13.7375	partly_thawed
2023-07-18	4	41.0063463	38.6072954	14.0625	partly_thawed
2023-07-19	4	43.5113186	45.2993445	12.375	partly_thawed
2023-07-20	4	58.1198302	49.9005766	12.875	partly_thawed
2023-07-21	4	44.4942575	42.4367119	12.525	partly_thawed
2023-07-22	4	37.1977352	37.2852589	12.2375	partly_thawed
2023-07-23	4	36.2617427	31.6168443	12.125	partly_thawed
2023-07-24	4	36.6393035	34.4014538	13.125	partly_thawed
2023-07-25	4	35.4331152	34.6989108	13.5	partly_thawed
2023-07-26	4	41.8456117	38.6393134	15.0125	partly_thawed
2023-07-27	4	49.2020487	47.3216293	16.6	partly_thawed
2023-07-28	4	55.169586	55.248497	16.5	partly_thawed
2023-07-29	4	46.2299463	43.1308362	15.95	partly_thawed
2023-07-30	4	51.4052057	48.68909	14.3375	partly_thawed
2023-07-31	4	38.8404046	35.8706909	14.0125	partly_thawed
2023-08-01	4	43.0606422	43.8458035	14.7	partly_thawed
2023-08-02	4	44.7060991	42.6706483	13.95	partly_thawed
2023-08-03	4	34.382709	38.5229968	14.9625	partly_thawed
2023-08-04	4	43.6758417	42.6097425	15.5375	partly_thawed
2023-08-05	4	28.8372025	34.7937105	13.825	partly_thawed
2023-08-06	4	59.0955896	62.788	13.8625	partly_thawed
2023-08-07	4	48.3871803	48.7196695	12.7	partly_thawed
2023-08-08	4	51.7724684	50.7905241	15.225	partly_thawed
2023-08-09	4	38.4434676	42.0341417	15.875	partly_thawed
2023-08-10	4	74.9909469	77.0483852	14.6875	partly_thawed

Table C5. Continued.

date	chamber_id	ch4_flux_mgch4m2d1_median	ch4_flux_mgch4m2d1_mean	peat_temp	thaw_stage
2023-08-11	4	55.5844904	60.3671212	13.8125	partly_thawed
2023-08-12	4	66.6026489	67.2746802	14.175	partly_thawed
2023-08-13	4	58.589253	64.0130665	12.8125	partly_thawed
2023-08-14	4	83.0673361	79.7021874	14.5625	partly_thawed
2023-08-15	4	89.1140624	89.2577606	15.975	partly_thawed
2023-08-16	4	87.0601228	90.9022928	13.4375	partly_thawed
2023-08-17	4	67.5630045	62.9590444	14.0625	partly_thawed
2023-08-18	4	74.5207843	70.3560364	12.675	partly_thawed
2023-08-19	4	72.6660605	76.2211604	12.525	partly_thawed
2023-08-20	4	47.6804448	52.417741	13	partly_thawed
2023-08-21	4	69.7409064	74.3706168	14.3125	partly_thawed
2023-08-22	4	103.851364	108.870645	15.0375	partly_thawed
2023-08-23	4	100.810651	103.065426	15.3375	partly_thawed
2023-08-24	4	98.2969009	93.9909804	13.5375	partly_thawed
2023-08-25	4	77.4292843	78.8877952	12.65	partly_thawed
2023-08-26	4	71.6129038	75.9783125	13.525	partly_thawed
2023-08-27	4	87.5944317	80.6300486	11.925	partly_thawed
2023-08-28	4	59.782811	60.123705	12.1625	partly_thawed
2023-08-29	4	96.4069224	103.531189	13.1375	partly_thawed
2023-08-30	4	109.6439	108.307258	14.275	partly_thawed
2023-05-19	5	−0.0251655	−0.2040148	5.55	intact
2023-05-20	5	−0.2815876	−0.1156674	6.8375	intact
2023-05-21	5	−0.0128425	−0.2529357	7.725	intact
2023-05-22	5	1.13846109	4.86783665	7.6875	intact
2023-05-23	5	0.03762361	5.35088145	7.075	intact
2023-05-24	5	0.68078451	0.52926372	5.9875	intact
2023-05-25	5	−0.0359756	−0.203844	4.55	intact
2023-05-26	5	0.04524934	0.04812912	3.65	intact
2023-05-27	5	−0.3080117	−0.0685212	4.65	intact
2023-05-28	5	0.05947033	0.15642894	6.675	intact
2023-05-29	5	−0.4193692	−0.2105441	5.3625	intact
2023-05-30	5	0.42612454	0.37590872	5.3	intact
2023-05-31	5	0.09737126	0.1007778	4.375	intact
2023-06-01	5	0.41931014	0.67524052	3.4375	intact
2023-06-02	5	0.51340476	−0.1051708	5.675	intact
2023-06-03	5	−0.3604455	−0.3624306	5.7875	intact
2023-06-04	5	−0.3352774	−0.3292613	5.8625	intact
2023-06-05	5	0.29650586	0.08976407	4.6	intact
2023-06-06	5	0.29522394	0.04881347	5.5125	intact
2023-06-07	5	0.41065004	0.14334422	6.5375	intact
2023-06-08	5	−0.2631071	0.09009892	5.3125	intact
2023-06-09	5	0.07342837	5.00581528	7.1875	intact
2023-06-10	5	0.05336857	4.94258043	7.775	intact
2023-06-11	5	0.72256387	3.05219001	9.2625	intact
2023-06-12	5	0.42412964	1.00882438	8.925	intact
2023-06-13	5	−0.3177511	−0.2192402	7.9375	intact
2023-06-14	5	−0.0623086	−0.0201624	8.325	intact
2023-06-15	5	0.12853273	0.01134575	8.2375	intact
2023-06-16	5	−0.5996864	−0.6132317	10.65	intact
2023-06-17	5	−0.3939054	−1.2309494	11.275	intact
2023-06-18	5	1.03784111	3.26013278	12.9625	intact
2023-06-19	5	0.64445063	4.70022052	14.1	intact
2023-06-20	5	−1.9160745	−1.3170517	15.825	intact
2023-06-21	5	1.43174456	4.94086096	14.675	intact
2023-06-22	5	14.5897185	27.5451175	15.95	intact
2023-06-23	5	14.5860744	25.1118206	14.4	intact
2023-06-24	5	3.67560803	2.52014476	11.1125	intact

Table C5. Continued.

date	chamber_id	ch4_flux_mgch4m2d1_median	ch4_flux_mgch4m2d1_mean	peat_temp	thaw_stage
2023-06-25	5	2.55655259	1.31037591	11.5875	intact
2023-06-26	5	9.05582828	14.1506646	13.95	intact
2023-06-27	5	19.4938737	18.5075612	15.7625	intact
2023-06-28	5	3.68693252	3.87986092	14.7	intact
2023-06-29	5	42.87176	55.3274336	14.8375	intact
2023-06-30	5	31.8379188	31.175372	15.7875	intact
2023-07-01	5	77.3669118	92.6742226	14.875	intact
2023-07-02	5	86.4779433	76.6820233	11.5875	intact
2023-07-03	5	42.2123819	53.1488351	11.7875	intact
2023-07-04	5	40.1150495	42.8141171	12.375	intact
2023-07-05	5	2.89235452	9.47502849	11.025	intact
2023-07-06	5	6.52251839	17.6682207	12.2375	intact
2023-07-07	5	19.3111916	19.58588	13.8875	intact
2023-07-08	5	7.72584268	14.8962392	13.925	intact
2023-07-09	5	4.05604454	2.17828788	13.525	intact
2023-07-10	5	23.7444273	36.3046591	13.7	intact
2023-07-11	5	39.538247	42.797092	15.8125	intact
2023-07-12	5	3.63369206	12.227283	14.0125	intact
2023-07-13	5	36.1857136	35.4577445	14.3125	intact
2023-07-14	5	17.8959163	22.0494318	14.6375	intact
2023-07-15	5	2.93729053	3.51853312	13.2	intact
2023-07-16	5	25.4409511	23.9423046	11.25	intact
2023-07-17	5	30.0283404	29.7213781	13.525	intact
2023-07-18	5	3.48866727	5.74666902	12.6625	intact
2023-07-19	5	8.49712006	7.90516831	11.725	intact
2023-07-20	5	79.9097731	80.9678286	12.4875	intact
2023-07-21	5	46.0929503	47.3835864	12.8	intact
2023-07-22	5	15.822715	22.6153466	12.125	intact
2023-07-23	5	25.9418801	26.9434791	12.4875	intact
2023-07-24	5	41.6494707	35.438396	13.7	intact
2023-07-25	5	51.2553575	52.2977835	14.625	intact
2023-07-26	5	50.7803873	60.1438815	15.0875	intact
2023-07-27	5	38.5916977	44.0686328	14.3375	intact
2023-07-28	5	40.664371	53.2797467	14.6125	intact
2023-07-29	5	10.9023469	12.1773874	14.3375	intact
2023-07-30	5	35.5344519	37.1523359	14.575	intact
2023-07-31	5	27.8033055	32.645376	14.5875	intact
2023-08-01	5	39.8192712	46.5040767	14.5875	intact
2023-08-02	5	33.1918338	40.9258595	14.4875	intact
2023-08-03	5	26.6571166	20.6653901	15.1625	intact
2023-08-04	5	32.2463183	44.9244439	14.9125	intact
2023-08-05	5	13.9493778	23.896496	12.6625	intact
2023-08-06	5	75.8253915	79.1372214	12.0625	intact
2023-08-07	5	62.0275455	64.2055756	12.675	intact
2023-08-08	5	46.1963654	54.0385145	15.5125	intact
2023-08-09	5	26.5256764	44.7651636	15.475	intact
2023-08-10	5	92.8947529	87.2108676	13.6875	intact
2023-08-11	5	85.7433681	78.3819607	13.0875	intact
2023-08-12	5	32.8176831	46.5376787	13.9	intact
2023-08-13	5	71.2841821	66.5311746	12.875	intact
2023-08-14	5	76.0603196	77.0281032	14.025	intact
2023-08-15	5	61.2518558	74.7160673	13.9125	intact
2023-08-16	5	74.938378	71.5146573	12.6	intact
2023-08-17	5	10.3617386	11.3624915	12.0625	intact
2023-08-18	5	20.8561353	25.9445849	10.9375	intact
2023-08-19	5	48.1623514	71.1001884	11.6	intact
2023-08-20	5	47.4928991	56.7325931	12.6125	intact

Table C5. Continued.

date	chamber_id	ch4_flux_mgch4m2d1_median	ch4_flux_mgch4m2d1_mean	peat_temp	thaw_stage
2023-08-21	5	59.9468901	48.8358025	13.4	intact
2023-08-22	5	56.257235	57.3824881	13.4875	intact
2023-08-23	5	54.5211725	58.7325399	13.35	intact
2023-08-24	5	73.8134836	77.1484314	12.75	intact
2023-08-25	5	78.2430376	89.5674388	12	intact
2023-08-26	5	70.5265326	66.6240402	12.0625	intact
2023-08-27	5	58.3734518	58.862783	11.2625	intact
2023-08-28	5	29.1387184	45.334858	11.775	intact
2023-08-29	5	43.3536866	50.8089725	12.45	intact
2023-08-30	5	96.3562445	93.1586661	12.55	intact
2023-05-19	6	8.22055435	8.36940269	2.7875	partly_thawed
2023-05-20	6	10.0807689	10.5066268	3.0875	partly_thawed
2023-05-21	6	18.0408983	20.3644724	4.025	partly_thawed
2023-05-22	6	20.0728355	19.6821984	3.8	partly_thawed
2023-05-23	6	19.8541094	18.4981734	4.4125	partly_thawed
2023-05-24	6	13.2493831	16.0246948	3.75	partly_thawed
2023-05-25	6	15.7558773	15.7560188	3.0125	partly_thawed
2023-05-26	6	14.6898552	16.3776553	3.0875	partly_thawed
2023-05-27	6	12.4038263	17.9471328	3.2625	partly_thawed
2023-05-28	6	14.3445595	15.3652945	4.4375	partly_thawed
2023-05-29	6	17.7840109	16.6526554	4.2375	partly_thawed
2023-05-30	6	20.0638626	20.1224406	3.975	partly_thawed
2023-05-31	6	21.5137204	22.4310255	3.9375	partly_thawed
2023-06-01	6	16.1449866	16.8554831	3.25	partly_thawed
2023-06-02	6	21.4132642	22.4076818	4.7875	partly_thawed
2023-06-03	6	23.4707426	23.0540833	5.6375	partly_thawed
2023-06-04	6	17.0908635	18.5687625	5.3	partly_thawed
2023-06-05	6	11.2882837	10.2126407	4.8625	partly_thawed
2023-06-06	6	16.9432259	16.8660376	5.55	partly_thawed
2023-06-07	6	23.442394	24.3577983	6.2	partly_thawed
2023-06-08	6	19.689198	21.7679062	5.75	partly_thawed
2023-06-09	6	30.7806593	30.0382616	6.5875	partly_thawed
2023-06-10	6	29.6977711	30.092162	6.3875	partly_thawed
2023-06-11	6	19.6793493	24.2542025	7.2625	partly_thawed
2023-06-12	6	16.157194	21.4507637	7.85	partly_thawed
2023-06-13	6	10.1582938	9.79526147	7.2625	partly_thawed
2023-06-14	6	20.2614767	20.6581517	7.5625	partly_thawed
2023-06-15	6	21.7092025	22.3232356	7.3375	partly_thawed
2023-06-16	6	38.2572792	35.2009128	8.175	partly_thawed
2023-06-17	6	39.1763921	34.2166381	8.7625	partly_thawed
2023-06-18	6	37.9001712	36.2820037	9.6	partly_thawed
2023-06-19	6	40.0347046	40.0491413	10.775	partly_thawed
2023-06-20	6	25.1664938	31.2181789	11.0625	partly_thawed
2023-06-21	6	39.1694686	42.1963156	11.9125	partly_thawed
2023-06-22	6	12.3492412	17.1607488	11.2375	partly_thawed
2023-06-23	6	43.5449617	47.1659297	13.275	partly_thawed
2023-06-24	6	40.9599485	39.947581	11.475	partly_thawed
2023-06-25	6	33.7630086	37.5147382	10.9875	partly_thawed
2023-06-26	6	13.5229454	24.8245029	10.1125	partly_thawed
2023-06-27	6	20.7579681	31.147547	11.325	partly_thawed
2023-06-28	6	34.0001316	38.2315613	11.9375	partly_thawed
2023-06-29	6	57.9189061	57.6365163	12.025	partly_thawed
2023-06-30	6	17.541349	26.1626504	12.1625	partly_thawed
2023-07-01	6	19.7927166	20.6067129	12.1875	partly_thawed
2023-07-02	6	32.9973847	38.1155083	10.9125	partly_thawed
2023-07-03	6	12.0365407	18.1963014	9.7625	partly_thawed
2023-07-04	6	77.5904311	67.8668564	9.3875	partly_thawed

Table C5. Continued.

date	chamber_id	ch4_flux_mgch4m2d1_median	ch4_flux_mgch4m2d1_mean	peat_temp	thaw_stage
2023-07-05	6	42.6626879	47.3393034	10.55	partly_thawed
2023-07-06	6	43.1515249	45.3354218	10.5375	partly_thawed
2023-07-07	6	20.2174368	38.4991831	10.7125	partly_thawed
2023-07-08	6	39.6743724	48.4818878	12.625	partly_thawed
2023-07-09	6	48.1502657	45.6027901	11.45	partly_thawed
2023-07-10	6	85.2151002	80.9096284	11.1875	partly_thawed
2023-07-11	6	62.5039758	65.9324879	12.2125	partly_thawed
2023-07-12	6	22.9181234	25.330108	12	partly_thawed
2023-07-13	6	23.9994698	34.1472324	11.8	partly_thawed
2023-07-14	6	19.2792223	37.3581303	11.7625	partly_thawed
2023-07-15	6	48.9913041	48.3724217	12.5125	partly_thawed
2023-07-16	6	20.0868713	33.8979963	10.25	partly_thawed
2023-07-17	6	64.236184	53.7913356	10.8	partly_thawed
2023-07-18	6	50.322429	52.7552287	12.025	partly_thawed
2023-07-19	6	49.8566426	55.3955589	10.925	partly_thawed
2023-07-20	6	58.7793876	69.4519487	10.5125	partly_thawed
2023-07-21	6	31.8481451	40.8008804	10.8875	partly_thawed
2023-07-22	6	26.4707146	26.8150754	10.8625	partly_thawed
2023-07-23	6	29.127419	31.8537345	10.6125	partly_thawed
2023-07-24	6	31.3779504	29.9220072	10.6375	partly_thawed
2023-07-25	6	32.8231256	34.8159151	11.475	partly_thawed
2023-07-26	6	50.4473485	54.8340509	11.9	partly_thawed
2023-07-27	6	110.332247	97.0265119	12.275	partly_thawed
2023-07-28	6	92.7295683	89.1958493	12.6375	partly_thawed
2023-07-29	6	60.3420529	59.6087259	13.575	partly_thawed
2023-07-30	6	53.361103	56.3148631	12.6375	partly_thawed
2023-07-31	6	29.3270414	28.8761465	12.2875	partly_thawed
2023-08-01	6	36.8111944	41.5758528	12.3	partly_thawed
2023-08-02	6	48.9128661	47.4309069	12.9375	partly_thawed
2023-08-03	6	27.0428055	28.6326007	13.25	partly_thawed
2023-08-04	6	48.4321356	48.9716458	13.925	partly_thawed
2023-08-05	6	59.7348555	66.1898182	13.0875	partly_thawed
2023-08-06	6	101.669452	107.152667	11.625	partly_thawed
2023-08-07	6	46.415161	51.7328859	11.875	partly_thawed
2023-08-08	6	50.7337198	60.983005	12.0125	partly_thawed
2023-08-09	6	50.8757148	56.5830926	13.8875	partly_thawed
2023-08-10	6	107.105636	111.843301	13.9375	partly_thawed
2023-08-11	6	56.2275049	64.0516535	13.3375	partly_thawed
2023-08-12	6	68.3311498	75.5072875	12.8	partly_thawed
2023-08-13	6	50.7633661	65.6487623	12.75	partly_thawed
2023-08-14	6	105.827707	117.849916	13.2875	partly_thawed
2023-08-15	6	104.659029	117.474173	13.8625	partly_thawed
2023-08-16	6	90.186093	111.175356	13.4	partly_thawed
2023-08-17	6	53.6937611	57.1817659	12.8875	partly_thawed
2023-08-18	6	68.4988103	94.2451418	12.1875	partly_thawed
2023-08-19	6	83.7797336	105.58579	11.8	partly_thawed
2023-08-20	6	65.4200639	73.8287304	11.975	partly_thawed
2023-08-21	6	86.6755397	98.7066985	13.1	partly_thawed
2023-08-22	6	101.218752	127.663228	13.7	partly_thawed
2023-08-23	6	105.18271	144.897213	13.9125	partly_thawed
2023-08-24	6	110.510497	142.388473	12.9	partly_thawed
2023-08-25	6	101.360275	101.964527	12.1375	partly_thawed
2023-08-26	6	110.248594	104.11099	12.1125	partly_thawed
2023-08-27	6	69.1696216	91.9143423	11.6375	partly_thawed
2023-08-28	6	63.0693781	67.8501806	12.025	partly_thawed
2023-08-29	6	97.0584329	114.239248	12.45	partly_thawed
2023-08-30	6	116.592803	122.524322	13	partly_thawed

Table C5. Continued.

date	chamber_id	ch4_flux_mgch4m2d1_median	ch4_flux_mgch4m2d1_mean	peat_temp	thaw_stage
2023-05-19	7	49.334863	47.8621745	2.0125	fully_thawed
2023-05-20	7	46.9200393	44.4316941	2.1	fully_thawed
2023-05-21	7	52.0751732	52.4462877	2.425	fully_thawed
2023-05-22	7	75.3469779	77.2452609	2.275	fully_thawed
2023-05-23	7	44.6685192	47.9344752	2.975	fully_thawed
2023-05-24	7	33.8936121	42.0889037	2.8375	fully_thawed
2023-05-25	7	37.6489882	40.4435532	2.75	fully_thawed
2023-05-26	7	34.7523409	36.5482176	2.55	fully_thawed
2023-05-27	7	39.9671258	38.7382302	2.4875	fully_thawed
2023-05-28	7	39.3415505	39.2518293	3.35	fully_thawed
2023-05-29	7	34.1545325	34.2216868	3.2875	fully_thawed
2023-05-30	7	36.1480781	41.6197173	3.15	fully_thawed
2023-05-31	7	31.5812416	39.6837059	3.2625	fully_thawed
2023-06-01	7	34.2491326	39.51766	2.75	fully_thawed
2023-06-02	7	36.3974991	44.3509345	3.6625	fully_thawed
2023-06-03	7	36.4606779	35.9005886	4.0125	fully_thawed
2023-06-04	7	33.4537363	33.4941482	4.2375	fully_thawed
2023-06-05	7	30.5260161	32.7818017	4.05	fully_thawed
2023-06-06	7	39.7875148	40.7727151	4.4625	fully_thawed
2023-06-07	7	44.0400964	48.0598024	4.3375	fully_thawed
2023-06-08	7	39.0480798	38.3578566	4.325	fully_thawed
2023-06-09	7	50.2600447	55.2714998	4.4125	fully_thawed
2023-06-10	7	72.8707437	68.8740667	4.2	fully_thawed
2023-06-11	7	54.8621741	66.7493228	4.8625	fully_thawed
2023-06-12	7	46.3315212	46.9956524	5.7625	fully_thawed
2023-06-13	7	46.4795599	46.4291483	5.575	fully_thawed
2023-06-14	7	49.2634297	50.9196366	5.625	fully_thawed
2023-06-15	7	52.4206463	51.1836335	5.95	fully_thawed
2023-06-16	7	74.340552	77.4791259	5.2375	fully_thawed
2023-06-17	7	80.1579366	81.5767077	5	fully_thawed
2023-06-18	7	92.6844436	111.973471	6.0875	fully_thawed
2023-06-19	7	112.902023	111.779864	6.6375	fully_thawed
2023-06-20	7	76.8289006	112.675045	7.7	fully_thawed
2023-06-21	7	103.716188	117.563215	8.55	fully_thawed
2023-06-22	7	64.6615473	66.5804132	7.775	fully_thawed
2023-06-23	7	104.424053	104.192511	8.5375	fully_thawed
2023-06-24	7	91.6352675	97.5669571	7.575	fully_thawed
2023-06-25	7	108.874606	105.322583	7.125	fully_thawed
2023-06-26	7	78.4405403	72.111787	6.7375	fully_thawed
2023-06-27	7	97.4924365	124.258865	7.7375	fully_thawed
2023-06-28	7	138.313482	164.993641	7.825	fully_thawed
2023-06-29	7	150.786801	156.450101	7.25	fully_thawed
2023-06-30	7	82.7247754	96.6420018	7.55	fully_thawed
2023-07-01	7	93.5174097	84.1863838	7.0875	fully_thawed
2023-07-02	7	84.1199896	114.774776	6.3375	fully_thawed
2023-07-03	7	68.8906932	81.4311045	5.2875	fully_thawed
2023-07-04	7	125.311515	128.833645	5.05	fully_thawed
2023-07-05	7	82.7811367	86.2692138	6.4	fully_thawed
2023-07-06	7	115.519992	106.05497	5.775	fully_thawed
2023-07-07	7	83.6127463	94.5363047	6.3875	fully_thawed
2023-07-08	7	117.799471	161.497365	7.1875	fully_thawed
2023-07-09	7	127.258105	154.346676	6.65	fully_thawed
2023-07-10	7	134.356642	153.716332	5.5	fully_thawed
2023-07-11	7	119.822284	127.748772	6.4375	fully_thawed
2023-07-12	7	63.2641997	81.4714608	6.6625	fully_thawed
2023-07-13	7	73.3970921	75.3129335	7.0875	fully_thawed
2023-07-14	7	64.4319988	69.1387471	7.3625	fully_thawed

Table C5. Continued.

date	chamber_id	ch4_flux_mgch4m2d1_median	ch4_flux_mgch4m2d1_mean	peat_temp	thaw_stage
2023-07-15	7	87.7517355	109.398006	8.0625	fully_thawed
2023-07-16	7	60.0648654	81.7113203	6.5875	fully_thawed
2023-07-17	7	86.8304636	115.092668	6.6875	fully_thawed
2023-07-18	7	91.537164	91.2504492	7.4875	fully_thawed
2023-07-19	7	104.248884	103.742601	7.1375	fully_thawed
2023-07-20	7	96.1184814	106.771965	7.55	fully_thawed
2023-07-21	7	72.9758352	75.4283374	7.9625	fully_thawed
2023-07-22	7	50.8879982	52.5804427	8.0875	fully_thawed
2023-07-23	7	47.890464	51.7904287	8.05	fully_thawed
2023-07-24	7	67.628543	70.1944301	8.025	fully_thawed
2023-07-25	7	66.104418	67.1867027	8.35	fully_thawed
2023-07-26	7	59.0960214	71.3616365	9.45	fully_thawed
2023-07-27	7	107.272419	122.411518	9.2625	fully_thawed
2023-07-28	7	125.58199	131.347129	9.5125	fully_thawed
2023-07-29	7	105.040756	126.584227	10.2875	fully_thawed
2023-07-30	7	71.9771293	84.8288918	9.475	fully_thawed
2023-07-31	7	49.8456284	48.3364605	9.825	fully_thawed
2023-08-01	7	67.1301054	59.9133549	10.2875	fully_thawed
2023-08-02	7	68.0543255	62.641913	9.8	fully_thawed
2023-08-03	7	53.418273	61.6375364	10.625	fully_thawed
2023-08-04	7	89.3546858	110.994566	11.725	fully_thawed
2023-08-05	7	107.694219	110.576869	11.2125	fully_thawed
2023-08-06	7	142.426043	141.600357	9.6875	fully_thawed
2023-08-07	7	59.0778337	62.8037329	10.45	fully_thawed
2023-08-08	7	70.8195516	75.7575534	11.5	fully_thawed
2023-08-09	7	61.1767954	59.970054	13.1625	fully_thawed
2023-08-10	7	122.236264	154.684266	13.15	fully_thawed
2023-08-11	7	76.1331003	77.7675547	12.675	fully_thawed
2023-08-12	7	86.5827151	112.533137	12.4	fully_thawed
2023-08-13	7	87.0160802	106.60389	11.9125	fully_thawed
2023-08-14	7	134.443476	127.821891	12.6625	fully_thawed
2023-08-15	7	177.273142	211.575752	13.0375	fully_thawed
2023-08-16	7	123.484146	131.965013	12.3375	fully_thawed
2023-08-17	7	126.096449	139.218056	12.0875	fully_thawed
2023-08-18	7	171.532134	182.269055	11.15	fully_thawed
2023-08-19	7	103.586558	136.989137	10.425	fully_thawed
2023-08-20	7	76.0763399	73.5902305	11.1875	fully_thawed
2023-08-21	7	89.1069265	106.405968	12.1875	fully_thawed
2023-08-22	7	147.526551	183.595578	12.725	fully_thawed
2023-08-23	7	190.143095	219.501071	12.85	fully_thawed
2023-08-24	7	242.91605	224.040046	11.7375	fully_thawed
2023-08-25	7	112.696976	146.411157	10.7875	fully_thawed
2023-08-26	7	187.9008	182.6657	10.5125	fully_thawed
2023-08-27	7	88.5555957	115.60819	9.9875	fully_thawed
2023-08-28	7	69.6624609	65.0229066	11	fully_thawed
2023-08-29	7	83.0563735	110.917223	11.6625	fully_thawed
2023-08-30	7	198.675869	202.666392	11.9375	fully_thawed
2023-05-19	8	34.7006239	34.6469628	8.8125	fully_thawed
2023-05-20	8	20.7060914	20.4918121	11.5875	fully_thawed
2023-05-21	8	39.7632249	40.1256783	11.55	fully_thawed
2023-05-22	8	51.4766506	51.0077644	12.075	fully_thawed
2023-05-23	8	39.2495605	38.8283208	10.375	fully_thawed
2023-05-24	8	33.4763883	34.4389857	8.775	fully_thawed
2023-05-25	8	21.6617507	30.9194817	6.9	fully_thawed
2023-05-26	8	31.3390259	31.7121132	4.725	fully_thawed
2023-05-27	8	32.3995898	30.6834427	6.7	fully_thawed
2023-05-28	8	19.3751497	20.1882238	10.0375	fully_thawed

Table C5. Continued.

date	chamber_id	ch4_flux_mgch4m2d1_median	ch4_flux_mgch4m2d1_mean	peat_temp	thaw_stage
2023-05-29	8	20.5861088	25.4842424	7.3375	fully_thawed
2023-05-30	8	37.5520532	34.8199607	6.675	fully_thawed
2023-05-31	8	23.703279	23.7309339	4.125	fully_thawed
2023-06-01	8	24.371716	22.3458104	5.6375	fully_thawed
2023-06-02	8	36.1691973	38.0274175	7.5375	fully_thawed
2023-06-03	8	35.2229112	32.9884145	7.525	fully_thawed
2023-06-04	8	34.5912683	34.2727808	8.1375	fully_thawed
2023-06-05	8	23.7471868	24.6726049	6.825	fully_thawed
2023-06-06	8	34.8645607	37.1863894	11.1875	fully_thawed
2023-06-07	8	51.7544084	47.2871867	10.8125	fully_thawed
2023-06-08	8	30.2154105	29.7787088	9.2125	fully_thawed
2023-06-09	8	55.8270964	58.2682072	18.1	fully_thawed
2023-06-10	8	58.3342632	59.9797712	18.575	fully_thawed
2023-06-11	8	63.8823588	51.5586709	13.3125	fully_thawed
2023-06-12	8	58.3933537	61.3947409	13.075	fully_thawed
2023-06-13	8	42.5780141	43.9541079	14.6625	fully_thawed
2023-06-14	8	38.3218216	38.8987401	16.4875	fully_thawed
2023-06-15	8	42.1898655	41.5978906	12.625	fully_thawed
2023-06-16	8	96.1384255	113.243998	21.425	fully_thawed
2023-06-17	8	97.7764602	97.7908683	21.6875	fully_thawed
2023-06-18	8	115.451319	129.218346	23.0875	fully_thawed
2023-06-19	8	104.867502	107.708625	23.675	fully_thawed
2023-06-20	8	93.700883	95.1999744	20.1375	fully_thawed
2023-06-21	8	86.0736841	92.2739545	18.6375	fully_thawed
2023-06-22	8	64.7044161	66.3194232	21.025	fully_thawed
2023-06-23	8	121.630873	115.917609	15.325	fully_thawed
2023-06-24	8	123.917059	120.159965	14.625	fully_thawed
2023-06-25	8	114.339939	113.91905	15.475	fully_thawed
2023-06-26	8	82.7727499	89.5042756	18.9	fully_thawed
2023-06-27	8	100.223707	109.170843	19.275	fully_thawed
2023-06-28	8	111.760012	123.168416	21.05	fully_thawed
2023-06-29	8	125.297228	136.714036	21.825	fully_thawed
2023-06-30	8	85.4755693	86.0490496	18.5125	fully_thawed
2023-07-01	8	74.3489467	83.5775367	17.4625	fully_thawed
2023-07-02	8	103.054436	106.944953	10.7125	fully_thawed
2023-07-03	8	83.7350237	91.4184859	10.9375	fully_thawed
2023-07-04	8	124.946855	118.949381	18.4125	fully_thawed
2023-07-05	8	89.2157471	89.1379505	11.8875	fully_thawed
2023-07-06	8	101.540381	99.0015504	18.4375	fully_thawed
2023-07-07	8	90.7057301	88.3942528	20.4	fully_thawed
2023-07-08	8	82.0840488	84.6694723	15.85	fully_thawed
2023-07-09	8	99.1335258	94.3421708	20.1125	fully_thawed
2023-07-10	8	103.139045	116.06328	19.025	fully_thawed
2023-07-11	8	91.7801651	85.9948847	20.175	fully_thawed
2023-07-12	8	42.8239454	53.3858829	20.35	fully_thawed
2023-07-13	8	60.9340832	73.6003756	16.7625	fully_thawed
2023-07-14	8	60.0526603	66.8935262	14.575	fully_thawed
2023-07-15	8	76.4054909	83.9482106	14.4625	fully_thawed
2023-07-16	8	45.7691207	46.8267716	13.4125	fully_thawed
2023-07-17	8	88.0293306	85.3056854	15.3375	fully_thawed
2023-07-18	8	79.4695261	73.9802775	16.05	fully_thawed
2023-07-19	8	72.7707008	98.8396103	12.5875	fully_thawed
2023-07-20	8	100.605945	97.1037608	13.6625	fully_thawed
2023-07-21	8	54.6632769	58.9828956	13.4125	fully_thawed
2023-07-22	8	49.1530095	50.0321278	13.55	fully_thawed
2023-07-23	8	52.0787468	52.0586663	14.4375	fully_thawed
2023-07-24	8	55.5108827	77.0189918	15.2375	fully_thawed

Table C5. Continued.

date	chamber_id	ch4_flux_mgch4m2d1_median	ch4_flux_mgch4m2d1_mean	peat_temp	thaw_stage
2023-07-25	8	55.0531341	75.2777923	15.3125	fully_thawed
2023-07-26	8	80.6270529	90.3159352	16.7	fully_thawed
2023-07-27	8	179.422789	177.185227	20.025	fully_thawed
2023-07-28	8	135.095657	136.476995	20.175	fully_thawed
2023-07-29	8	121.325816	140.213709	19.425	fully_thawed
2023-07-30	8	112.376703	123.029358	16.4625	fully_thawed
2023-07-31	8	65.010212	62.6815346	17.85	fully_thawed
2023-08-01	8	98.6857163	93.9872872	15.55	fully_thawed
2023-08-02	8	98.081123	88.0297787	15.125	fully_thawed
2023-08-03	8	55.3702881	63.9778193	17.075	fully_thawed
2023-08-04	8	114.624674	116.300391	16.5125	fully_thawed
2023-08-05	8	138.729082	138.288381	14.4375	fully_thawed
2023-08-06	8	194.554335	193.395251	14.275	fully_thawed
2023-08-07	8	68.9633448	81.0578537	14.075	fully_thawed
2023-08-08	8	72.2752781	79.3467784	17.675	fully_thawed
2023-08-09	8	73.333636	129.937336	18.3625	fully_thawed
2023-08-10	8	158.331138	159.917908	14	fully_thawed
2023-08-11	8	73.1789191	78.7288633	14.1875	fully_thawed
2023-08-12	8	96.4098046	124.391776	13.925	fully_thawed
2023-08-13	8	74.9828709	135.380888	13.5875	fully_thawed
2023-08-14	8	140.817714	150.033294	15.4625	fully_thawed
2023-08-15	8	249.731429	236.124016	16.4	fully_thawed
2023-08-16	8	151.419455	175.272705	12.3125	fully_thawed
2023-08-17	8	151.557401	179.81294	15.075	fully_thawed
2023-08-18	8	155.843219	193.997706	11.8375	fully_thawed
2023-08-19	8	80.9519732	122.660288	13.675	fully_thawed
2023-08-20	8	62.6858435	70.4797608	15.2375	fully_thawed
2023-08-21	8	84.8247269	210.635347	14.85	fully_thawed
2023-08-22	8	197.024031	212.686385	14.8375	fully_thawed
2023-08-23	8	225.034049	227.98486	14.625	fully_thawed
2023-08-24	8	154.545038	207.369594	13.2625	fully_thawed
2023-08-25	8	100.121819	150.12795	14.1875	fully_thawed
2023-08-26	8	142.596869	154.284122	13.975	fully_thawed
2023-08-27	8	68.0651359	131.91971	13.9625	fully_thawed
2023-08-28	8	61.5780643	61.3165775	13	fully_thawed
2023-08-29	8	89.8932177	111.008369	12.8375	fully_thawed
2023-08-30	8	194.667128	196.736206	14.975	fully_thawed
2023-05-19	9	21.8601571	22.8400082	1.325	fully_thawed
2023-05-20	9	11.6146665	11.0711051	1.3	fully_thawed
2023-05-21	9	18.8943766	17.5897242	1.525	fully_thawed
2023-05-22	9	27.3975222	35.2203079	0.975	fully_thawed
2023-05-23	9	22.424599	24.7424736	1.5125	fully_thawed
2023-05-24	9	12.2903458	27.0290205	1.4875	fully_thawed
2023-05-25	9	20.4846225	18.5515487	1.6625	fully_thawed
2023-05-26	9	18.8217039	17.8283651	1.6875	fully_thawed
2023-05-27	9	29.0562812	28.973108	1.7	fully_thawed
2023-05-28	9	25.1520191	25.883117	1.55	fully_thawed
2023-05-29	9	19.1497958	22.3258512	1.8875	fully_thawed
2023-05-30	9	28.5140197	30.4782789	1.8125	fully_thawed
2023-05-31	9	12.2806488	26.9543911	1.725	fully_thawed
2023-06-01	9	28.7907459	30.7969776	2.0375	fully_thawed
2023-06-02	9	31.7277975	34.5188892	2.85	fully_thawed
2023-06-03	9	12.843581	14.051345	3	fully_thawed
2023-06-04	9	15.4399248	16.8971211	3.025	fully_thawed
2023-06-05	9	10.3431169	8.68856537	2.9125	fully_thawed
2023-06-06	9	17.1475016	17.7663835	3.5	fully_thawed
2023-06-07	9	30.6175896	28.9055717	3.375	fully_thawed

Table C5. Continued.

date	chamber_id	ch4_flux_mgch4m2d1_median	ch4_flux_mgch4m2d1_mean	peat_temp	thaw_stage
2023-06-08	9	19.1719179	21.2954023	3.0375	fully_thawed
2023-06-09	9	29.2840512	45.483657	3.57142857	fully_thawed
2023-06-10	9	25.4503584	41.9297051	2.75	fully_thawed
2023-06-11	9	28.7861429	42.4575503	2.6	fully_thawed
2023-06-12	9	18.1588137	27.1200648	3.4875	fully_thawed
2023-06-13	9	15.6149258	19.7926886	3.3375	fully_thawed
2023-06-14	9	20.2457051	20.3574749	3.1375	fully_thawed
2023-06-15	9	24.7602037	23.8131516	3.125	fully_thawed
2023-06-16	9	36.6875552	43.5213909	2.9875	fully_thawed
2023-06-17	9	43.4093611	54.1996233	1.7	fully_thawed
2023-06-18	9	33.2430488	79.997975	1.5125	fully_thawed
2023-06-19	9	53.2388994	67.303491	1.4875	fully_thawed
2023-06-20	9	35.0823231	46.0291915	1.7375	fully_thawed
2023-06-21	9	44.3443703	50.4739139	2.8375	fully_thawed
2023-06-22	9	24.7112247	30.5857029	1.7875	fully_thawed
2023-06-23	9	66.3432432	75.0238727	3.775	fully_thawed
2023-06-24	9	71.9940645	68.0269518	3.9125	fully_thawed
2023-06-25	9	66.9624634	69.5681375	4.4	fully_thawed
2023-06-26	9	34.4875342	37.4454253	3.7	fully_thawed
2023-06-27	9	32.1128129	49.3668859	2.55	fully_thawed
2023-06-28	9	35.4868038	70.5200094	3.7375	fully_thawed
2023-06-29	9	56.0230485	66.4854346	2.8	fully_thawed
2023-06-30	9	35.0536483	37.9166821	3.7625	fully_thawed
2023-07-01	9	36.3572308	34.5227723	2.875	fully_thawed
2023-07-02	9	62.9398655	70.2667796	4.3125	fully_thawed
2023-07-03	9	43.9137521	62.711237	3.95	fully_thawed
2023-07-04	9	84.1333927	112.883854	2.7625	fully_thawed
2023-07-05	9	74.1425748	69.6787019	4.875	fully_thawed
2023-07-06	9	55.6372893	60.342801	3.75	fully_thawed
2023-07-07	9	54.1536993	63.6827046	2.75	fully_thawed
2023-07-08	9	57.1462326	111.17401	5.0625	fully_thawed
2023-07-09	9	84.4408589	114.402167	3.9375	fully_thawed
2023-07-10	9	125.758643	202.354261	3.7875	fully_thawed
2023-07-11	9	90.4711308	145.271263	4.3375	fully_thawed
2023-07-12	9	49.3281588	48.1279533	3.7875	fully_thawed
2023-07-13	9	67.5695327	70.2440776	4.5625	fully_thawed
2023-07-14	9	64.166318	99.5091083	5.9125	fully_thawed
2023-07-15	9	83.0417302	110.576682	7.2125	fully_thawed
2023-07-16	9	55.9762745	109.767193	6.0125	fully_thawed
2023-07-17	9	116.356878	129.690126	6.15	fully_thawed
2023-07-18	9	79.6578928	85.2373324	7.9875	fully_thawed
2023-07-19	9	96.2904357	110.851157	8.075	fully_thawed
2023-07-20	9	94.3315022	145.789704	7.9125	fully_thawed
2023-07-21	9	77.8990507	74.6335483	8.8625	fully_thawed
2023-07-22	9	72.2680472	63.7881582	8.975	fully_thawed
2023-07-23	9	65.4965943	64.8153473	8.4875	fully_thawed
2023-07-24	9	75.7396548	88.8207036	8.775	fully_thawed
2023-07-25	9	67.8346061	63.1338917	9.3	fully_thawed
2023-07-26	9	97.3968974	151.103139	9.3875	fully_thawed
2023-07-27	9	191.247927	185.297682	9.625	fully_thawed
2023-07-28	9	193.206865	171.693767	10.2	fully_thawed
2023-07-29	9	92.986422	120.613128	11.225	fully_thawed
2023-07-30	9	117.88812	117.570781	10.85	fully_thawed
2023-07-31	9	83.9161709	76.4805586	10.675	fully_thawed
2023-08-01	9	91.1760178	96.5148396	11.0125	fully_thawed
2023-08-02	9	123.072066	122.536646	11.5	fully_thawed
2023-08-03	9	96.5049759	91.5312138	11.6625	fully_thawed

Table C5. Continued.

date	chamber_id	ch4_flux_mgch4m2d1_median	ch4_flux_mgch4m2d1_mean	peat_temp	thaw_stage
2023-08-04	9	116.419955	113.372383	12.7875	fully_thawed
2023-08-05	9	102.427354	141.310221	12.9125	fully_thawed
2023-08-06	9	239.310565	229.744061	12.075	fully_thawed
2023-08-07	9	94.2441887	109.598875	12.2	fully_thawed
2023-08-08	9	88.0675217	83.2518536	10.9375	fully_thawed
2023-08-09	9	104.1454	107.21431	12.575	fully_thawed
2023-08-10	9	202.513157	176.289944	13.4125	fully_thawed
2023-08-11	9	109.054042	117.815556	13.1625	fully_thawed
2023-08-12	9	100.641251	146.806711	12.4125	fully_thawed
2023-08-13	9	90.3502941	126.836101	12.5875	fully_thawed
2023-08-14	9	118.76462	188.582827	12.375	fully_thawed
2023-08-15	9	268.856306	254.511493	12.7125	fully_thawed
2023-08-16	9	233.716298	315.282061	12.6125	fully_thawed
2023-08-17	9	153.002257	205.716302	12.3625	fully_thawed
2023-08-18	9	161.186907	178.491091	12.15	fully_thawed
2023-08-19	9	205.850834	193.125026	11.525	fully_thawed
2023-08-20	9	115.506318	140.382822	11.225	fully_thawed
2023-08-21	9	156.318628	270.920632	11.6875	fully_thawed
2023-08-22	9	285.042443	310.843272	12.4875	fully_thawed
2023-08-23	9	273.472399	358.147244	12.6	fully_thawed
2023-08-24	9	146.866361	232.216088	11.95	fully_thawed
2023-08-25	9	132.775318	168.704937	11.375	fully_thawed
2023-08-26	9	244.950784	252.266715	11.2125	fully_thawed
2023-08-27	9	160.286048	152.657018	11.1125	fully_thawed
2023-08-28	9	95.1710018	100.324303	10.8375	fully_thawed
2023-08-29	9	164.601244	235.245973	11.4125	fully_thawed
2023-08-30	9	375.879582	372.361953	11.6375	fully_thawed

Table C6. Results of generalized additive models (GAM) used for determining CH_4 flux season values. Note: Intact 2 plot GAM $R^2_{adj} < 0.1$, and the CH_4 flux periods are based on moving 7 d medians. CI = 95 % confidence interval.

Chamber	R^2_{adj}	p-value	CH_4 flux period	CH_4 flux period value ($mg\,CH_4\,m^{-2}\,d^{-1}$)	95 % CI	CH_4 flux period date (YYYY-MM-DD)
Intact 1	0.32	< 0.001	Early	−0.1	−0.6–0.3	2023-05-19
			Middle	0.4	0.2–0.6	2023-08-16
			Peak	1.2	0.7–1.9	2023-08-30
Intact 2	–	–	Early	0.3	–	2023-05-19
			Middle	0.4	–	2023-07-06
			Peak	1.0	–	2023-08-15
Intact 3	0.85	<0.001	Early	5.8	3.8–8.9	2023-06-25
			Middle	29.9	19.6–45.4	2023-07-26
			Peak	56.8	36.7–88.1	2023-08-25
Partly thawed 1	0.76	<0.001	Early	9.8	7.9–12.0	2023-06-16
			Middle	32.8	26.6–40.4	2023-07-16
			Peak	61.5	41.1–91.8	2023-08-30
Partly thawed 2	0.82	<0.001	Early	20.4	17.8–23.4	2023-06-23
			Middle	53.4	46.4–61.4	2023-08-08
			Peak	92.9	71.5–120.8	2023-08-30
Partly thawed 3	0.67	<0.001	Early	22.0	19.9–24.4	2023-06-13
			Middle	54.6	49.7–60.1	2023-08-01
			Peak	93.5	80.4–108.7	2023-08-30
Fully thawed 1	0.66	<0.001	Early	50.6	38.9–66.0	2023-05-19
			Middle	85.0	73.8–97.8	2023-06-21
			Peak	127.5	109.5–148.4	2023-08-25
Fully thawed 2	0.66	<0.001	Early	40.1	33.9–47.3	2023-06-07
			Middle	77.7	65.9–91.6	2023-06-18
			Peak	120.2	101.0–142.9	2023-08-20
Fully thawed 3	0.83	<0.001	Early	35.4	32.3–38.9	2023-06-19
			Middle	116.9	106.3–128.5	2023-08-04
			Peak	214.4	180.0–255.2	2023-08-30

Code availability. The R code used for data processing and analysis can be accessed via Zenodo (https://doi.org/10.5281/zenodo.20718440, Määttä, 2026).

Data availability. The belowground trait and vegetation survey data together with edaphic variables (Määttä and Malhotra, 2026) can be openly accessed at https://doi.org/10.5281/zenodo.18269229. The porewater CH_4 and $\delta^{13}C$ data (Wilson et al., 2026) is available with open access at https://doi.org/10.5281/zenodo.18363867 (Wilson et al., 2026). The daily-aggregated automated chamber CH_4 flux data from the productive season and the peat moisture data are shown in the Appendices (Tables C5 and C3, respectively). The full chamber CH_4 flux dataset will be published in the EMERGE-DB database (Bolduc et al., 2020).

Author contributions. TM and AM conceptualized the study and prepared the original manuscript draft. Data curation and provision of resources was done by TM, RV, PC, SH, RW, SB, and JC. TM conducted the formal analysis, investigation, and visualization, and collected and processed the belowground trait data. Chamber CH_4 flux data was collected and provided by RV and PC, and porewater gas data by SH, SB, RW and JC. AM and TM acquired funding for the study and coordinated the project. AM supervised the project. All authors contributed to the review and editing of the manuscript.

Competing interests. The contact author has declared that none of the authors has any competing interests.

Disclaimer. Publisher's note: Copernicus Publications remains neutral with regard to jurisdictional claims made in the text, published maps, institutional affiliations, or any other geographical representation in this paper. The authors bear the ultimate responsibility for providing appropriate place names. Views expressed in the text are those of the authors and do not necessarily reflect the views of the publisher.

Acknowledgements. We thank Melina Bucher and Charmaine Bassfeld for their assistance in the field and laboratory work. We are grateful to Yves Brügger and Thomas Keller for their help in the laboratory at the University of Zurich, and also to Martina Peter, Felix Zimmermann, and Mara Wieser for providing access to, and support in, the laboratory at the Swiss Federal Research Institute WSL. We also thank Christina Biasi and Maija Marushchak for providing the peat moisture data, and Apryl Perry, Carmody McCalley and Cheristy Jones for automated chamber CH_4 flux data, and Nitin Chaudhary for valuable insights. We thank Alisa Heuchel, the Swedish Polar Research Secretariat and SITES for the support of the work done at the Abisko Scientific Research Station. SITES is supported by the Swedish Research Council. Porewater and automated chamber flux data were collected and analyzed using funding from the EMERGE Biology Integration Institute, funded by the National Science Foundation, Biology Integration Institutes Program, Award #2022070 awarded to Virginia Rich and RV.

Financial support. This research has been supported by the Schweizerischer Nationalfonds zur Förderung der Wissenschaftlichen Forschung (grant no. 200021_215214 to AM), the Universität Zürich, Foundation for Research in Science and the Humanities (grant no. STWF-22-028 to AM), the Swiss Polar Institute Polar Access Grant (grant no. PAF-2023-001 to TM) and an Early Career Award from the U.S. Department of Energy, Office of Science, Biological and Environmental Research to AM. RV was funded by the US Department of Energy's Genomic Sciences Program grant (grant no. DE-SC0023456).

Review statement. This paper was edited by Jack Middelburg and reviewed by Tim Moore and one anonymous referee.

References

Armstrong, W., Justin, S. H. F. W., Beckett, P. M., and Lythe, S.: Root adaptation to soil waterlogging, Aquat. Bot., 39, 57–73, https://doi.org/10.1016/0304-3770(91)90022-w, 1991.

Bardgett, R. D., Mommer, L., and De Vries, F. T.: Going underground: root traits as drivers of ecosystem processes, Trends Ecol. Evol., 29, 692–699, https://doi.org/10.1016/j.tree.2014.10.006, 2014.

Bäckstrand, K., Crill, P. M., Mastepanov, M., Christensen, T. R., and Bastviken, D.: Non-methane volatile organic compound flux from a subarctic mire in Northern Sweden, Tellus B, 60, 226, https://doi.org/10.1111/j.1600-0889.2007.00331.x, 2008.

Bergmann, J., Weigelt, A., van der Plas, F., Laughlin, D. C., Kuyper, T. W., Guerrero-Ramirez, N., Valverde-Barrantes, O. J., Bruelheide, H., Freschet, G. T., Iversen, C. M., Kattge, J., McCormack, M. L., Meier, I. C., Rillig, M. C., Roumet, C., Semchenko, M., Sweeney, C. J., van Ruijven, J., York, L. M., and Mommer, L.: The fungal collaboration gradient dominates the root economics space in plants, Sci. Adv., 6, https://doi.org/10.1126/sciadv.aba3756, 2020.

Bhullar, G. S., Edwards, P. J., and Olde Venterink, H.: Variation in the plant-mediated methane transport and its importance for methane emission from intact wetland peat mesocosms, J. Plant Ecol., 6, 298–304, https://doi.org/10.1093/jpe/rts045, 2013.

Billings, W. D., Peterson, K. M., and Shaver, G. R.: Growth, turnover, and respiration rates of roots and tillers in tundra graminoids, in: Ecological Studies, Springer New York, New York, NY, 415–434, https://doi.org/10.1007/978-1-4612-6307-4_18, 1978.

Blume-Werry, G., Wilson, S. D., Kreyling, J., and Milbau, A.: The hidden season: growing season is 50 % longer below than above ground along an arctic elevation gradient, New Phytol., 209, 978–986, https://doi.org/10.1111/nph.13655, 2016.

Blume-Werry, G., Milbau, A., Teuber, L. M., Johansson, M., and Dorrepaal, E.: Dwelling in the deep – strongly increased root growth and rooting depth enhance plant interactions with thawing permafrost soil, New Phytol., 223, 1328–1339, https://doi.org/10.1111/nph.15903, 2019.

Bolduc, B., Hodgkins, S. B., Varner, R. K., Crill, P. M., McCalley, C. K., Chanton, J. P., Tyson, G. W., Riley, W. J., Palace, M., Duhaime, M. B., Hough, M. A., Saleska, S. R., Sullivan, M. B., Rich, V. I., and IsoGenie Project Coordinators, IsoGenie Project Team, A2A Project Team: The IsoGenie database: an interdisciplinary data management solution for ecosystems biology and environmental research, PeerJ, 8, e9467, https://doi.org/10.7717/peerj.9467, 2020.

Bouchard, V., Frey, S. D., Gilbert, J. M., and Reed, S. E.: Effects of macrophyte functional group richness on emergent freshwater wetland functions, Ecology, 88, 2903–2914, https://doi.org/10.1890/06-1144.1, 2007.

Bubier, J., Crill, P., Mosedale, A., Frolking, S., and Linder, E.: Peatland responses to varying interannual moisture conditions as measured by automatic CO_2 chambers, Global Biogeochem. Cy., 17, https://doi.org/10.1029/2002gb001946, 2003.

Chanton, J. P.: The effect of gas transport on the isotope signature of methane in wetlands, Org. Geochem., 36, 753–768, https://doi.org/10.1016/j.orggeochem.2004.10.007, 2005.

Chanton, J. P. and Dacey, J. W. H.: Effects of vegetation on methane flux, reservoirs, and carbon isotopic composition, in: Trace Gas Emissions by Plants, Elsevier, 65–92, https://doi.org/10.1016/b978-0-12-639010-0.50008-x, 1991.

Christensen, T. R., Johansson, T., Åkerman, H. J., Mastepanov, M., Malmer, N., Friborg, T., Crill, P., and Svensson, B. H.: Thawing sub-arctic permafrost: Effects on vegetation and methane emissions, Geophys. Res. Lett., 31, https://doi.org/10.1029/2003gl018680, 2004.

Crill, P., McCalley, C., and Crew, A. F.: Manual active layer and and water table depth measurements from the autochamber sites at Stordalen Mire, northern Sweden (2003–2017), https://doi.org/10.5281/zenodo.10420396, 2023.

Delwiche, K. B., Knox, S. H., Malhotra, A., Fluet-Chouinard, E., McNicol, G., Feron, S., Ouyang, Z., Papale, D., Trotta, C., Canfora, E., Cheah, Y.-W., Christianson, D., Alberto, Ma. C. R., Alekseychik, P., Aurela, M., Baldocchi, D., Bansal, S., Billesbach, D. P., Bohrer, G., Bracho, R., Buchmann, N., Campbell, D. I., Celis, G., Chen, J., Chen, W., Chu, H., Dalmagro, H. J., Dengel, S., Desai, A. R., Detto, M., Dolman, H., Eichelmann, E., Euskirchen, E., Famulari, D., Fuchs, K., Goeckede, M., Gogo, S., Gondwe, M. J., Goodrich, J. P., Gottschalk, P., Graham, S. L., Heimann, M., Helbig, M., Helfter, C., Hemes, K. S., Hirano, T., Hollinger, D., Hörtnagl, L., Iwata, H., Jacotot, A., Jurasinski, G., Kang, M., Kasak, K., King, J., Klatt, J., Koebsch, F., Krauss, K. W., Lai, D. Y. F., Lohila, A., Mammarella, I., Belelli Marchesini, L., Manca, G., Matthes, J. H., Maximov, T., Merbold, L., Mitra, B., Morin, T. H., Nemitz, E., Nilsson, M. B., Niu, S., Oechel, W. C., Oikawa, P. Y., Ono, K., Peichl, M., Peltola, O., Reba, M. L., Richardson, A. D., Riley, W., Runkle, B. R. K., Ryu, Y., Sachs, T., Sakabe, A., Sanchez, C. R., Schuur, E. A., Schäfer, K. V. R., Sonnentag, O., Sparks, J. P., Stuart-Haëntjens, E., Sturtevant, C., Sullivan, R. C., Szutu, D. J., Thom, J. E., Torn, M. S., Tuittila, E.-S., Turner, J., Ueyama, M., Valach, A. C., Vargas, R., Varlagin, A., Vazquez-Lule, A., Verfaillie, J. G., Vesala, T., Vourlitis, G. L., Ward, E. J., Wille, C., Wohlfahrt, G., Wong, G. X., Zhang, Z., Zona, D., Windham-Myers, L., Poulter, B., and Jackson, R. B.: FLUXNET-CH_4: a global, multi-ecosystem dataset and analysis of methane seasonality from freshwater wetlands , Earth Syst. Sci. Data, 13, 3607–3689, https://doi.org/10.5194/essd-13-3607-2021, 2021.

Dong, N., Prentice, I. C., Wright, I. J., Evans, B. J., Togashi, H. F., Caddy-Retalic, S., McInerney, F. A., Sparrow, B., Leitch, E., and Lowe, A. J.: Components of leaf-trait variation along environmental gradients, New Phytol., 228, 82–94, https://doi.org/10.1111/nph.16558, 2020.

Eissenstat, D. M., Wells, C. E., Yanai, R. D., and Whitbeck, J. L.: Building roots in a changing environment: implications for root longevity, New Phytol., 147, 33–42, https://doi.org/10.1046/j.1469-8137.2000.00686.x, 2000.

Eklundh, L. and Jönsson, P.: TIMESAT: A software package for time-series processing and assessment of vegetation dynamics, in: Remote Sensing Time Series, Springer International Publishing, Cham, 141–158, https://doi.org/10.1007/978-3-319-15967-6_7, 2015.

Freschet, G. T., Pagès, L., Iversen, C. M., Comas, L. H., Rewald, B., Roumet, C., Klimešová, J., Zadworny, M., Poorter, H., Postma, J. A., Adams, T. S., Bagniewska-Zadworna, A., Bengough, A. G., Blancaflor, E. B., Brunner, I., Cornelissen, J. H. C., Garnier, E., Gessler, A., Hobbie, S. E., Meier, I. C., Mommer, L., Picon-Cochard, C., Rose, L., Ryser, P., Scherer-Lorenzen, M., Soudzilovskaia, N. A., Stokes, A., Sun, T., Valverde-Barrantes, O. J., Weemstra, M., Weigelt, A., Wurzburger, N., York, L. M., Batterman, S. A., Gomes de Moraes, M., Janeček, Š., Lambers, H., Salmon, V., Tharayil, N., and McCormack, M. L.: A starting guide to root ecology: strengthening ecological concepts and standardising root classification, sampling, processing and trait measurements, New Phytol., 232, 973–1122, https://doi.org/10.1111/nph.17572, 2021a.

Freschet, G. T., Roumet, C., Comas, L. H., Weemstra, M., Bengough, A. G., Rewald, B., Bardgett, R. D., De Deyn, G. B., Johnson, D., Klimešová, J., Lukac, M., McCormack, M. L., Meier, I. C., Pagès, L., Poorter, H., Prieto, I., Wurzburger, N., Zadworny, M., Bagniewska-Zadworna, A., Blancaflor, E. B., Brunner, I., Gessler, A., Hobbie, S. E., Iversen, C. M., Mommer, L., Picon-Cochard, C., Postma, J. A., Rose, L., Ryser, P., Scherer-Lorenzen, M., Soudzilovskaia, N. A., Sun, T., Valverde-Barrantes, O. J., Weigelt, A., York, L. M., and Stokes, A.: Root traits as drivers of plant and ecosystem functioning: current understanding, pitfalls and future research needs, New Phytol., 232, 1123–1158, https://doi.org/10.1111/nph.17072, 2021b.

Fritz, C., Pancotto, V. A., Elzenga, J. T. M., Visser, E. J. W., Grootjans, A. P., Pol, A., Iturraspe, R., Roelofs, J. G. M., and Smolders, A. J. P.: Zero methane emission bogs: extreme rhizosphere oxygenation by cushion plants in Patagonia, New Phytol., 190, 398–408, https://doi.org/10.1111/j.1469-8137.2010.03604.x, 2011.

Gao, Y., Wang, H., Yang, F., Dai, X., Meng, S., Hu, M., Kou, L., and Fu, X.: Relationships between root exudation and root morphological and architectural traits vary with growing season, Tree Physiol., 44, 118, https://doi.org/10.1093/treephys/tpad118, 2024.

Ge, M., Korrensalo, A., Putkinen, A., Laiho, R., Kohl, L., Pihlatie, M., Lohila, A., Mäkiranta, P., Siljanen, H., Tuittila, E.-S., Wang, J., and Koskinen, M.: CH_4 transport in wetland plants under controlled environmental conditions – separating the impacts of phenology from environmental variables, Plant Soil, 507, 671–691, https://doi.org/10.1007/s11104-024-06756-x, 2025.

Gorham, E.: Northern peatlands: Role in the carbon cycle and probable responses to climatic warming, Ecol. Appl., 1, 182–195, https://doi.org/10.2307/1941811, 1991.

Gray, A., Levy, P. E., Cooper, M. D. A., Jones, T., Gaiawyn, J., Leeson, S. R., Ward, S. E., Dinsmore, K. J., Drewer, J., Sheppard, L. J., Ostle, N. J., Evans, C. D., Burden, A., and Zieliński, P.: Methane indicator values for peatlands: a comparison of species and functional groups, Glob. Change Biol., 19, 1141–1150, https://doi.org/10.1111/gcb.12120, 2013.

Greenup, A., Bradford, M., Mcnamara, N., Ineson, P., and Lee, J.: The role of Eriophorum vaginatum in CH_4 flux from an ombrotrophic peatland, Plant Soil, 227, 265–272, 2000.

Guyonnet, J. P., Cantarel, A. A. M., Simon, L., and Haichar, F. E. Z.: Root exudation rate as functional trait involved in plant nutrient-use strategy classification, Ecol. Evol., 8, 8573–8581, https://doi.org/10.1002/ece3.4383, 2018.

Hackney, C. T. and De La Cruz, A. A.: In situ decomposition of roots and rhizomes of two tidal marsh plants, Ecology, 61, 226–231, https://doi.org/10.2307/1935178, 1980.

Henneberg, A., Brix, H., and Sorrell, B. K.: The interactive effect of Juncus effusus and water table position on mesocosm methanogenesis and methane emissions, Plant Soil, 400, 45–54, https://doi.org/10.1007/s11104-015-2707-y, 2016.

Hewitt, R. E., Taylor, D. L., Genet, H., McGuire, A. D., and Mack, M. C.: Below-ground plant traits influence tundra plant acquisition of newly thawed permafrost nitrogen, J. Ecol., 107, 950–962, https://doi.org/10.1111/1365-2745.13062, 2019.

Hodgkins, S. B., Tfaily, M. M., McCalley, C. K., Logan, T. A., Crill, P. M., Saleska, S. R., Rich, V. I., and Chanton, J. P.: Changes in peat chemistry associated with permafrost thaw increase greenhouse gas production, P. Natl. Acad. Sci. USA, 111, 5819–5824, https://doi.org/10.1073/pnas.1314641111, 2014.

Hogg, E. H.: Decay potential of hummock and hollow sphagnum peats at different depths in a Swedish raised bog, Oikos, 66, 269, https://doi.org/10.2307/3544814, 1993.

Holmes, M. E., Crill, P. M., Burnett, W. C., McCalley, C. K., Wilson, R. M., Frolking, S., Chang, K.-Y., Riley, W. J., Varner, R. K., Hodgkins, S. B., McNichol, A. P., Saleska, S. R., Rich, V. I., Chanton, J. P., IsoGenie Project Coordinators, and IsoGenie Field Team: Carbon accumulation, flux, and fate in stordalen mire, a permafrost peatland in transition, Global Biogeochem. Cy., 36, https://doi.org/10.1029/2021gb007113, 2022.

Hough, M., McCabe, S., Vining, S. R., Pickering Pedersen, E., Wilson, R. M., Lawrence, R., Chang, K.-Y., Bohrer, G., IsoGenie Coordinators, Riley, W. J., Crill, P. M., Varner, R. K., Blazewicz, S. J., Dorrepaal, E., Tfaily, M. M., Saleska, S. R., and Rich, V. I.: Coupling plant litter quantity to a novel metric for litter quality explains C storage changes in a thawing permafrost peatland, Glob. Change Biol., 28, 950–968, https://doi.org/10.1111/gcb.15970, 2022.

Husby, C.: Biology and functional ecology of Equisetum with emphasis on the giant horsetails, Bot. Rev., 79, 147–177, https://doi.org/10.1007/s12229-012-9113-4, 2013.

Hyvönen, T., Ojala, A., Kankaala, P., and Martikainen, P. J.: Methane release from stands of water horsetail (Equisetum fluviatile) in a boreal lake, Freshwater Biol., 40, 275–284, https://doi.org/10.1046/j.1365-2427.1998.00351.x, 1998.

Iversen, C. M., Murphy, M. T., Allen, M. F., Childs, J., Eissenstat, D. M., Lilleskov, E. A., Sarjala, T. M., Sloan, V. L., and Sullivan, P. F.: Advancing the use of minirhizotrons in wetlands, Plant Soil, 352, 23–39, https://doi.org/10.1007/s11104-011-0953-1, 2012.

Iversen, C. M., Sloan, V. L., Sullivan, P. F., Euskirchen, E. S., McGuire, A. D., Norby, R. J., Walker, A. P., Warren, J. M., and Wullschleger, S. D.: The unseen iceberg: plant roots in arctic tundra, New Phytol., 205, 34–58, https://doi.org/10.1111/nph.13003, 2015.

Jackson, M. and Armstrong, W.: Formation of aerenchyma and the processes of plant ventilation in relation to soil flooding and submergence, Plant Biol.-Stuttg., 1, 274–287, https://doi.org/10.1055/s-2007-978516, 1999.

Joabsson, A. and Christensen, T. R.: Methane emissions from wetlands and their relationship with vascular plants: an Arctic example: METHANE EMISSION and VASCULAR PLANTS, Glob. Change Biol., 7, 919–932, https://doi.org/10.1046/j.1354-1013.2001.00044.x, 2001.

Johansson, T., Malmer, N., Crill, P. M., Friborg, T., Åkerman, J. H., Mastepanov, M., and Christensen, T. R.: Decadal vegetation changes in a northern peatland, greenhouse gas fluxes and net radiative forcing, Glob. Change Biol., 12, 2352–2369, https://doi.org/10.1111/j.1365-2486.2006.01267.x, 2006.

Johnston, C. E., Ewing, S. A., Harden, J. W., Varner, R. K., Wickland, K. P., Koch, J. C., Fuller, C. C., Manies, K., and Jorgenson, M. T.: Effect of permafrost thaw on CO_2 and CH_4 exchange in a western Alaska peatland chronosequence, Environ. Res. Lett., 9, 085004, https://doi.org/10.1088/1748-9326/9/8/085004, 2014.

Jönsson, P. and Eklundh, L.: Seasonality extraction by function fitting to time-series of satellite sensor data, IEEE T. Geosci. Remote, 40, 1824–1832, https://doi.org/10.1109/tgrs.2002.802519, 2002.

Kankaala, P. and Bergström, I.: Emission and oxidation of methane in Equisetum fluviatile stands growing on organic sediment and sand bottoms, Biogeochemistry, 67, 21–37, https://doi.org/10.1023/b:biog.0000015277.17288.7a, 2004.

Keuper, F., Dorrepaal, E., van Bodegom, P. M., van Logtestijn, R., Venhuizen, G., van Hal, J., and Aerts, R.: Experimentally increased nutrient availability at the permafrost thaw front selectively enhances biomass production of deep-rooting subarctic peatland species, Glob. Change Biol., 23, 4257–4266, https://doi.org/10.1111/gcb.13804, 2017.

Kichenin, E., Wardle, D. A., Peltzer, D. A., Morse, C. W., and Freschet, G. T.: Contrasting effects of plant inter- and intraspecific variation on community-level trait measures along an environmental gradient, Funct. Ecol., 27, 1254–1261, https://doi.org/10.1111/1365-2435.12116, 2013.

Knoblauch, C., Beer, C., Liebner, S., Grigoriev, M. N., and Pfeiffer, E.-M.: Methane production as key to the greenhouse gas budget of thawing permafrost, Nat. Clim. Change, 8, 309–312, https://doi.org/10.1038/s41558-018-0095-z, 2018.

Knox, S. H., Bansal, S., McNicol, G., Schafer, K., Sturtevant, C., Ueyama, M., Valach, A. C., Baldocchi, D., Delwiche, K., Desai, A. R., Euskirchen, E., Liu, J., Lohila, A., Malhotra, A., Melling, L., Riley, W., Runkle, B. R. K., Turner, J., Vargas, R., Zhu, Q., Alto, T., Fluet-Chouinard, E., Goeckede, M., Melton, J. R., Sonnentag, O., Vesala, T., Ward, E., Zhang, Z., Feron, S., Ouyang, Z., Alekseychik, P., Aurela, M., Bohrer, G., Campbell, D. I., Chen, J., Chu, H., Dalmagro, H. J., Goodrich, J. P., Gottschalk, P., Hirano, T., Iwata, H., Jurasinski, G., Kang, M., Koebsch, F., Mammarella, I., Nilsson, M. B., Ono, K., Peichl, M., Peltola, O., Ryu, Y., Sachs, T., Sakabe, A., Sparks, J. P., Tuittila, E.-S., Vourlitis, G. L., Wong, G. X., Windham-Myers, L., Poulter, B., and Jackson, R. B.: Identifying dominant environmental predictors of freshwater wetland methane fluxes across diurnal to seasonal time scales, Glob. Change Biol., 27, 3582–3604, https://doi.org/10.1111/gcb.15661, 2021.

Koelbener, A., Ström, L., Edwards, P. J., and Olde Venterink, H.: Plant species from mesotrophic wetlands cause relatively high methane emissions from peat soil, Plant Soil, 326, 147–158, https://doi.org/10.1007/s11104-009-9989-x, 2010.

Končalová, H.: Anatomical adaptations to waterlogging in roots of wetland graminoids: limitations and drawbacks, Aquat. Bot., 38, 127–134, https://doi.org/10.1016/0304-3770(90)90102-q, 1990.

Körner, C., Möhl, P., and Hiltbrunner, E.: Four ways to define the growing season, Ecol. Lett., 26, 1277–1292, https://doi.org/10.1111/ele.14260, 2023.

Kummerow, J. and Russell, M.: Seasonal root growth in the arctic tussock tundra, Oecologia, 47, 196–199, https://doi.org/10.1007/BF00346820, 1980.

Laanbroek, H. J.: Methane emission from natural wetlands: interplay between emergent macrophytes and soil microbial processes. A mini-review, Ann. Bot., 105, 141–153, https://doi.org/10.1093/aob/mcp201, 2010.

Laine, A. M., Korrensalo, A., and Tuittila, E.-S.: Plant functional traits play the second fiddle to plant functional types in explaining peatland CO_2 and CH_4 gas exchange, Sci. Total Environ., 834, 155352, https://doi.org/10.1016/j.scitotenv.2022.155352, 2022.

Łakomiec, P., Holst, J., Friborg, T., Crill, P., Rakos, N., Kljun, N., Olsson, P.-O., Eklundh, L., Persson, A., and Rinne, J.: Field-scale CH_4 emission at a subarctic mire with heterogeneous permafrost thaw status, Biogeosciences, 18, 5811–5830, https://doi.org/10.5194/bg-18-5811-2021, 2021.

Larmola, T., Tuittila, E.-S., Tiirola, M., Nykänen, H., Martikainen, P. J., Yrjälä, K., Tuomivirta, T., and Fritze, H.: The role of Sphagnum mosses in the methane cycling of a boreal mire, Ecology, 91, 2356–2365, https://doi.org/10.1890/09-1343.1, 2010.

Lawrence, D. M., Slater, A. G., Romanovsky, V. E., and Nicolsky, D. J.: Sensitivity of a model projection of near-surface permafrost degradation to soil column depth and representation of soil organic matter, J. Geophys. Res., 113, https://doi.org/10.1029/2007jf000883, 2008.

Lê, S., Josse, J., and Husson, F.: FactoMineR: AnR-Package for Multivariate Analysis, J. Stat. Softw., 25, https://doi.org/10.18637/jss.v025.i01, 2008.

Lundin, E., Crill, P., Grudd, H., Holst, J., Kristoffersson, A., Meire, A., Mölder, M., and Rakos, N.: ETC L2 Fluxnet (half-hourly) from Abisko-Stordalen Palsa Bog, 2021-12-31–2023-08-31, ICOS RI [data set], https://hdl.handle.net/11676/JFtuqWbso4iTRa0UFYalE-4X (last access: 15 November 2025), 2023

Luoto, M., Heikkinen, R. K., and Carter, T. R.: Loss of palsa mires in Europe and biological consequences, Environ. Conserv., 31, 30–37, https://doi.org/10.1017/s0376892904001018, 2004.

Määttä, T.: Code for Increased plant mediated methane transport along a peatland permafrost thaw gradient, version v1, Zenodo [code], https://doi.org/10.5281/zenodo.20718440, 2026.

Määttä, T. and Malhotra, A.: The hidden roots of wetland methane emissions, Glob. Change Biol., 30, e17127, https://doi.org/10.1111/gcb.17127, 2024.

Määttä, T. and Malhotra, A.: Plant belowground trait and vegetation survey data from the Stordalen mire 2023, Zenodo [data set], https://doi.org/10.5281/zenodo.18269229, 2026.

Malhotra, A. and Roulet, N. T.: Environmental correlates of peatland carbon fluxes in a thawing landscape: do transitional thaw stages matter?, Biogeosciences, 12, 3119–3130, https://doi.org/10.5194/bg-12-3119-2015, 2015.

Man, M., Kalčík, V., Macek, M., Brůna, J., Hederová, L., Wild, J., and Kopecký, M.: myClim: Microclimate data handling and standardised analyses in R, Methods Ecol. Evol., 14, 2308–2320, 2023.

McCalley, C. K., Woodcroft, B. J., Hodgkins, S. B., Wehr, R. A., Kim, E.-H., Mondav, R., Crill, P. M., Chanton, J. P., Rich, V. I., Tyson, G. W., and Saleska, S. R.: Methane dynamics regulated by microbial community response to permafrost thaw, Nature, 514, 478–481, https://doi.org/10.1038/nature13798, 2014.

McCormack, M. L., Dickie, I. A., Eissenstat, D. M., Fahey, T. J., Fernandez, C. W., Guo, D., Helmisaari, H.-S., Hobbie, E. A., Iversen, C. M., Jackson, R. B., Leppälammi-Kujansuu, J., Norby, R. J., Phillips, R. P., Pregitzer, K. S., Pritchard, S. G., Rewald, B., and Zadworny, M.: Redefining fine roots improves understanding of below-ground contributions to terrestrial biosphere processes, New Phytol., 207, 505–518, https://doi.org/10.1111/nph.13363, 2015.

McGuire, A. D., Anderson, L. G., Christensen, T. R., Dallimore, S., Guo, L., Hayes, D. J., Heimann, M., Lorenson, T. D., Macdonald, R. W., and Roulet, N.: Sensitivity of the carbon cycle in the Arctic to climate change, Ecol. Monogr., 79, 523–555, https://doi.org/10.1890/08-2025.1, 2009.

Merritt, D. A., Hayes, J. M., and Des Marais, D. J.: Carbon isotopic analysis of atmospheric methane by isotope-ratio-monitoring gas chromatography-mass spectrometry, J. Geophys. Res., 100, 1317–1326, https://doi.org/10.1029/94jd02689, 1995.

Metsävainio, K.: Untersuchungen über das Wurzelsystem der Moorpflanzen, Annales Botanici Societatis Zoologicae-Botanicae Fennicae Vanamo, 1, 1–422, 1931.

Mollenkopf, M., Lenge, K., Drabesch, S., Monteux, S., van Grinsven, S., Joshi, P., Dorrepaal, E., Wild, B., Kappler, A., and Muehe, E. M.: Graminoids increase greenhouse gas emissions from thawed permafrost at the end of the growing season, Glob. Change Biol., 32, e70783, https://doi.org/10.1111/gcb.70783, 2026.

Mondav, R., Woodcroft, B. J., Kim, E.-H., McCalley, C. K., Hodgkins, S. B., Crill, P. M., Chanton, J., Hurst, G. B., VerBerkmoes, N. C., Saleska, S. R., Hugenholtz, P., Rich, V. I., and Tyson, G. W.: Discovery of a novel methanogen prevalent in thawing permafrost, Nat. Commun., 5, 3212, https://doi.org/10.1038/ncomms4212, 2014.

Moor, H., Rydin, H., Hylander, K., Nilsson, M. B., Lindborg, R., and Norberg, J.: Towards a trait-based ecology of wetland vegetation, J. Ecol., 105, 1623–1635, https://doi.org/10.1111/1365-2745.12734, 2017.

Noyce, G. L., Varner, R. K., Bubier, J. L., and Frolking, S.: Effect ofCarex rostrataon seasonal and interannual variability in peatland methane emissions, J. Geophys. Res.-Biogeo., 119, 24–34, https://doi.org/10.1002/2013jg002474, 2014.

Noyce, G. L., Smith, A. J., Kirwan, M. L., Rich, R. L., and Megonigal, J. P.: Oxygen priming induced by elevated CO_2 reduces carbon accumulation and methane emissions in coastal wetlands, Nat. Geosci., 16, 63–68, https://doi.org/10.1038/s41561-022-01070-6, 2023.

Oksanen, J., Simpson, G. L., Blanchet, F. G., Kindt, R., Legendre, P., Minchin, P. R., O'Hara, R. B., Solymos, P., Stevens, M. H. H., Szoecs, E., Wagner, H., Barbour, M., Bedward, M., Bolker, B., Borcard, D., Carvalho, G., Chirico, M., De Caceres, M., Durand, S., Evangelista, H., FitzJohn, R., Friendly, M., Furneaux, B., Hannigan, G., Heida, I., Hill, M. O., Lahti, L., Martino, C., McGlinn, D., Ouellette, M.-H., Ribeiro Cunha, E., Smith, T., Stier, A., Ter Braak, C. J. F., and Weedon, J.: vegan: Community Ecology Package, R package version 2.7-2, CRAN [code], https://doi.org/10.32614/CRAN.package.vegan, 2025.

Olefeldt, D., Turetsky, M. R., Crill, P. M., and McGuire, A. D.: Environmental and physical controls on northern terrestrial methane emissions across permafrost zones, Glob. Change Biol., 19, 589–603, https://doi.org/10.1111/gcb.12071, 2013.

Olvmo, M., Holmer, B., Thorsson, S., Reese, H., and Lindberg, F.: Sub-arctic palsa degradation and the role of climatic drivers in the largest coherent palsa mire complex in Sweden (Vissátvuopmi), 1955–2016, Sci. Rep., 10, 8937, https://doi.org/10.1038/s41598-020-65719-1, 2020.

Öquist, M. G. and Svensson, B. H.: Vascular plants as regulators of methane emissions from a subarctic mire ecosystem, J. Geophys. Res.-Atmos., 107, ACL 10-1–ACL 10-10, https://doi.org/10.1029/2001JD001030, 2002.

Ouyang, W., Mueller, F., Hjelmare, M., Lundberg, E., and Zimmer, C.: ImJoy: an open-source computational platform for the deep learning era, Nat. Methods, 16, 1199–1200, https://doi.org/10.1038/s41592-019-0627-0, 2019.

Palace, M., Herrick, C., DelGreco, J., Finnell, D., Garnello, A. J., McCalley, C., McArthur, K., Sullivan, F., and Varner, R. K.: Determining subarctic peatland vegetation using an unmanned aerial system (UAS), Remote Sens.-Basel, 10, 1498, https://doi.org/10.3390/rs10091498, 2018.

Palace, M., Varner, R., Crill, P. M., Frolking, S., McCalley, C. K., Burke, S. A., Chanton, J. P., and Holmes, M. E.: Isogenie Project Coordinators, and Saleska, S.: Stordalen Mire ground cover classifications, based on 2014 WorldView-2 satellite imagery (version 0.0.0), EMERGE Biology Integration Institute, Ohio

State University [data set], https://emerge-db.asc.ohio-state.edu/datasources/0145_Wv2-2014_GroundCoverClassifications (last access: 9 July 2025), 2022.

Pan, Y., Cieraad, E., and van Bodegom, P. M.: Are ecophysiological adaptive traits decoupled from leaf economics traits in wetlands?, Funct. Ecol., 33, 1202–1210, https://doi.org/10.1111/1365-2435.13329, 2019.

Pastorello, G., Trotta, C., Canfora, E., Chu, H., Christianson, D., Cheah, Y.-W., Poindexter, C., Chen, J., Elbashandy, A., Humphrey, M., Isaac, P., Polidori, D., Reichstein, M., Ribeca, A., van Ingen, C., Vuichard, N., Zhang, L., Amiro, B., Ammann, C., Arain, M. A., Ardö, J., Arkebauer, T., Arndt, S. K., Arriga, N., Aubinet, M., Aurela, M., Baldocchi, D., Barr, A., Beamesderfer, E., Belelli Marchesini, L., Bergeron, O., Beringer, J., Bernhofer, C., Berveiller, D., Billesbach, D., Black, T. A., Blanken, P. D., Bohrer, G., Boike, J., Bolstad, P. V., Bonal, D., Bonnefond, J.-M., Bowling, D. R., Bracho, R., Brodeur, J., Brümmer, C., Buchmann, N., Burban, B., Burns, S. P., Buysse, P., Cale, P., Cavagna, M., Cellier, P., Chen, S., Chini, I., Christensen, T. R., Cleverly, J., Collalti, A., Consalvo, C., Cook, B. D., Cook, D., Coursolle, C., Cremonese, E., Curtis, P. S., D'Andrea, E., da Rocha, H., Dai, X., Davis, K. J., De Cinti, B., de Grandcourt, A., De Ligne, A., De Oliveira, R. C., Delpierre, N., Desai, A. R., Di Bella, C. M., di Tommasi, P., Dolman, H., Domingo, F., Dong, G., Dore, S., Duce, P., Dufrêne, E., Dunn, A., Dušek, J., Eamus, D., Eichelmann, U., ElKhidir, H. A. M., Eugster, W., Ewenz, C. M., Ewers, B., Famulari, D., Fares, S., Feigenwinter, I., Feitz, A., Fensholt, R., Filippa, G., Fischer, M., Frank, J., Galvagno, M., Gharun, M., Gianelle, D., Gielen, B., Gioli, B., Gitelson, A., Goded, I., Goeckede, M., Goldstein, A. H., Gough, C. M., Goulden, M. L., Graf, A., Griebel, A., Gruening, C., Grünwald, T., Hammerle, A., Han, S., Han, X., Hansen, B. U., Hanson, C., Hatakka, J., He, Y., Hehn, M., Heinesch, B., Hinko-Najera, N., Hörtnagl, L., Hutley, L., Ibrom, A., Ikawa, H., Jackowicz-Korczynski, M., Janouš, D., Jans, W., Jassal, R., Jiang, S., Kato, T., Khomik, M., Klatt, J., Knohl, A., Knox, S., Kobayashi, H., Koerber, G., Kolle, O., Kosugi, Y., Kotani, A., Kowalski, A., Kruijt, B., Kurbatova, J., Kutsch, W. L., Kwon, H., Launiainen, S., Laurila, T., Law, B., Leuning, R., Li, Y., Liddell, M., Limousin, J.-M., Lion, M., Liska, A. J., Lohila, A., López-Ballesteros, A., López-Blanco, E., Loubet, B., Loustau, D., Lucas-Moffat, A., Lüers, J., Ma, S., Macfarlane, C., Magliulo, V., Maier, R., Mammarella, I., Manca, G., Marcolla, B., Margolis, H. A., Marras, S., Massman, W., Mastepanov, M., Matamala, R., Matthes, J. H., Mazzenga, F., McCaughey, H., McHugh, I., McMillan, A. M. S., Merbold, L., Meyer, W., Meyers, T., Miller, S. D., Minerbi, S., Moderow, U., Monson, R. K., Montagnani, L., Moore, C. E., Moors, E., Moreaux, V., Moureaux, C., Munger, J. W., Nakai, T., Neirynck, J., Nesic, Z., Nicolini, G., Noormets, A., Northwood, M., Nosetto, M., Nouvellon, Y., Novick, K., Oechel, W., Olesen, J. E., Ourcival, J.-M., Papuga, S. A., Parmentier, F.-J., Paul-Limoges, E., Pavelka, M., Peichl, M., Pendall, E., Phillips, R. P., Pilegaard, K., Pirk, N., Posse, G., Powell, T., Prasse, H., Prober, S. M., Rambal, S., Rannik, Ü., Raz-Yaseef, N., Rebmann, C., Reed, D., Resco de Dios, V., Restrepo-Coupe, N., Reverter, B. R., Roland, M., Sabbatini, S., Sachs, T., Saleska, S. R., Sánchez-Cañete, E. P., Sanchez-Mejia, Z. M., Schmid, H. P., Schmidt, M., Schneider, K., Schrader, F., Schroder, I., Scott, R. L., Sedlák, P., Serrano-Ortíz, P., Shao, C., Shi, P., Shironya, I., Siebicke, L., Šigut, L., Silberstein, R., Sirca, C., Spano, D., Steinbrecher, R., Stevens, R. M., Sturtevant, C., Suyker, A., Tagesson, T., Takanashi, S., Tang, Y., Tapper, N., Thom, J., Tomassucci, M., Tuovinen, J.-P., Urbanski, S., Valentini, R., van der Molen, M., van Gorsel, E., van Huissteden, K., Varlagin, A., Verfaillie, J., Vesala, T., Vincke, C., Vitale, D., Vygodskaya, N., Walker, J. P., Walter-Shea, E., Wang, H., Weber, R., Westermann, S., Wille, C., Wofsy, S., Wohlfahrt, G., Wolf, S., Woodgate, W., Li, Y., Zampedri, R., Zhang, J., Zhou, G., Zona, D., Agarwal, D., Biraud, S., Torn, M., and Papale, D.: The FLUXNET2015 dataset and the ONEFlux processing pipeline for eddy covariance data, Sci. Data, 7, 225, https://doi.org/10.1038/s41597-020-0534-3, 2020.

Perryman, C. R., McCalley, C. K., Malhotra, A., Fahnestock, M. F., Kashi, N. N., Bryce, J. G., Giesler, R., and Varner, R. K.: Thaw transitions and redox conditions drive methane oxidation in a permafrost peatland, J. Geophys. Res.-Biogeo., 125, https://doi.org/10.1029/2019jg005526, 2020.

Phillips, R. P., Erlitz, Y., Bier, R., and Bernhardt, E. S.: New approach for capturing soluble root exudates in forest soils, Funct. Ecol., 22, 990–999, https://doi.org/10.1111/j.1365-2435.2008.01495.x, 2008.

Picon-Cochard, C., Pilon, R., Tarroux, E., Pagès, L., Robertson, J., and Dawson, L.: Effect of species, root branching order and season on the root traits of 13 perennial grass species, Plant Soil, 353, 47–57, https://doi.org/10.1007/s11104-011-1007-4, 2012.

Pinheiro, J. and Bates, D. M.: Mixed-effects models in S and S-PLUS, 1st edn., Springer, New York, NY, 528 pp., https://doi.org/10.1007/b98882, 2000.

Pinheiro, J., Bates, D., and R Core Team: nlme: Linear and Nonlinear Mixed Effects Models, CRAN [code], https://doi.org/10.32614/CRAN.package.nlme, 2023.

Polarforskningssekretariatet and SMHI: Abisko Aut (ID 188790) Lufttemperatur (dygn) 1985–2025, SMHI Öppna data: meteorologiska observationer, SMHI, Sveriges meteorologiska och hydrologiska institut [data set], https://www.smhi.se/data/hitta-data-for-en-plats/ladda-ner-vaderobservationer/airtemperatureMean24h/188790 (last access: 9 July 2025), 2025a.

Polarforskningssekretariatet and SMHI: Abisko Aut (ID 188790) Nederbördsmängd (dygn) 1985–2025, SMHI Öppna data: meteorologiska observationer, SMHI, Sveriges meteorologiska och hydrologiska institut [data set], https://www.smhi.se/data/hitta-data-for-en-plats/ladda-ner-vaderobservationer/precipitation24HourSum/188790 (last access: 9 July 2025), 2025b.

Putkinen, A., Larmola, T., Tuomivirta, T., Siljanen, H. M., Bodrossy, L., Tuittila, E.-S., and Fritze, H.: Peatland succession induces a shift in the community composition of Sphagnum-associated active methanotrophs, FEMS Microbiol. Ecol., 88, 596–611, https://doi.org/10.1111/1574-6941.12327, 2014.

Raivonen, M., Smolander, S., Backman, L., Susiluoto, J., Aalto, T., Markkanen, T., Mäkelä, J., Rinne, J., Peltola, O., Aurela, M., Lohila, A., Tomasic, M., Li, X., Larmola, T., Juutinen, S., Tuittila, E.-S., Heimann, M., Sevanto, S., Kleinen, T., Brovkin, V., and Vesala, T.: HIMMELI v1.0: HelsinkI Model of MEthane buiLd-up and emIssion for peatlands, Geosci. Model Dev., 10, 4665–4691, https://doi.org/10.5194/gmd-10-4665-2017, 2017.

R Core Team: R: A Language and Environment for Statistical Computing, R Foundation for Statistical Computing, Vienna, Austria, https://www.R-project.org (last access: 15 May 2026), 2025.

Rose, L.: Pitfalls in root trait calculations: How ignoring diameter heterogeneity can lead to overestimation of functional traits, Front. Plant Sci., 8, 898, https://doi.org/10.3389/fpls.2017.00898, 2017.

Saarnio, S., Wittenmayer, L., and Merbach, W.: Rhizospheric exudation of Eriophorum vaginatum L. – Potential link to methanogenesis, Plant Soil, 267, 343–355, https://doi.org/10.1007/s11104-005-0140-3, 2004.

Schaefer, K., Lantuit, H., Romanovsky, V. E., Schuur, E. A. G., and Witt, R.: The impact of the permafrost carbon feedback on global climate, Environ. Res. Lett., 9, 085003, https://doi.org/10.1088/1748-9326/9/8/085003, 2014.

Scheffer, R. A. and Aerts, R.: Root decomposition and soil nutrient and carbon cycling in two temperate fen ecosystems, Oikos, 91, 541–549, https://doi.org/10.1034/j.1600-0706.2000.910316.x, 2000.

Schimel, J. P.: Plant transport and methane production as controls on methane flux from arctic wet meadow tundra, Biogeochemistry, 28, 183–200, https://doi.org/10.1007/BF02186458, 1995.

Schneider, C. A., Rasband, W. S., and Eliceiri, K. W.: NIH Image to ImageJ: 25 years of image analysis, Nat. Methods, 9, 671–675, https://doi.org/10.1038/nmeth.2089, 2012.

Schuur, E. A. G., Bockheim, J., Canadell, J. G., Euskirchen, E., Field, C. B., Goryachkin, S. V., Hagemann, S., Kuhry, P., Lafleur, P. M., Lee, H., Mazhitova, G., Nelson, F. E., Rinke, A., Romanovsky, V. E., Shiklomanov, N., Tarnocai, C., Venevsky, S., Vogel, J. G., and Zimov, S. A.: Vulnerability of permafrost carbon to climate change: Implications for the global carbon cycle, Bioscience, 58, 701–714, https://doi.org/10.1641/b580807, 2008.

Shaver, G. R.: Ecology of roots and rhizomes in graminoid plants of the Alaskan coastal tundra, PhD thesis, Duke University, Durham, NC, USA, https://www.proquest.com/openview/ad750e00eb95eeb7721530f62152090f/1?cbl=18750&diss=y (last access: 20 January 2026), 1976.

Shaver, G. R. and Billings, W. D.: Root production and root turnover in a wet tundra ecosystem, barrow, Alaska, Ecology, 56, 401–409, https://doi.org/10.2307/1934970, 1975.

Shaver, G. R. and Billings, W. D.: Effects of daylength and temperature on root elongation in tundra graminoids, Oecologia, 28, 57–65, https://doi.org/10.1007/BF00346836, 1977.

Singleton, C. M., McCalley, C. K., Woodcroft, B. J., Boyd, J. A., Evans, P. N., Hodgkins, S. B., Chanton, J. P., Frolking, S., Crill, P. M., Saleska, S. R., Rich, V. I., and Tyson, G. W.: Methanotrophy across a natural permafrost thaw environment, ISME J., 12, 2544–2558, https://doi.org/10.1038/s41396-018-0065-5, 2018.

Smith, B., Prentice, C., and Sykes, M. T.: Representation of vegetation dynamics in the modelling of terrestrial ecosystems: comparing two contrasting approaches within European climate space, Global Ecol. Biogeogr., 10, 621–637, https://doi.org/10.1046/j.1466-822X.2001.t01-1-00256.x, 2001.

Smith, B., Wårlind, D., Arneth, A., Hickler, T., Leadley, P., Siltberg, J., and Zaehle, S.: Implications of incorporating N cycling and N limitations on primary production in an individual-based dynamic vegetation model, Biogeosciences, 11, 2027–2054, https://doi.org/10.5194/bg-11-2027-2014, 2014.

Snedecor, G. W. and Cochran, W. G.: Statistical Methods, 8th Edn., Iowa State University Press, Ames, ISBN 0-8138-1561-4, 1989.

Ström, L. and Christensen, T. R.: Below ground carbon turnover and greenhouse gas exchanges in a subarctic wetland, Soil Biol. Biochem., 39, 1689–1698, https://doi.org/10.1016/j.soilbio.2007.01.019, 2007.

Ström, L., Ekberg, A., Mastepanov, M., and Røjle Christensen, T.: The effect of vascular plants on carbon turnover and methane emissions from a tundra wetland, Glob. Change Biol., 9, 1185–1192, https://doi.org/10.1046/j.1365-2486.2003.00655.x, 2003.

Ström, L., Mastepanov, M., and Christensen, T. R.: Species-specific Effects of Vascular Plants on Carbon Turnover and Methane Emissions from Wetlands, Biogeochemistry, 75, 65–82, https://doi.org/10.1007/s10533-004-6124-1, 2005.

Ström, L., Tagesson, T., Mastepanov, M., and Christensen, T. R.: Presence of Eriophorum scheuchzeri enhances substrate availability and methane emission in an Arctic wetland, Soil Biol. Biochem., 45, 61–70, https://doi.org/10.1016/j.soilbio.2011.09.005, 2012.

Turetsky, M. R., Kotowska, A., Bubier, J., Dise, N. B., Crill, P., Hornibrook, E. R. C., Minkkinen, K., Moore, T. R., Myers-Smith, I. H., Nykänen, H., Olefeldt, D., Rinne, J., Saarnio, S., Shurpali, N., Tuittila, E.-S., Waddington, J. M., White, J. R., Wickland, K. P., and Wilmking, M.: A synthesis of methane emissions from 71 northern, temperate, and subtropical wetlands, Glob. Change Biol., 20, 2183–2197, https://doi.org/10.1111/gcb.12580, 2014.

van den Berg, M., van den Elzen, E., Ingwersen, J., Kosten, S., Lamers, L. P. M., and Streck, T.: Contribution of plant-induced pressurized flow to CH_4 emission from a Phragmites fen, Sci. Rep., 10, 12304, https://doi.org/10.1038/s41598-020-69034-7, 2020.

Varner, R. K., Crill, P. M., Frolking, S., McCalley, C. K., Burke, S. A., Chanton, J. P., Holmes, M. E., Isogenie Project Coordinators, Saleska, S., and Palace, M. W.: Permafrost thaw driven changes in hydrology and vegetation cover increase trace gas emissions and climate forcing in Stordalen Mire from 1970 to 2014, Philos. T. R. Soc. A, 380, 20210022, https://doi.org/10.1098/rsta.2021.0022, 2022.

Violle, C., Reich, P. B., Pacala, S. W., Enquist, B. J., and Kattge, J.: The emergence and promise of functional biogeography, P. Natl. Acad. Sci. USA, 111, 13690–13696, https://doi.org/10.1073/pnas.1415442111, 2014.

Visser, E. J. W., Bögemann, G. M., VAN DE Steeg, H. M., Pierik, R., and Blom, C. W. P. M.: Flooding tolerance of Carex species in relation to field distribution and aerenchyma formation: RESEARCH Flooding tolerance of Carex species, New Phytol., 148, 93–103, https://doi.org/10.1046/j.1469-8137.2000.00742.x, 2000.

Vroom, R. J. E., van den Berg, M., Pangala, S. R., van der Scheer, O. E., and Sorrell, B. K.: Physiological processes affecting methane transport by wetland vegetation – A review, Aquat. Bot., 182, 103547, https://doi.org/10.1016/j.aquabot.2022.103547, 2022.

Waldo, N. B., Hunt, B. K., Fadely, E. C., Moran, J. J., and Neumann, R. B.: Plant root exudates increase methane emissions through direct and indirect pathways, Biogeochemistry, 145, 213–234, https://doi.org/10.1007/s10533-019-00600-6, 2019.

Wallén, B.: Above and below ground dry mass of the three main vascular plants on hummocks on a subarctic peat bog, Oikos, 46, 51, https://doi.org/10.2307/3565379, 1986.

Wang, P., Mommer, L., van Ruijven, J., Berendse, F., Maximov, T. C., and Heijmans, M. M. P. D.: Seasonal changes and vertical distribution of root standing biomass of graminoids and shrubs at a Siberian tundra site, Plant Soil, 407, 55–65, https://doi.org/10.1007/s11104-016-2858-5, 2016.

Wen, Z., White, P. J., Shen, J., and Lambers, H.: Linking root exudation to belowground economic traits for resource acquisition, New Phytol., 233, 1620–1635, https://doi.org/10.1111/nph.17854, 2022.

Whiticar, M. J.: Carbon and hydrogen isotope systematics of bacterial formation and oxidation of methane, Chem. Geol., 161, 291–314, 1999.

Wild, J., Kopecký, M., Macek, M., Šanda, M., Jankovec, J., and Haase, T.: Climate at ecologically relevant scales: A new temperature and soil moisture logger for long-term microclimate measurement, Agr. Forest Meteorol., 268, 40–47, 2019.

Wilson, D., Alm, J., Riutta, T., Laine, J., Byrne, K. A., Farrell, E. P., and Tuittila, E.-S.: A high resolution green area index for modelling the seasonal dynamics of CO_2 exchange in peatland vascular plant communities, Plant Ecol., 190, 37–51, https://doi.org/10.1007/s11258-006-9189-1, 2007.

Wilson, R., Bosman, S., and Chanton, J.: CH? and DIC concentrations and δ13C from porewater at Stordalen Mire, July 2023, Zenodo, https://doi.org/10.5281/zenodo.18363867, 2026.

Wilson, R. M., Hough, M. A., Verbeke, B. A., Hodgkins, S. B., IsoGenie Coordinators, Chanton, J. P., Saleska, S. D., Rich, V. I., and Tfaily, M. M.: Plant organic matter inputs exert a strong control on soil organic matter decomposition in a thawing permafrost peatland, Sci. Total Environ., 820, 152757, https://doi.org/10.1016/j.scitotenv.2021.152757, 2022.

Wood, S. N.: Fast stable restricted maximum likelihood and marginal likelihood estimation of semiparametric generalized linear models, J. R. Stat. Soc. B, 73, 3–36, https://doi.org/10.1111/j.1467-9868.2010.00749.x, 2011.

Wood, S. N.: Generalized additive models: An introduction with R, Chapman and Hall/CRC, https://doi.org/10.1201/9781315370279, 2017.

Ye, Z. and Ryser, P.: Root porosity contributes to root trait space of wetland monocotyledons independently of economics traits, Plant Soil, 471, 301–314, https://doi.org/10.1007/s11104-021-05186-3, 2022.

Zhuang, Q., Melillo, J. M., Kicklighter, D. W., Prinn, R. G., McGuire, A. D., Steudler, P. A., Felzer, B. S., and Hu, S.: Methane fluxes between terrestrial ecosystems and the atmosphere at northern high latitudes during the past century: A retrospective analysis with a process-based biogeochemistry model, Global Biogeochem. Cy., 18, https://doi.org/10.1029/2004gb002239, 2004.